

REDUCING EMISSIONS OF A LARGE BORE TWO STROKE CYCLE ENGINE USING A  
NATURAL GAS AND HYDROGEN MIXTURE

by

VINCENT RAY VAN NORDEN

B.S., Kansas State University, 2006

A THESIS

submitted in partial fulfillment of the requirements for the degree

MASTER OF SCIENCE

Department of Mechanical and Nuclear Engineering  
College of Engineering

KANSAS STATE UNIVERSITY  
Manhattan, Kansas

2008

Approved by:

Major Professor  
Kirby S. Chapman, Ph.D.

## **Abstract**

The United States Environmental Protection Agency (EPA) continues to tighten pollutant emission regulations throughout the United States. As a result, the need to reduce air pollutants such as nitrogen oxides ( $\text{NO}_x$ ) and carbon monoxide (CO) remains a challenge for pipeline operators.  $\text{NO}_x$  formation is primarily a function of in-cylinder combustion temperatures. A challenge for engine researchers is to identify methods to lower combustion temperatures while maintaining complete combustion. Blending hydrogen into an engine's fuel can lower in-cylinder combustion temperatures and reduce pollutant emissions. Hydrogen has a wider flammability range in comparison to natural gas, which allows for leaner engine operation and lower combustion temperatures. Specifically, the very high molecular diffusivity of hydrogen creates a more uniform mixture of fuel and air. Hydrogen also has very low ignition energy, which translates into easier combustion. This paper presents test results of using hydrogen as a fuel additive for a large bore, two stroke cycle, single cylinder, natural gas fueled Ajax engine in a test laboratory. The engine was first operated at the test point on pure natural gas and allowed to stabilize. Then a mixture of hydrogen and natural gas at various molar percentages was introduced. The engine was operated entirely on the blended fuel without a pre-combustion chamber first. Next, a pre-combustion chamber was installed and the blended fuel was supplied to it while the main combustion chamber operated on pure natural gas. Engine and emissions data were recorded and physical observations were also noted, such as engine misfires. Results showed that the addition of hydrogen into the fuel gas without the use of a pre-combustion chamber reduced emissions. The addition of the pre-combustion chamber reduced  $\text{NO}_x$  emissions without the use of hydrogen. For both configurations, the engine ran smoother with no noticeable increase in misfires or detonation. The pollutant emission reduction and engine combustion stability suggest that hydrogen as a fuel additive would be a good method to meet emissions requirements.

## Table of Contents

List of Figures .....	vi
List of Tables .....	viii
Acronyms .....	ix
Nomenclature .....	x
Greek Variables .....	xii
Subscripts .....	xiii
Chemical Substances .....	xiv
Acknowledgements .....	xv
CHAPTER 1 - Introduction .....	1
CHAPTER 2 - Literature Review .....	6
Engines Used in the Industry .....	6
Environmental Protection Agency Regulations.....	7
Combustion Processes .....	8
Complete Combustion .....	8
Incomplete Combustion .....	9
Emissions .....	9
Oxides of Nitrogen.....	12
Carbon Monoxide .....	13
Addition of Hydrogen.....	14
Hydrogen/Methane Engine Testing .....	17
Ford F-150 .....	18
K4X Lean Burn.....	21
Pre-Combustion Chambers .....	25
Methods of Hydrogen Generation .....	26
Steam Methane Reforming .....	27
Partial Oxidation .....	28
Autothermal Reforming .....	29
Exhaust Gas Fuel Reforming .....	29

Partial Oxidation vs. Steam Methane Reforming .....	32
Major Findings.....	33
CHAPTER 3 - Governing Equations.....	34
Brake Horsepower .....	34
Mass Flow Rate of Fuel .....	34
Fuel Blending Calculations.....	36
Accounting for Hydrogen Addition.....	41
Measures of Efficiency .....	41
Equivalence Ratio .....	42
Delivery Ratio.....	43
Emissions .....	45
Uncertainty Analysis.....	46
CHAPTER 4 - Experimental Setup .....	48
Test Engine .....	48
Dynamometer.....	50
Pre-Combustion Chamber.....	51
Blending System.....	53
Data Collection and Instrumentation .....	57
CHAPTER 5 - Testing .....	64
Test Plan for Non-PCC Configuration.....	64
Test Results and Discussion for Non-PCC Configuration.....	65
Uncertainty in Experimental Results .....	66
Physical Observations .....	66
In-Cylinder Peak Pressure.....	66
Brake Specific Fuel Consumption .....	71
Exhaust Temperature .....	73
NO <sub>x</sub> Emissions .....	75
CO Emissions.....	77
Trapped Equivalence Ratio.....	79
Summary of Non-PCC Tests .....	80
Test Plan for PCC Configuration.....	80

Test Results and Discussion for PCC Configuration.....	81
In-Cylinder Peak Pressure.....	82
Brake Specific Fuel Consumption .....	85
NO <sub>x</sub> Emissions .....	86
CO Emissions.....	87
Trapped Equivalence Ratio.....	88
Summary of PCC Tests.....	89
CHAPTER 6 - Conclusions and Recommendations.....	91
References.....	95
Appendix A - Real Gas Fuel Blending Sample Calculation.....	99
Appendix B - Compressibility Factors .....	101
Appendix C - Ideal Gas Fuel Blending Sample Calculation .....	102

## List of Figures

Figure 1-1 Diagram of the Four Stroke Cycle .....	2
Figure 1-2 Diagram of the Two Stroke Cycle .....	3
Figure 2-1 Pollutant Formation in a Spark Ignited Engine.....	10
Figure 2-2 Concentration of HC, CO, and NO vs. Equivalence Ratio .....	12
Figure 2-3 Low Percentage Blend Ford F-150 .....	18
Figure 2-4 Graph Showing the Time to Accelerate Ford F-150 to 60mph Operating on Various Fuel Blends .....	20
Figure 2-5 Schematic of Simplified TCR Reformer.....	22
Figure 2-6 Mixer Hardware Installed at Dresser-Rand.....	23
Figure 2-7 Steam Methane Reforming Process .....	28
Figure 2-8 Example of Engine-Reformer System .....	30
Figure 2-9 Parameters Affecting the Quality and Quantity of Reformed Fuel.....	31
Figure 3-1 Orifice Plate in a Pipe .....	35
Figure 4-1 Hydraulic Governor Installed on Test Engine .....	49
Figure 4-2 Air Plenum Installed on Test Engine .....	50
Figure 4-3 Dynamometer Coupled to Test Engine.....	51
Figure 4-4 Pre-Combustion Chamber.....	52
Figure 4-5 Pre-Combustion Chamber Installed on Test Engine.....	52
Figure 4-6 Blending Chamber .....	54
Figure 4-7 Blending Manifold .....	55
Figure 4-8 Adjustable Pressure Regulator at Engine.....	55
Figure 4-9 Schematic of Fuel Delivery System.....	56
Figure 4-10 Data Acquisition Setup .....	59
Figure 4-11 User Interface.....	60
Figure 4-12 AETC Mapping Program.....	60
Figure 4-13 Heat Emissions Sample Line .....	62
Figure 5-1 In-Cylinder Peak Pressure.....	67
Figure 5-2 Standard Deviation of In-Cylinder Peak Pressure .....	68

Figure 5-3 In-Cylinder Peak Pressure Coefficient of Variation .....	69
Figure 5-4 Average Location of Peak Pressure .....	71
Figure 5-5 Brake Specific Fuel Consumption.....	72
Figure 5-6 Measured Exhaust Temperature.....	73
Figure 5-7 Corrected Exhaust Temperature.....	74
Figure 5-8 NO <sub>x</sub> Emissions .....	75
Figure 5-9 NO Emissions.....	76
Figure 5-10 NO <sub>2</sub> Emissions .....	77
Figure 5-11 CO Emissions.....	78
Figure 5-12 Equivalence Ratio .....	79
Figure 5-13 In-Cylinder Peak Pressure with PCC .....	82
Figure 5-14 Standard Deviation in Peak Pressure with PCC.....	83
Figure 5-15 In-Cylinder Peak Pressure Coefficient of Variation with PCC.....	84
Figure 5-16 Brake Specific Fuel Consumption with PCC.....	85
Figure 5-17 NO <sub>x</sub> Emissions with PCC.....	86
Figure 5-18 CO Emissions with PCC .....	88
Figure 5-19 Trapped Equivalence Ratio with PCC .....	89
Figure 6-1 Summary of Literature Results .....	93

## List of Tables

Table 2-1 Combustion Values of Hydrogen and Other Fuels.....	14
Table 2-2 Properties of Hydrogen, Methane, and Gasoline.....	15
Table 2-3 Emission Test Results (gram/mile) for Ford F-150 Operating on 30% Hydrogen .....	19
Table 2-4 Percentage Reduction in Emissions for 30% Hydrogen and CNG Blend vs. Gasoline Ford F-150 .....	20
Table 2-5 Chart of Fuel Economy and Range for Ford F-150 with Various Fuel Blends.....	21
Table 3-1 Real Gas and Ideal Gas Mixture Pressures.....	40
Table 3-2 Gas Density Factors for Emissions Calculations.....	45
Table 4-1 Test Engine Specifications .....	48
Table 4-2 Instrumentation Used to Analyze the Impact of Hydrogen.....	57
Table 4-3 Safety Shutdowns .....	61
Table 5-1 Non-PCC Test Matrix.....	65
Table 5-2 Uncertainties.....	66
Table 5-3 PCC Test Matrix.....	81

## Acronyms

AETC	Advanced Engine Technologies
ATDC	After Top Dead Center
ATR	Autothermal Reforming
BTDC	Before Top Dead Center
CI	Compression Ignition
CNG	Compressed Natural Gas
CV	Coefficient of Variation
EPA	Environmental Protection Agency
GTI	Gas Technology Institute
HCCI	Homogeneous Charge Compression Ignition
NGML	National Gas Machinery Lab
PCC	Pre-Combustion Chamber
SI	Spark Ignition
SMR	Steam Methane Reforming
TCR	Thermochemical Recuperation

## Nomenclature

$A$	Area
$AF$	Air-to-Fuel Ratio
$BSFC$	Brake Specific Fuel Consumption
$c_p$	Specific Heat at Constant Pressure
$c_v$	Specific Heat at Constant Volume
$d$	Diameter
$DR$	Delivery Ratio
$HHV$	Higher Heating Value
$LHV$	Lower Heating Value
$M$	Molecular Weight
$\dot{m}$	Mass Flow Rate
$N$	Rotational Speed
$n$	Number of Moles
$p$	Pressure
$R_u$	Universal Gas Constant
$T$	Temperature
$V$	Velocity
$\Psi$	Volume
$\dot{V}$	Volumetric Flow Rate
$\bar{v}$	Molar Specific Volume
$\dot{W}$	Power
$w$	Humidity Ratio

$y$	Mole Fraction
$Z$	Compressibility Factor

## Greek Variables

$\Delta$	Change in a Condition
$\phi$	Equivalence Ratio
$\sigma$	Uncertainty
$\rho$	Density
$\tau$	Torque
$\mu$	Mean

## Subscripts

<i>amb</i>	Ambient Conditions
<i>b</i>	Brake
<i>c</i>	Critical
<i>H</i>	Hydrogen
<i>i</i>	Species within a Mixture
<i>N</i>	Natural Gas
<i>R</i>	Reduced
<i>sat</i>	Saturated
<i>st</i>	Standard Conditions
<i>stoich</i>	Stoichiometric
<i>th</i>	Thermal
<i>Tr</i>	Trapped
<i>u</i>	Universal
<i>v</i>	Vapor

## Chemical Substances

C	Carbon
CH <sub>4</sub>	Methane
CO	Carbon Monoxide
CO <sub>2</sub>	Carbon Dioxide
H, H <sub>2</sub>	Hydrogen
HC	Unburned Hydrocarbons
HO <sub>2</sub>	Hydroperoxyl
H <sub>2</sub> O	Water
N, N <sub>2</sub>	Nitrogen
NO	Nitric Oxide
NO <sub>2</sub>	Nitrogen Dioxide
NO <sub>x</sub>	Nitrogen Oxides
O, O <sub>2</sub>	Oxygen
OH	Hydroxyl

## **Acknowledgements**

First, I would like to thank my advisor Dr. Kirby S. Chapman, the director of the National Gas Machinery Laboratory (NGML). He allowed me to work on this research, and was always there to answer questions and help me through difficult decisions. I want to thank Dr. Ali Keshavarz. He was very supportive and was always there to look over my research and add insight. I also want to thank Dr. Donald L. Fenton and Dr. Keith L. Hohn for being members of my defense committee. Dr. Fenton is an excellent instructor, and always took the time to help me even if it wasn't related to coursework. I took many classes from him and thoroughly enjoyed them all. Dr. Hohn was especially helpful with my catalyst research and took time out of his busy schedule to meet with me on multiple occasions.

Throughout my project, Ajax continued to provide guidance and support. Bruce Chrisman and Drake Pate spent a considerable amount of time helping tune up the engine on-site. Not only did this ensure reliable data for my testing, but gave me valuable knowledge of the engine I would not have received otherwise. Without Ajax's support and donations, conducting my research would have been much more difficult.

Since my research relied heavily on emissions data, a reliable emissions analyzer was necessary. ECOM not only agreed to donate an analyzer, but took the time to look at the NGML's needs. This resulted in an analyzer that gave excellent data for my research, and was versatile enough that other graduate students could use it for their research as well. This analyzer proved to be invaluable for my testing, and will continue to be that way for future research.

## CHAPTER 1 - Introduction

The goal of this research is to investigate the impact of hydrogen addition on performance and exhaust gas emissions of a two stroke cycle, lean burn, single cylinder engine. This engine is similar to those operated within the natural gas exploration and production sector and gives a representation of one cylinder in the transmission sector's multi-cylinder engines. A review of the literature indicates that the need for reducing pollutant emissions such as nitrogen oxides (NO<sub>x</sub>) and carbon monoxide (CO), and greenhouse gases such as carbon dioxide (CO<sub>2</sub>) remains a challenge for pipeline operators. Blending hydrogen into an engine's fuel system can lower in-cylinder combustion temperatures and reduce pollutant emissions. To thoroughly study hydrogen blending on a laboratory engine, the objectives of this thesis research are:

- Research the properties of hydrogen and its use as a fuel
- Design and build a fuel blending system
- Collect experimental data from operation on hydrogen blended fuels
- Collect experimental data from pre-combustion chamber operation on a hydrogen blended fuel
- Determine if emissions are lowered with hydrogen addition
- Consider performance parameters to determine engine stability on hydrogen blended fuels

The internal combustion engine was first developed in the late 1800s. Since then, it has become the dominant prime mover in several industries. The basic components of the internal combustion engine have remained unchanged since the late 1800s. Improvements have come in increased thermal efficiency and lower emissions. Lower emissions are particularly important, and are a constant subject of research.

There are two major cycles used in internal combustion engines. These are the Otto and Diesel cycles. The Diesel cycle engine is also referred to as the compression ignition (CI) engine. In a CI engine, the fuel auto-ignites when it is injected into the combustion chamber. The Otto cycle engine is also called a spark ignition (SI) engine. Here, a spark is used to ignite the fuel-air mixture in the combustion chamber. Both the Otto and Diesel cycles can operate on

either a four or two stroke cycle. Since the research presented does not deal with the Diesel cycle, only the Otto cycle will be addressed in detail.

The four stroke Otto cycle is shown in Figure 1-1. Here, the intake stroke draws a combustible mixture of fuel and air into the cylinder. Then, the compression stroke raises the temperature and pressure of the mixture. At the end of the compression stroke, a spark ignites the mixture and the power stroke results from the combustion of the fuel-air mixture. Finally, an exhaust stroke pushes out the burned gases.

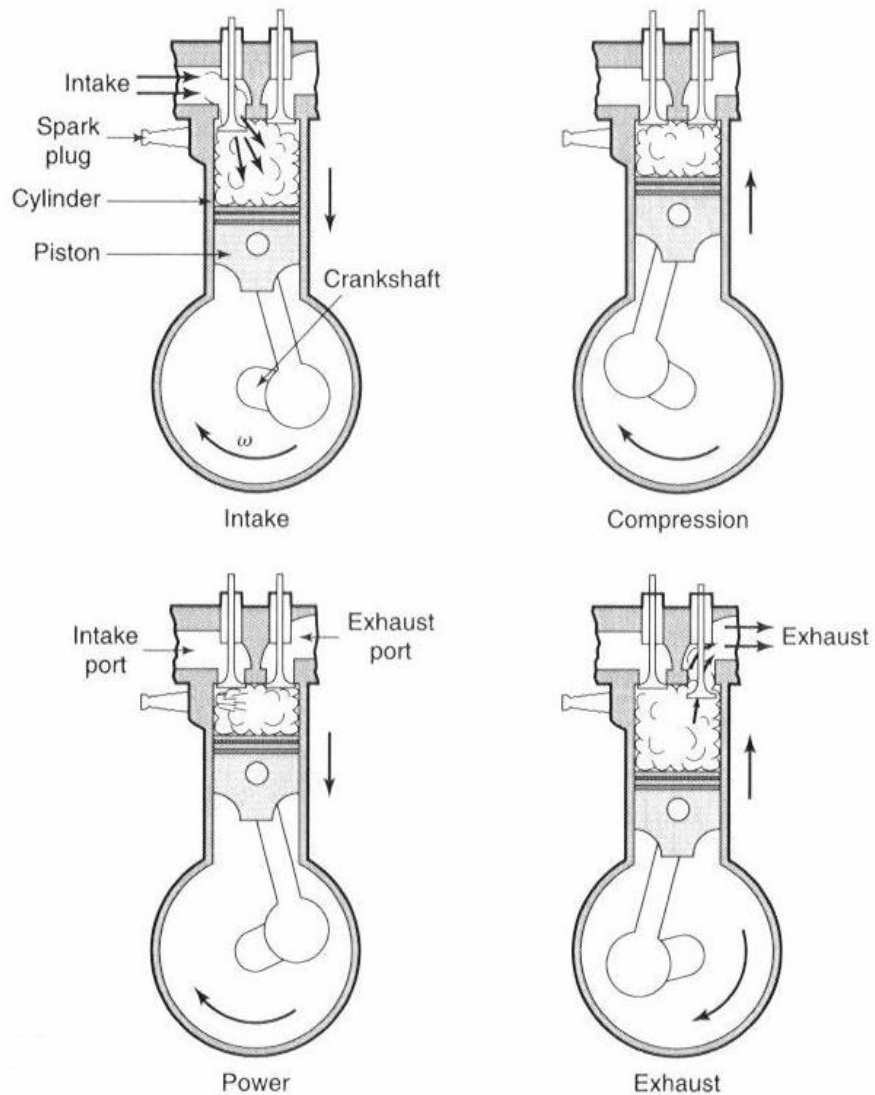


**Figure 1-1 Diagram of the Four Stroke Cycle**

Source: (Ferguson and Kirkpatrick, 2001)

The two stroke Otto cycle is shown in Figure 1-2. Here, as the name implies, only two strokes of the piston are needed to complete the cycle instead of four. The two stroke cycle starts with a compression stroke that first closes the inlet and exhaust ports. Next, the cylinder contents are compressed by the top of the piston and a sub-atmospheric pressure is induced on the back side of the piston to draw a fresh intake charge into the crankcase. Here, the piston movement completes this step, but the use of turbochargers, blowers, and other methods can achieve the same results. This intake charge can be either a fuel and air mixture or just air depending on if the engine is carbureted. At the end of compression, a spark initiates combustion and the power stroke. During the power stroke, the exhaust ports are uncovered first, which starts the exhaust blowdown process. Next, the intake ports are uncovered, and the fresh intake charge that has been compressed in the crankcase flows into the cylinder, where it continues to push out the exhaust gases in the scavenging process. If the engine is carbureted, the intake charge is a mixture of fuel and air. During scavenging, some of the fuel could escape through the exhaust port. This is why fuel injected two stroke cycle engines are more efficient, since their intake charge contains only air.

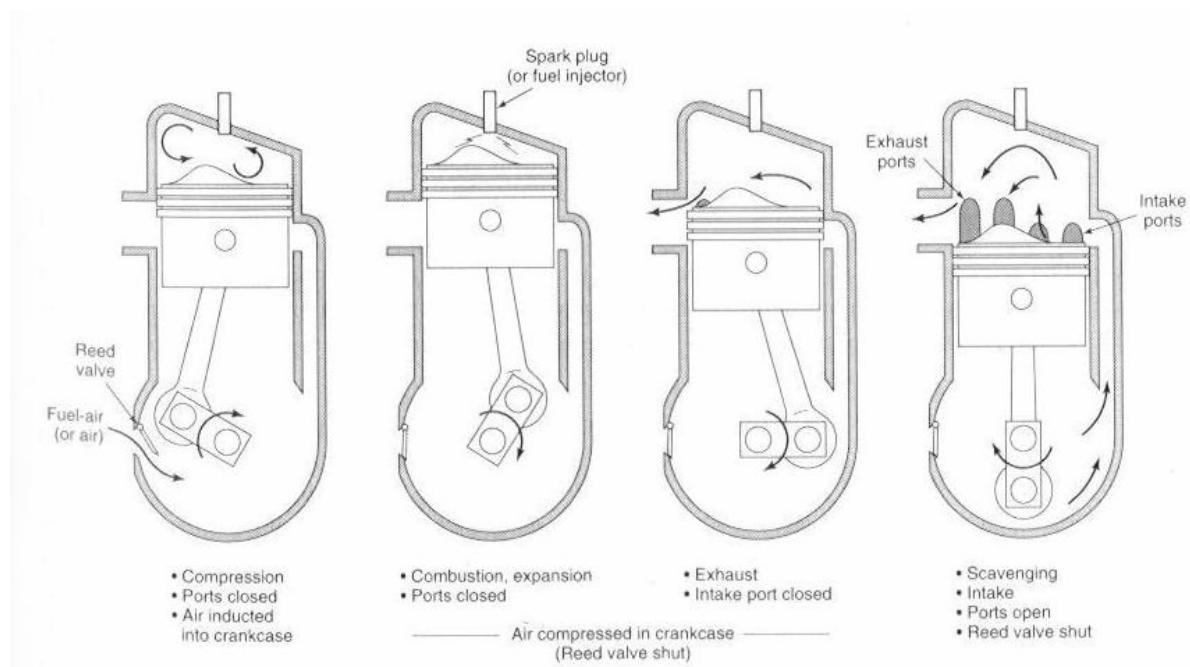


**Figure 1-2 Diagram of the Two Stroke Cycle**

Source: (Ferguson and Kirkpatrick, 2001)

The two stroke cycle has a power stroke every revolution. Two stroke cycle engines are also mechanically simpler than four stroke cycle engines. Most two stroke cycle engines use reed valves and ports instead of poppet valves like that of most four stroke cycle engines. Reed valves do not require mechanical actuation like poppet valves, which simplifies the design.

Some engines are rich burn. This means that they burn a mixture of fuel and air that is near stoichiometric. Some engines are lean burn, meaning their fuel-air mixture is on the lean side of stoichiometric. Either way, the engine will produce pollutant emissions such as NO<sub>x</sub> and CO, as well as greenhouse gases such as CO<sub>2</sub>. Pollutant emissions from combustion have become of great concern due to their impact on health and the environment. The United States Environmental Protection Agency (EPA) continues to tighten pollutant emission regulations throughout the United States. As a result, the need to reduce air pollutants remains a challenge.

Engine researchers continually evaluate methods to reduce exhaust gas emissions such as NO<sub>x</sub> and CO to enable engine operators to meet regulatory requirements. The formation of NO<sub>x</sub> is primarily a function of the peak in-cylinder temperature and the duration at these peak in-cylinder temperatures. Since higher temperatures produce more NO<sub>x</sub>, one strategy that has been adopted to reduce NO<sub>x</sub> formation is to lower peak in-cylinder combustion temperatures while maintaining complete combustion. Additionally, if the duration at these peak in-cylinder combustion temperatures can be reduced, NO<sub>x</sub> emissions can be reduced even further. If the engine is fueled by natural gas, blending hydrogen with the natural gas has been suggested as a means to lower combustion temperatures and reduce emissions (Karner and Francfort, 2003). This is due to how hydrogen acts as a fuel.

The flammability limits for hydrogen range from a low of 4% to a high of 75%. These limits are in contrast to the narrower limits of natural gas (methane), which are 5.3% to 17% (Swain, 2003). The wider flammability range, and more specifically, the lower flammability limit, allows for leaner engine operation and, in turn, lower combustion temperatures. These lower temperatures then result in lower NO<sub>x</sub> emissions. A second promising physical property of hydrogen is the diffusivity. The diffusivity is 0.61 cm<sup>2</sup>/s compared to that of natural gas (methane), which is 0.189 cm<sup>2</sup>/s (Karim, 2003). The relatively high diffusivity of hydrogen creates a more uniform mixture of fuel and air when compared to natural gas. Hydrogen also has an ignition energy of 0.017 mJ, which is 94% lower than that of pure methane (Swain, 2003). This low ignition energy, coupled with the relatively high laminar flame speed of 6.23 ft/s,

serves to lower the combustion duration and thus NO<sub>x</sub> emissions (Karim, 2003). Potentially, hydrogen-enhanced natural gas fuel blends can consistently and reliably reduce NO<sub>x</sub> emissions to below 1.0 g/hp-hr levels. Furthermore, hydrogen-methane fuel blends may enhance the capability of retrofit technologies such as pre-combustion chambers that have been developed for two stroke cycle engines to further lower NO<sub>x</sub> emissions.

The available literature indicates that hydrogen addition to natural gas fuel will reduce NO<sub>x</sub> emissions. Chapter 2 describes the engines used in the natural gas industry, discusses emissions regulations as well as the combustion process and formation of emissions. The properties of hydrogen are then discussed followed by a description of research that has already been conducted. Pre-combustion chambers are discussed as a retrofit technology that may benefit from hydrogen addition. The chapter finishes with a discussion of hydrogen production methods. Since many of the engines used in the industry are in remote locations, it may be necessary to produce hydrogen on-site. Chapter 3 describes the governing equations that were applied with analyzing the experimental data. Chapter 4 describes the test setup that was used to collect the experimental data. Each component of the test cell is discussed in detail. Chapter 5 discusses the test plans, each followed by experimental results and analysis.

## **CHAPTER 2 - Literature Review**

The literature review gives some background into the engines used in the natural gas industry. It was important to understand the industry and what it expects from its engines while setting up the experiment. In the following literature review, a discussion of emissions regulations describes the obstacles faced by engine operators. Next, the combustion process is described, followed by the methods of emissions formation within an internal combustion engine. Information on hydrogen addition and the properties that make it advantageous for lowering emissions is given. This information is supported by experimental results found by other researchers whose work is summarized. Since a typical low-emission, two stroke cycle engine used in the gas industry includes pre-combustion chambers, a description of their operation and purpose is presented. The pre-combustion chamber is another location where blended fuel can be utilized. The literature review concludes with descriptions of how hydrogen can be generated in the field. This is particularly important because many of the engines are located in remote regions. If hydrogen blended fuels were to be used with these engines, a method of on-site hydrogen generation may be necessary. The information presented in this chapter is the first step in achieving the objective of this research.

### **Engines Used in the Industry**

The effective and efficient delivery of natural gas involves the use of an extensive transportation system. Often, gas from a well has to be transported hundreds of miles to reach the consumer. The natural gas industry is separated into three primary areas: exploration and production (E&P), transmission, and local distribution. The transmission sector uses large engines to transport natural gas in large pipelines throughout the nation. Approximately 70% of the engines used in the transmission sector are two stroke cycle engines manufactured by Cooper and Clark (Beshouri et al., 2005). The exploration and production sector uses much smaller engines than the transmission sector. There are literally tens of thousands of engines used within this sector. They are four and two stroke cycle engines, with most being less than 100 hp. Many of the engines are two stroke cycle engines manufactured by Ajax. The remaining engines are four stroke cycle engines manufactured by Waukesha, Arrow, and Caterpillar (Chapman,

December 2003). These engines are used to collect natural gas from the well head and transfer it to processing facilities and pipelines. Often, a processing plant is located between the well head and the pipeline to remove unwanted components such as sulfur and hydrocarbons including butane, ethane, and propane. These components are often then sold. The local distribution systems deliver gas to the end consumer. The local distributor does not usually need the use of engines and compressors since they receive the gas at a high pressure from the transmission system.

### **Environmental Protection Agency Regulations**

In both E&P and transmission, the engines were designed and built during a time when reliability and durability were valued more than emissions and fuel consumption (Pratapap et al., 2007). These engine's continued existence and use shows that the engineers succeeded in this regard. They are fueled by natural gas and emit NO<sub>x</sub>, CO, CO<sub>2</sub>, and unburned non-methane hydrocarbons. New technologies for these engines are typically aimed at reducing NO<sub>x</sub> emissions (Frey and Li, 2001). Impending emissions regulations promise to require lower NO<sub>x</sub> and CO emissions, not only on large engines, but also on engines as small as 25 hp. These regulatory requirements will necessitate the development and implementation of low-cost emissions reduction strategies on the smaller engine fleet (less than 300 hp) (Agrawal et al., 2004).

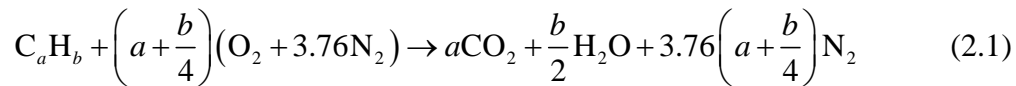
Until recently, the EPA has limited most of its emissions regulations to stationary engines larger than 300 hp. Now, emissions constraints on engines as small as 25 hp are being put into place. Furthermore, the EPA continues to tighten pollutant emissions regulations throughout the United States, and was recently given right by the Supreme Court to regulate greenhouse gases (Agrawal et al., 2004). Typically, technologies that reduce emissions from the smaller engines can be readily modified to serve as emissions reduction technologies on the larger engines used in the natural gas transmission industry. Most gathering engines will now be regulated by very tight limits, many of which currently have no emissions controls. Major capital investments by the gas industry would be required if these engines had to be replaced. Effective low cost solutions for reducing emissions while maintaining combustion stability and engine performance must become available for these legacy engines. Gathering companies are scrambling to see what can be done with these engines so that they can meet the new limits.

## Combustion Processes

Combustion is a chemical reaction that releases a large amount of energy. It is the driving force behind an internal combustion engine. It is separated into complete combustion and incomplete combustion. Often, it is useful to study combustion by assuming that the reaction is complete. However, this is most likely not the case with actual combustion.

### *Complete Combustion*

With sufficient oxygen, a hydrocarbon fuel can be completely oxidized. Complete oxidation allows for the carbon in the fuel to be converted to CO<sub>2</sub> while the hydrogen in the fuel is converted to water (H<sub>2</sub>O). The general form of a complete combustion reaction is given by (Heywood, 1988):



Equation (2.1) defines the stoichiometric, or theoretical, proportion of fuel and air to achieve complete combustion. This means that there is just enough oxygen for all of the fuel to burn. Notice that the products contain no excess oxygen and no unburned fuel.

If the amount of air is in excess of the stoichiometric amount, the mixture is called lean. Similarly, if there is less air than stoichiometric, the mixture is called rich. Referring to Equation (2.1), the stoichiometric mass air-to-fuel ratio ( $AF_{stoich}$ ) is defined as:

$$AF_{stoich} = \left(a + \frac{b}{4}\right) \frac{4.76 \times M_{air}}{M_{fuel}} \quad (2.2)$$

Dividing this value by the actual mass air-to-fuel ratio ( $AF$ ) of the engine will give the fuel-air equivalence ratio as given by (Ferguson and Kirkpatrick, 2001):

$$\phi = \frac{AF_{stoich}}{AF} \quad (2.3)$$

If this value is greater than one, then the mixture is rich. A value less than one means the mixture is lean. If the value is equal to one, the mixture is stoichiometric.

In actual combustion, it is common to use a lean mixture to control the temperature of the combustion chamber. Excess air in the combustion chamber absorbs heat, therefore lowering the temperature. The combustion reaction of methane and air with 50% excess air is:



Notice in Equation (2.4) that the excess air is passed into the products.

### ***Incomplete Combustion***

The combustion process is incomplete if the combustion products contain unburned fuel, carbon (C), hydrogen (H<sub>2</sub>), carbon monoxide (CO), nitric oxide (NO), or hydroxyl (OH). Sometimes, incomplete combustion is caused by a rich mixture, where there is insufficient oxygen for the fuel. This causes some of the fuel to not burn and be passed out of the exhaust. Excess oxygen may also cause incomplete combustion. If too much air is in the cylinder, incomplete mixing may occur. Since there is a limited amount of time that the air and fuel are in contact, some regions of the cylinder may be too lean to combust while others are rich (Heywood, 1988). This is when ignition timing and the method of fuel introduction is important. The mixture should be ignited at the proper time to ensure the fuel and air have been properly mixed. It is also important to introduce the fuel in such a way that promotes thorough mixing. These are only some of the causes for incomplete combustion. Combustion is a complicated process that is dependent on many factors such as temperature, pressure, and equivalence ratio.

### **Emissions**

All combustion processes produce emissions. Some of these emissions are regulated, while others are not. Examples of unregulated emissions are CO<sub>2</sub> and water vapor. Hereafter, regulated emissions will be collectively referred to as emissions. The amount of emissions depends on the conditions that were present during combustion. For example, the combustion process could have been complete or incomplete, and the mixture rich or lean. When dealing with two stroke cycle engines, the mixture is usually lean. As a result, CO and unburned hydrocarbon (HC) emissions are lower. NO<sub>x</sub> and CO are the emissions of primary concern. The first step in controlling emissions is to understand how they form.

In general, the concentration of emissions in combustion engines is different from the values calculated assuming chemical equilibrium. This goes back to equilibrium, chemical

kinetics, improper mixing, and other conditions within the combustion chamber. The processes by which pollutants form within the cylinder of a spark ignited engine are shown in Figure 2-1.

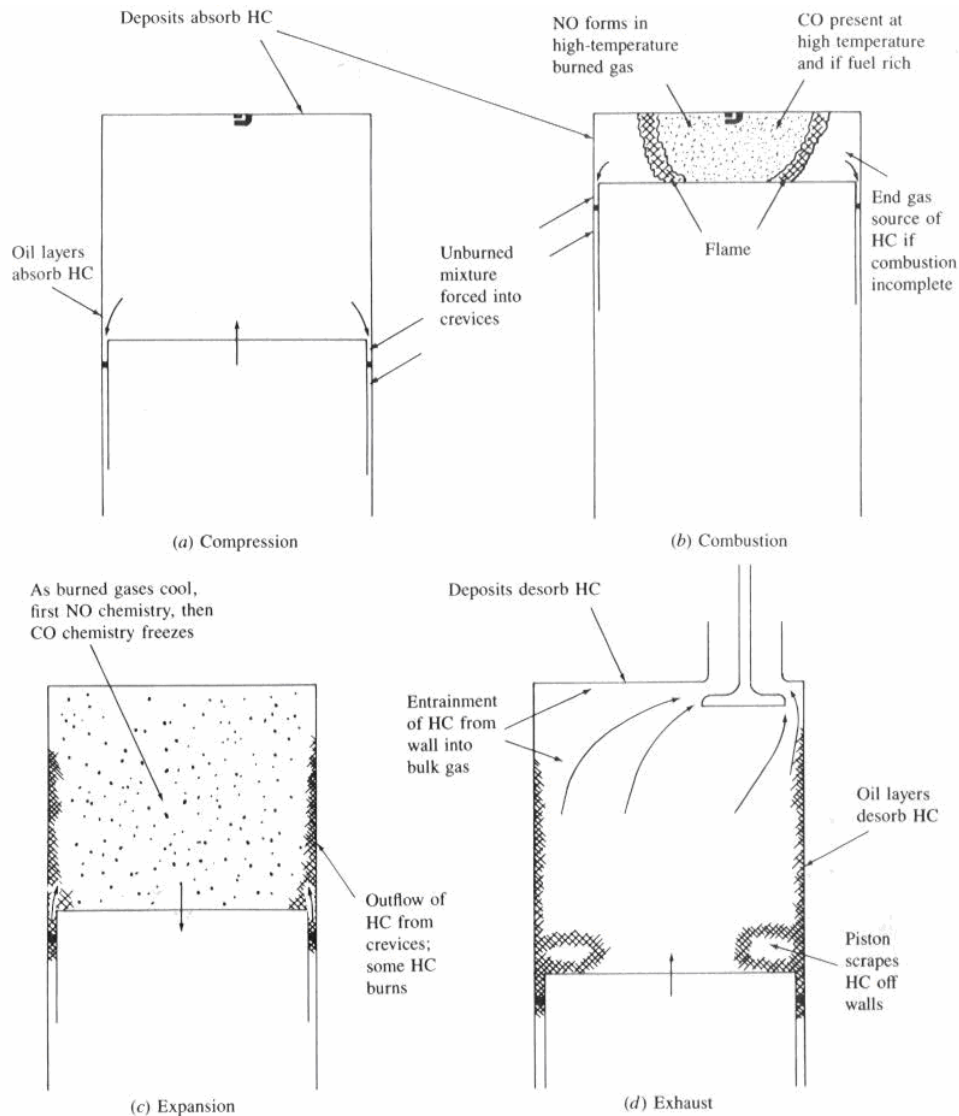


**Figure 2-1 Pollutant Formation in a Spark Ignited Engine**

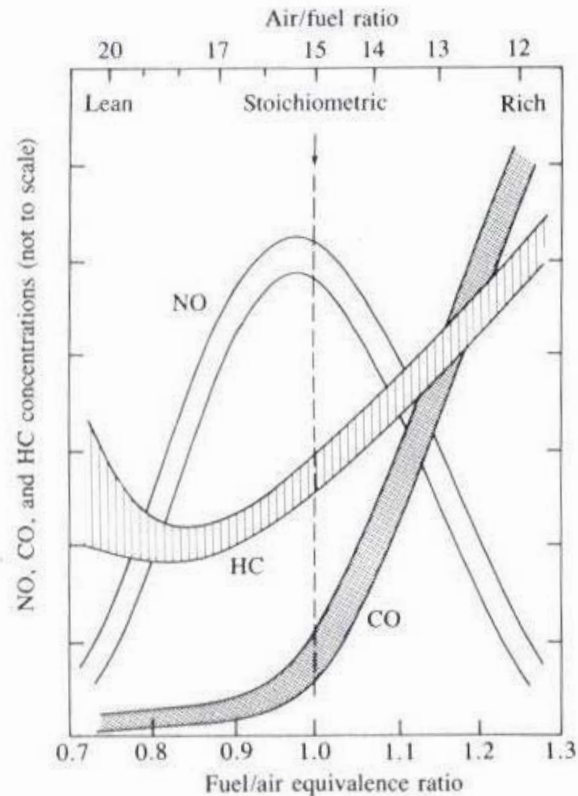
**Source:** (Heywood, 1988)

Figure 2-1 shows the combustion chamber during four different times of the cycle: compression, combustion, expansion, and exhaust. NO forms in the high temperature regions behind the flame through chemical reactions involving nitrogen and oxygen. Higher temperature regions form more NO. If the fuel-air mixture is rich, there is insufficient oxygen to burn all of

the carbon in the fuel to  $\text{CO}_2$ , and  $\text{CO}$  is formed. Even if the mixture is lean, high temperature regions cause  $\text{CO}_2$  dissociation and the subsequent production of  $\text{CO}$  occurs. When the burned gas temperature lowers during the expansion stroke, the  $\text{NO}$  and  $\text{CO}$  reactions stop with the  $\text{CO}$  reactions stopping last (Heywood, 1988).

$\text{HC}$  emissions have several different sources. During compression and combustion, some gas is forced into crevices in the cylinder such as between the piston and cylinder wall. Much of this gas is an unburned fuel-air mixture since the flame cannot reach into these small crevices. This gas becomes a source of  $\text{HC}$  emissions when it leaves the crevices during the expansion and exhaust processes.  $\text{HC}$  emissions can also come from the quenching that occurs very close to the cylinder walls ( $<0.004$  in.). If the cylinder walls have any carbon build up on them, more  $\text{HC}$  emissions are produced from quenching. Another source of  $\text{HC}$  emissions is any oil layer that is left on the cylinder wall. This oil layer can absorb fuel components before combustion and desorb them after combustion (Heywood, 1988). These are only some of the sources of  $\text{HC}$  emissions. Other factors such as equivalence ratio and spark timing affect all emissions levels, including  $\text{HC}$ .

One of the most important variables affecting engine emissions is equivalence ratio. Figure 2-2 shows the variation of  $\text{HC}$ ,  $\text{CO}$ , and  $\text{NO}$  concentration as equivalence ratio changes in a spark ignited engine. Leaner mixtures give lower emissions as can be seen in the figure. As the mixture becomes leaner and the equivalence ratio smaller, the combustion process will become unstable and misfires will occur. It is these misfires and unstable combustion that cause the increase in  $\text{HC}$  emissions at low equivalence ratios (Heywood, 1988). The figure also shows that  $\text{NO}$  production peaks on the slightly lean side of stoichiometric. This corresponds to the highest in-cylinder combustion temperature.



**Figure 2-2 Concentration of HC, CO, and NO vs. Equivalence Ratio**

Source: (Heywood, 1988)

### ***Oxides of Nitrogen***

NO<sub>x</sub> refers to the sum of nitric oxide (NO) and nitrogen dioxide (NO<sub>2</sub>). While NO and NO<sub>2</sub> are lumped together as NO<sub>x</sub>, there are distinctive differences between these two pollutants. NO is a colorless and odorless gas, while NO<sub>2</sub> is a reddish-brown gas with a pungent odor. Both gases are considered toxic, but NO<sub>2</sub> has a level of toxicity five times greater than that of NO. NO is formed after combustion in high temperature regions (Agrawal et al., 2004).

The three principle reactions for the formation of NO are expressed by:



These equations are often called the extended Zeldovich mechanism (Heywood, 1988). The formed NO can oxidize into NO<sub>2</sub> through:



Dissociation can also occur, where NO and NO<sub>2</sub> will rearrange. Dissociation from NO<sub>2</sub> into NO can be a significant contributor to NO emissions. (Bowman, 1975) gives this dissociation as:



Formation of NO<sub>x</sub> is not significant when temperatures are below approximately 2900°F (Agrawal et al., 2004). This means that if temperatures in the combustion region can be kept below this value, or at least the duration above this threshold is limited, the NO<sub>x</sub> emissions will be lower. This set of reactions is the most widely used and recognized mechanism for NO formation. It can be seen that the formation of NO<sub>2</sub> results only from the oxidation of NO, so the total amount of NO<sub>x</sub> is not affected by the amount of NO<sub>2</sub> formed.

### *Carbon Monoxide*

Carbon monoxide is toxic and in high concentrations can cause asphyxiation and even death. CO emissions from internal combustion engines are heavily dependent on equivalence ratio. For rich mixtures, CO emissions rise with increasing equivalence ratio. For lean mixtures, CO emissions are almost zero for an equivalence ratio of 0.7, and do not significantly increase until a stoichiometric mixture is reached (Heywood, 1988). This can be seen in Figure 2-2. CO formed during combustion is then oxidized to CO<sub>2</sub> through the following reaction:



Equation (2.10) occurs at a relatively slow rate. This is one reason internal combustion engines have CO emissions. The residence time is not long enough and temperatures fall too rapidly in spark ignited engines to oxidize all of the CO (Turns, 2000).

After CO<sub>2</sub> has been formed, it may dissociate under the high temperatures of combustion. This endothermic reaction will result in CO as given by (Heywood, 1988):



Although CO formation is highly dependent on equivalence ratio, other factors can also contribute to its production. A couple of these are quenching by cold surfaces, and partial oxidation of unburned fuel (Turns, 2000). Just as NO<sub>2</sub> is formed through the oxidation of NO, CO<sub>2</sub> heavily relies on the existence and oxidation of CO.

### **Addition of Hydrogen**

The utilization of a blended fuel system is one method to reduce emissions. An engine equipped with a blended fuel system can operate on a combination of fuels. Hydrogen enriched combustion is a proven way to extend the lean limit of natural gas engines and also increases the level of exhaust gas recirculation on rich burn engines (Pratapas et al., 2007). The use of hydrogen in blended fuel engines can lower combustion temperatures and reduce emissions. The majority of blended fuel engines that utilize hydrogen operate with a hydrogen and natural gas mixture (Department of Energy, 2001a). The hydrogen content of this gas mixture can range from pure hydrogen to hardly any hydrogen. When operated with less than 30% hydrogen in the fuel gas mixture, these engines offer many advantages over other blended fuel engines. The engines perform well in all weather conditions, require no warm-up, have no cold-start problems, and are highly fuel efficient (Department of Energy, 2001b). All of these advantages result from hydrogen's fuel characteristics. Table 2-1 shows some of the combustion properties of hydrogen compared to other fuels.

**Table 2-1 Combustion Values of Hydrogen and Other Fuels**

Source: (Swain, 2003)

<b>Property</b>	<b>Hydrogen</b>	<b>Methane</b>	<b>Propane</b>	<b>Gasoline</b>
Lower Flammability Limit (%)	4	5.3	1.7	1.3
Lower Detonation Limit (%)	18.3	6.3	3.1	1.1
Upper Detonation Limit (%)	59	13.5	9.2	3.3
Upper Flammability Limit (%)	75	17	10.9	6.0
Auto Ignition Temperature (°F)	1085	1000	840	420
Minimum Ignition Energy (mJ)	0.017	0.274	0.240	0.240

Hydrogen has a wide range of flammability in comparison with all other fuels. Hydrogen's flammability range is 4% to 75% by volume in air, while methane's flammability range is 5.3% to 17% by volume in air (Swain, 2003). As a result, hydrogen can be combusted over a wide range of air to fuel ratios. The lean mixture also means that there is more air during combustion. The additional air absorbs heat and lowers the combustion temperature.

Hydrogen also has very low ignition energy. Hydrogen's ignition energy is 0.017 mJ at a 30% volumetric concentration compared to 0.25 mJ for other hydrocarbon fuels (Swain, 2003). The amount of energy needed to ignite hydrogen is about an order of magnitude less than that of gasoline. This helps with the ability to operate with a lean mixture and allows the engine to start easier, even in cold environments, and shortens warm-up time. Unfortunately, this low ignition energy also means that hot spots in the cylinder can cause pre-ignition. This, and a wide flammability range, causes premature ignition and backfires, which are the two main challenges when operating an engine on hydrogen. Table 2-2 shows some properties of hydrogen, methane, and gasoline. It can be seen that the properties vary from one fuel to another.

**Table 2-2 Properties of Hydrogen, Methane, and Gasoline**

Source: (Karim, 2003)

<b>Property</b>	<b>Hydrogen</b>	<b>Methane</b>	<b>Gasoline</b>
Density at 1 atm and 300 K (kg/ m <sup>3</sup> )	0.082	0.717	5.11
<i>HHV</i> (MJ/kg)	141.7	52.68	48.29
<i>LHV</i> (MJ/kg)	119.7	46.72	44.79
<i>HHV</i> (MJ/m <sup>3</sup> )	12.1	37.71	233.29
<i>LHV</i> (MJ/ m <sup>3</sup> )	10.22	33.95	216.38
Diffusion Coefficient into air at STP (cm <sup>2</sup> /s)	0.61	0.189	0.05

Looking at the table above, hydrogen's mass specific heating values are over twice that of methane, but the volume specific heating values are nearly 1/3 that of methane and 1/20 that of gasoline. This is due to hydrogen's extremely low density. For a given equivalent volume, the amount of energy released in the combustion of pure hydrogen and air is much lower than that of the other two fuels. It is for this reason that overall engine power declines with hydrogen blended fuels near stoichiometric equivalence ratios (Karim, 2003).

Hydrogen has a very high diffusivity. It is the lightest of all elements with a specific gravity about 1/14 that of air. As a result, hydrogen is buoyant and rapidly disperses when released into air. Hydrogen's diffusivity is  $0.61 \text{ cm}^2/\text{s}$  compared to that of natural gas (methane), which is  $0.189 \text{ cm}^2/\text{s}$  (Karim, 2003). Not only does hydrogen diffuse nearly three times faster than methane, but it diffuses ten times faster than gasoline (Swain, 2003). The relatively high diffusivity of hydrogen creates a more uniform mixture of fuel and air when compared to natural gas. This, coupled with a low ignition energy and the relatively high laminar flame speed of  $6.23 \text{ ft/s}$ , serves to lower the combustion duration. Since less time is spent at the peak in-cylinder temperature,  $\text{NO}_x$  emissions are lowered. The more uniform mixture of fuel and air increases power output from fuel mixtures near the lean operating limit where combustion stability is typically reduced (Karim, 2003).

Backfires can also be caused by hydrogen's small quenching gap (0.025 in). This distance describes the flame extinguishing properties of a fuel when used in an engine. This is the distance from the cylinder wall that the flame extinguishes due to heat losses. Hydrogen's quenching gap is approximately three times smaller than other fuels, which means that the addition of hydrogen causes the flame to travel closer to the cylinder wall. Since the flame travels very close to the cylinder wall, there is a better chance of it slipping through a nearly closed intake valve than the flame from a hydrocarbon fuel (Department of Energy, 2001a). Despite its low ignition energy, hydrogen has a high auto-ignition temperature, which is why it is primarily used in SI engines. Hydrogen has a low density. This means that a large volume is necessary to store enough hydrogen for a vehicle to operate on, which can be a design constraint (Department of Energy, 2001b).

Hydrogen is most commonly mixed with compressed natural gas since both gases can be stored in the same tank. Methane also has a relatively high octane number of approximately 120 (Heywood, 1988). This makes it resistant to pre-ignition. Since hydrogen is susceptible to pre-ignition, the addition of hydrogen to methane results in the formation of a fuel mixture with more resistance to pre-ignition than hydrogen and other fuels. This is important since pre-ignition is a main concern with hydrogen blended fuels. If a blended fuel engine is to operate with hydrogen and another fuel, the fuels usually have to be stored separately and mixed in the gaseous state before being sent to the engine. If the other fuel is a liquid, then the hydrogen would float on top and not mix. Liquid fuels are also stored at lower pressures than gaseous fuels, so very little

hydrogen could be added without increasing the pressure too much. If the hydrogen is stored in liquid form, it will freeze other fuels due to its low boiling point. Since hydrogen requires a lot of storage space, other fuels with the same problem, such as propane, are not used with hydrogen (Department of Energy, 2001b).

### **Hydrogen/Methane Engine Testing**

The primary focus of this research is stationary, two stroke cycle, lean burn, natural gas fueled engines. A review of the literature shows that some research has been conducted with these engines and hydrogen addition. The results from this research are particularly important because it establishes feasibility and grounds for further testing. However, while looking through the literature, it was found that most hydrogen and natural gas blending research was being conducted on automobile engines. Even though automobile engines are rich burn, four stroke cycle engines, the results of these tests are useful for developing test plans and getting an idea of expected results.

(Bauer and Forest, 2001) investigated the effects of hydrogen addition on natural gas engine performance. They noted that hydrogen addition up to 60% by volume resulted in a 26% decrease in carbon dioxide emissions, a 40% decrease in carbon monoxide emissions, and a 60% decrease in hydrocarbon emissions. However, for equivalence ratios near stoichiometric, they observed a 30% increase in nitrogen oxide emissions. Because of this increase, the results show that more hydrogen is not necessarily better.

(Shrestha and Karim, 1999) investigated the effects of hydrogen addition to natural gas fueled engines. They examined hydrogen concentrations from 0% to 80% by volume and concluded that the presence of more than 20% hydrogen in the blended fuel resulted in decreased power output due to the lower volume specific heating value of hydrogen as opposed to methane. However, as they decreased the equivalence ratio, power significantly increased in the lean operating region. They ultimately concluded that the optimum concentration of hydrogen in the fuel mixture for avoiding knock and producing power is 20% to 25% by volume.

(Karim et al., 1996) also investigated the effects of hydrogen addition to natural gas fueled engines. They observed a decrease in exhaust emissions including CO, methane (CH<sub>4</sub>), and CO<sub>2</sub>. Their main finding was that spark timing needed to be adjusted as hydrogen was added. They concluded that operation with extremely lean mixtures containing hydrogen

requires relatively late spark timing for optimum engine performance and lower emissions due to the higher flame speed of hydrogen.

The previous paragraphs summarize the major conclusions of testing done with mixtures of hydrogen and natural gas. The following are more detailed descriptions of similar tests and give more insight into the setup and procedures used in such testing. They also provide more detailed data for analyses.

### ***Ford F-150***

A few auto manufactures have developed vehicles that are fully hydrogen powered. BMW has displayed multiple hydrogen powered 750i vehicles around the world. Ford has introduced a number of hydrogen based vehicles including the P2000, the Focus based H2RV, and the Model U (Department of Energy, 2005). However, it is unlikely that these vehicles will be used by the public because there are few places to refuel or maintain them.

A more realistic approach to using hydrogen is blending it with natural gas. Compressed natural gas (CNG) is becoming more popular, especially with energy companies and government organizations. Blending hydrogen with CNG lowers combustion temperatures. To determine the effects of this blending, a 2001 Ford F-150 shown in Figure 2-3 was tested with 100% CNG, 15% hydrogen, and 30% hydrogen. The pickup was modified by installing two 3600 psig carbon steel fuel tanks with an 85 liter capacity, supercharging, ignition modifications, and exhaust gas recirculation.



**Figure 2-3 Low Percentage Blend Ford F-150**

Source: (Karner and Francfort, 2003)

Two different emissions tests were performed while the F-150 operated on a blend of 30% hydrogen. The first test was the Inspection and Maintenance Driving Cycle (IM240) test. This test lasted 240 seconds and 1.96 miles. The truck reached a top speed of 56.7 mph and averaged 29.4 mph, but this test did not take into account starting conditions. The second test was the Federal Test Procedure (FTP-75). This was a more comprehensive test since it took into account cold start, transient, and hot start conditions. It took 1,874 seconds and 11.04 miles to complete, during which the truck averaged 21.2 mph. The results from the FTP-75 test can be compared to the California emission standards for ultra low emission vehicles (ULEV) and super ultra low emission vehicles (SULEV). These standards are based on a new vehicle. The results showed that the F-150 averaged 0.255 gram/mile in carbon monoxide emissions, which is far below the California SULEV standard of 1 gram/mile. NO<sub>x</sub> emissions averaged 0.078 gram/mile, which is about the same as the California ULEV standard of 0.07 gram/mile (Karner and Francfort, 2003). The full emissions data for both tests can be seen in Table 2-3. There is a substantial decrease in the emissions for a 30% hydrogen and CNG blend compared to a gasoline fueled F-150, as shown in Table 2-4. This is due to the cleaner burning CNG and the lower combustion temperatures brought by the addition of hydrogen. All emissions decreased by operating on a blend of CNG and hydrogen except for methane, which is expected from vehicles operating on CNG (Karner and Francfort, 2003).

**Table 2-3 Emission Test Results (gram/mile) for Ford F-150 Operating on 30% Hydrogen**

Source: (Karner and Francfort, 2003)

Test Date	Mileage	NMHC	CH <sub>4</sub>	HC	CO	NO <sub>x</sub>	CO <sub>2</sub>
<b>FTP-75</b>							
5/2/2001	1592	0.011	0.075	0.094	0.237	0.063	440.606
5/3/2001	1613	0.019	0.084	0.118	0.249	0.094	441.442
5/4/2001	1636	0.024	0.082	0.121	0.267	0.094	437.370
5/8/2001	1657	0.017	0.099	0.133	0.257	0.084	439.940
6/14/2001	2148	0.028	0.091	0.136	0.223	0.104	435.899
8/30/2001	3890	0.028	0.074	0.116	0.348	0.051	442.515
8/31/2001	3915	0.028	0.067	0.107	0.210	0.053	437.009
<b>Average</b>		<b>0.022</b>	<b>0.081</b>	<b>0.117</b>	<b>0.255</b>	<b>0.078</b>	<b>439.254</b>
<b>IM240</b>							
5/2/2001	1592	0.062	0.050	0.124	0.135	0.040	392.720
5/3/2001	1625	0.008	0.042	0.057	0.118	0.025	402.205
5/4/2001	1647	0.014	0.054	0.078	0.146	0.023	410.147
5/8/2001	1670	0.016	0.069	0.098	0.101	0.022	411.302
8/30/2001	3901	0.014	0.054	0.078	0.077	0.089	397.635
8/30/2001	3903	0.016	0.028	0.049	0.125	0.051	402.614
8/31/2001	3928	0.013	0.045	0.066	0.101	0.019	397.634
8/31/2001	3931	0.013	0.026	0.045	0.095	0.033	396.020
<b>Average</b>		<b>0.019</b>	<b>0.046</b>	<b>0.074</b>	<b>0.112</b>	<b>0.037</b>	<b>401.285</b>

NMHC = nonmethane hydrocarbons  
 CH<sub>4</sub> = methane  
 HC = total hydrocarbons  
 CO = carbon monoxide  
 NO<sub>x</sub> = oxides of nitrogen  
 CO<sub>2</sub> = carbon dioxide

**Table 2-4 Percentage Reduction in Emissions for 30% Hydrogen and CNG Blend vs. Gasoline Ford F-150**

Source: (Karner and Francfort, 2003)

HC	CO	NO <sub>x</sub>	CO <sub>2</sub>
7.6%	83.5%	53.4%	29.4%

HC = total hydrocarbons.  
 CO = carbon monoxide.  
 NO<sub>x</sub> = oxides of nitrogen.  
 CO<sub>2</sub> = carbon dioxide.

Acceleration testing was also performed with the F-150. Tests were conducted four times for each different fuel blend. The fuel blends used were 100% CNG, 15% hydrogen, and 30% hydrogen. The time in seconds to accelerate from 0 to 60 mph are shown in Figure 2-4.

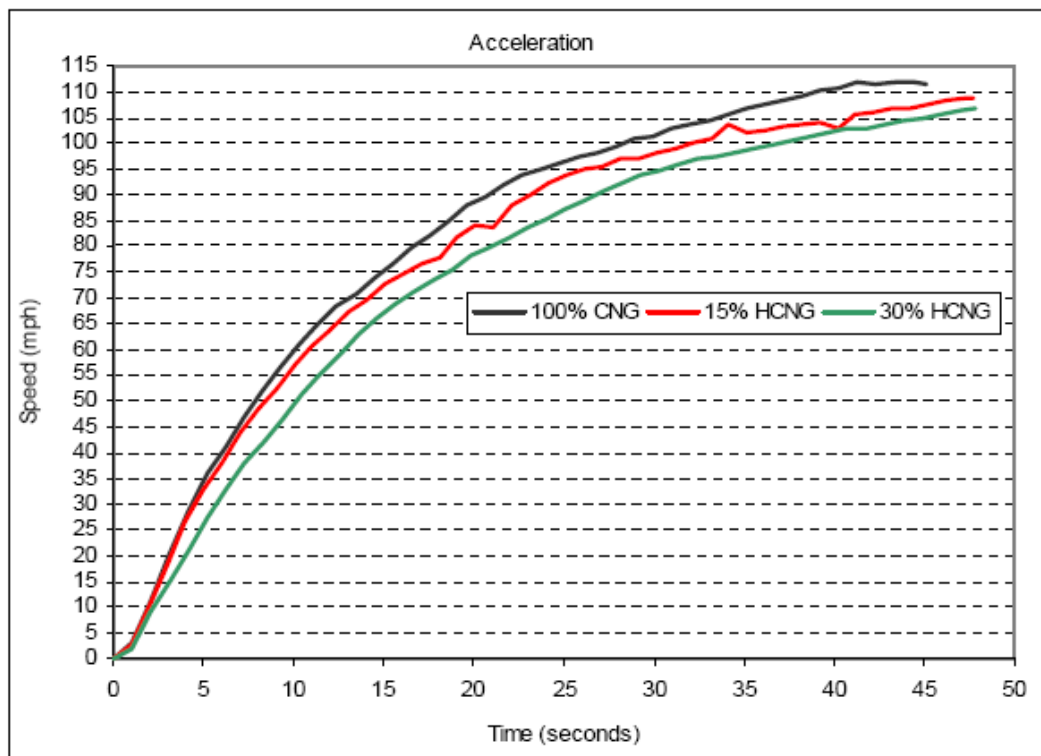


**Figure 2-4 Graph Showing the Time to Accelerate Ford F-150 to 60mph Operating on Various Fuel Blends**

Source: (Karner and Francfort, 2003)

The addition of more hydrogen slowed the acceleration time. But this small decrease in acceleration comes with a decrease in emissions as well, which is usually more important. This decrease in acceleration can be eliminated by either increasing the amount of fuel and air entering the cylinders, or by directly injecting the hydrogen, which will avoid the displacement of air by the hydrogen (Karner and Francfort, 2003).

The range of the F-150 with 100% CNG, 15% hydrogen, and 30% hydrogen was also tested. Tests were performed at a constant speed of 45 mph using a high speed oval track. The vehicle was driven 60 miles on each fuel blend and the amount of fuel used was determined by examining the relationship between pressure, temperature, and mass for each fuel. Table 2-5 shows the fuel economy for each blend of fuel in miles per gallon of gasoline. This allows for an easier comparison of how the blends performed. As can be seen in this table, the range decreased as hydrogen was added. This is due to the lower energy content of hydrogen compared to CNG in terms of volume. The problem with a lower range is the need to then increase fuel storage space. With the test F-150, an additional 14 liter fuel tank would need to be installed in order to have the same range with 30% hydrogen as with 100% CNG (Karner and Francfort, 2003). Even though the range decreased with the addition of hydrogen, the fuel efficiency stayed about the same over all fuel blends.

**Table 2-5 Chart of Fuel Economy and Range for Ford F-150 with Various Fuel Blends**

Source: (Karner and Francfort, 2003)

Fuel Blend	Vehicle Mileage	Fuel Economy (miles/gge)	Range (miles)
CNG	32,465	23.3	122
15% HCNG	31,951	22.6	110
30% HCNG	31,769	23.5	102

### ***K4X Lean Burn***

As stated earlier, there has been some research into hydrogen addition on lean burn stationary engines such as those used in the natural gas industry. Dresser-Rand and the Gas Technology Institute (GTI) evaluated the technical and economic feasibility of using thermochemical recuperation (TCR) to increase efficiency and reduce emissions from pipeline compressor engines (Pratapas et al., 2007).

TCR is a method of generating hydrogen that can be added to the fuel gas for combustion. A simplified schematic is shown in Figure 2-5. The major equipment includes heat exchangers, a recuperative reforming reactor, and a heat recovery steam generator. Here, steam and natural gas are mixed and passed into the reformer. The reformed fuel that is produced inside the reformer contains a percentage of hydrogen, typically as much as 25-30% by volume (Pratapas et al., 2007). Overall, the reforming reactions are endothermic. The heat used to drive the reactions is provided by the hot engine exhaust. The use of this waste heat increases the cycle efficiency.

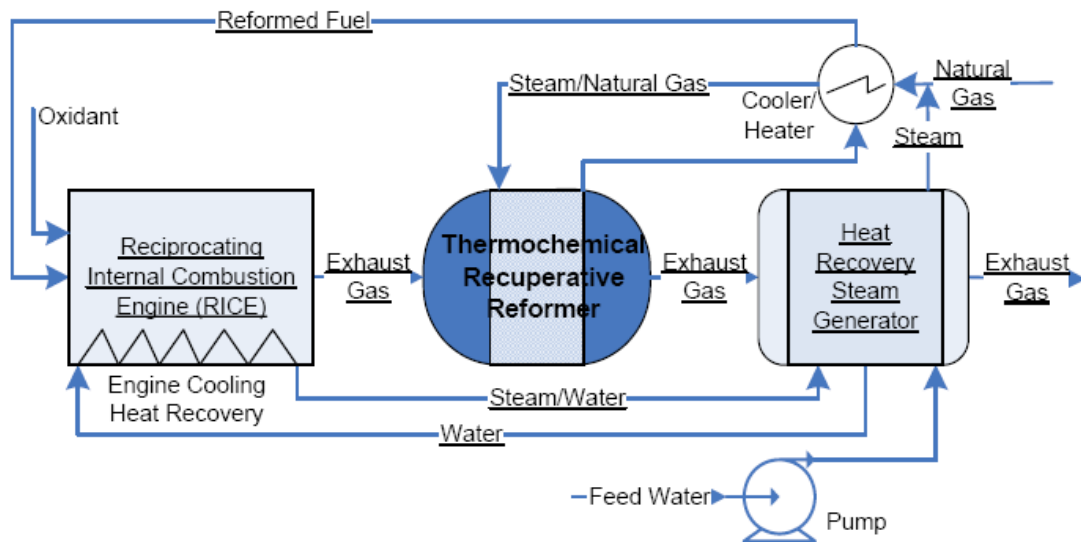


**Figure 2-5 Schematic of Simplified TCR Reformer**

Source: (Pratapas et al., 2007)

Before building a TCR system, it was decided that Dresser-Rand would install a fuel blending system at its engine test facility in Painted Post, NY. The fuel blending system would be capable of simulating the reformed fuel composition expected from the TCR system. The reformed fuel compositions were predicted using CHEMKIN (Pratapas et al., 2007). A K4X test engine was fitted with the fuel blending system. This unit is a lean burn, two cylinder, four stroke cycle engine that develops 750 hp at 350 rpm. It has a 17 inch bore and a 22 inch stroke.

Dresser-Rand designed the fuel blending system, shown in Figure 2-6, to deliver calculated flow rates of H<sub>2</sub>, N<sub>2</sub>, CO, CO<sub>2</sub>, and natural gas to the K4X engine. The fuel was blended continuously with control valves regulating the flow rates of each component in real

time. The required fuel component flows were calculated with the use of CHEMKIN. A 2:1 steam-to-methane molar ratio was used for fuel reforming. The extra steam helped add heat to the reaction and produce more hydrogen. In the TCR process, the hot reformed fuel stream will contain some water vapor. The fuel blending system was designed with the capability of adding steam through a spray bar, however that function was not used in the testing. Assuming that the reformed fuel was cooled to the maximum allowable fuel temperature of 120°F recommended by Dresser-Rand, the moisture content would be about 4% by volume. Dresser-Rand engineers expressed concern that combustion chamber moisture of that amount could cause engine damage and collapsed oil filters on the K4X (Pratapas et al., 2007).



**Figure 2-6 Mixer Hardware Installed at Dresser-Rand**

Source: (Pratapas et al., 2007)

Data was collected for variable air manifold pressures and multiple spark timings. Testing was done with 5%, 15%, and 25% hydrogen blended by volume with natural gas. Tests were also performed with blends of H<sub>2</sub>, N<sub>2</sub>, CO<sub>2</sub>, CO, and natural gas which simulated reformed fuel from the TCR. The engine was also tested with and without a screw-in pre-combustion chamber (PCC) (Pratapas et al., 2007).

Data from the PCC testing showed that combustion stability with hydrogen addition was equivalent to combustion stability when operating on pure natural gas. NO<sub>x</sub> emissions also appeared to be the same with and without hydrogen addition, while CO emissions decreased slightly with hydrogen addition. The explanation offered for the absence of combustion improvement with hydrogen addition is that a PCC operating on pure natural gas supplies sufficient energy to ignite very lean mixtures. Therefore, an engine operating with a PCC does not need hydrogen to extend its lean limit (Pratapas et al., 2007). Other literature dealing with hydrogen addition to lean burn engines do not include PCC testing, so other data is not available to compare these results. The addition of the other gases that simulated reformed fuel did not appear to have a significant impact on engine performance or emissions.

With the engine in non-PCC configuration, data showed it was possible to reach NO<sub>x</sub> levels as low as what is currently achievable with PCC technology. A decrease in misfires was found with volume percentages of hydrogen above 5%. When air manifold pressure was increased from 20 psig to 23 psig, an increase in misfires was observed. This increase was eliminated by the addition of 25% hydrogen. Hydrogen addition worked for all spark timings tested and showed improvement in combustion stability and a decrease in NO<sub>x</sub>. No combustion knock problems were experienced with mixtures of 25% or less hydrogen by volume (Pratapas et al., 2007). Just as with the PCC configuration, the addition of other gases to simulate the reformed fuel did not have a significant impact on engine performance or emissions. Changing the hydrogen content of the fuel had the most impact.

While further testing is desired by GTI and Dresser-Rand, the results from this testing show that operating a large bore, slow speed, lean burn, natural gas fueled engine with hydrogen addition is possible and produces positive results. Generally, hydrogen rich gas mixtures have a tendency to promote engine knock. However, during the course of this blended fuel testing, the K4X engine did not experience abnormal knock (Pratapas et al., 2007).

In another project, GTI prepared a detailed cost estimate of TCR for a Cummins QSK60G engine. The installed cost of a recuperative reformer was estimated to be \$168,000 (\$42/hp). Depending on the brake thermal efficiency of the engine (assumed to be between 33% and 37%), the cost of natural gas (assumed to be between \$6 and \$7 per MMBtu), and the relative efficiency gain with TCR (assumed to be 5%), the calculated payback period was estimated to range from 2.4 to 3.5 years (Pratapas et al., 2007).

### **Pre-Combustion Chambers**

When igniting very lean fuel-air mixtures, much more energy has to be supplied. Additionally, because of non-homogeneous mixing, it becomes less likely that an ignitable and sustainable mixture of air and fuel will be present near the spark plug at the time of ignition. This is especially the case with two-stroke engines. Multi-spark ignition systems have been developed that can effectively ignite lean mixtures. However, these systems do not provide enough energy when extremely lean mixtures are used (Kidder and Potter, 2002).

The purpose of a pre-combustion chamber is to produce a large amount of ignition energy to ignite a lean mixture of fuel and air. Pre-combustion chambers provide several orders of magnitude more energy than standard multi-spark ignition systems (Haimov et al., 1998). It does this by providing an additional volume where a near-stoichiometric mixture is created. A small amount of fuel is added to the pre-combustion chamber and air is forced in during compression. The spark plug in the pre-combustion chamber ignites this near-stoichiometric mixture, and a large flame is expelled into the engine cylinder. This large flame ignites the lean mixture in the cylinder. It also has a larger surface area and penetration than the flame produced from spark ignition. This provides a more rapid and complete combustion of the lean mixture in the cylinder (Kidder and Potter, 2002). Most pre-combustion chambers screw into an existing spark plug hole and require a fuel line as well as two lines for cooling, making installation simple. Some models require a separate hole in the cylinder head and require no external lines for cooling. These models may require the use of a new cylinder head.

Pre-combustion chambers allow for leaner engine operation and reduced emissions. However, since the combustion in the pre-combustion chamber is near-stoichiometric, a large amount of  $\text{NO}_x$  is formed. Amounts of  $\text{NO}_x$  formed in the pre-combustion chamber can be a large percentage of the overall  $\text{NO}_x$  emission from the engine. Since hydrogen can lower  $\text{NO}_x$

production, even in rich mixtures, the pre-combustion chamber may benefit from a blended fuel. Using a blended fuel in only the pre-combustion chamber has the possibility of lowering engine  $\text{NO}_x$  levels further while consuming a smaller quantity of hydrogen. As will be discussed next, having hydrogen on-site can be difficult. Reducing hydrogen consumption not only reduces the amount required on-site at any given time, but also decreases the size and complexity of a fuel blending system.

## **Methods of Hydrogen Generation**

To operate an engine on a mixture of hydrogen and methane requires both substances to be present. E&P engines are in remote locations. Natural gas is present for a fuel, but hydrogen is not. To mix hydrogen for these engines would require either hydrogen being physically delivered to the site or some type of piping system being built. Many of these engines are not visited regularly, so physical delivery of hydrogen would be difficult. The molecules of hydrogen are smaller than all other gases, so it can diffuse through many materials that are considered to be airtight or impermeable to other gases.

Constant exposure to hydrogen can cause hydrogen embrittlement in many materials. The embrittlement can lead to leakages or even catastrophic failures in not only metals, but some non-metals as well. The mechanisms that cause hydrogen embrittlement are not well known, but some factors that influence its rate and severity are. These factors include the hydrogen concentration, hydrogen pressure, temperature, stress level, stress rate, stress cycles, metal composition, microstructure, and heat treatment history. Moisture content within the hydrogen gas may also lead to hydrogen embrittlement since it accelerates the formation of fatigue cracks (Department of Energy, 2001a). Hydrogen storage containers and pipelines would have to be constantly checked for damage.

Hydrogen is also difficult to compress since the molecule is so small. This, and the fact that there is not a hydrogen distribution system in place, makes piping hydrogen to the engine site very difficult. The best way to get hydrogen on-site is to produce it there. There is more than one way to produce hydrogen. All of the processes are based on the separation of hydrogen from a hydrogen-containing feedstock. Depending on what feedstock is used, the appropriate extraction method can be obtained.

## *Steam Methane Reforming*

Currently, about 95% of the hydrogen produced in the United States uses a thermal process called steam methane reformation (SMR). This process uses high temperature steam (1300-1450°F) to produce hydrogen from a methane source, which is usually natural gas. It is very similar to the TCR process discussed earlier. The difference is that TCR uses heat recovered from the exhaust stream of the engine, while SMR uses an external burner.

There are two primary steps to the process. In the first step, the methane reacts with steam under 3-25 bar pressure (1 bar = 14.5 psi) in the presence of a catalyst to produce hydrogen, carbon monoxide, and a relatively small amount of carbon dioxide. The reaction is shown in Equation (2.12). The catalyst is usually a nickel on alumina material (Epperly, 2004). SMR is highly endothermic, so heat must be supplied to the process for the reaction to proceed. This is where the difference in TCR and SMR shows up. TCR performs basically the first step of the SMR process. The temperature the catalyst needs to be maintained at is at the high end of the expected exhaust temperature of a lean burn engine. Since the reactions are endothermic, and high temperature steam has to be produced from the exhaust stream as well as heating the catalyst, the reactions take place at lower temperatures in TCR than in SMR. This results in lower amounts of hydrogen in the reformed fuel and more natural gas that passes through the catalyst un-reacted in TCR than SMR.



The second step involves a water-gas shift reaction. Here, the carbon monoxide produced in the first reaction is reacted with steam over a catalyst. The reaction is shown in Equation (2.13). First, there is a high temperature shift (HTS) at 660°F and then a lower temperature shift (LTS) at 370-410°F (Padro et al., 2003). This produces carbon dioxide and more hydrogen and eliminates most of the carbon monoxide produced in the first step.



If very pure hydrogen is needed, a third step can be performed involving pressure-swing absorption. This removes carbon dioxide and other impurities from the gas stream and leaves essentially pure hydrogen. SMR can be performed with other fuels such as ethanol, propane, or

even gasoline (Department of Energy, 2006). For the needs of this research, natural gas will be concentrated on since it is already on-site. Figure 2-7 shows the entire SMR process.

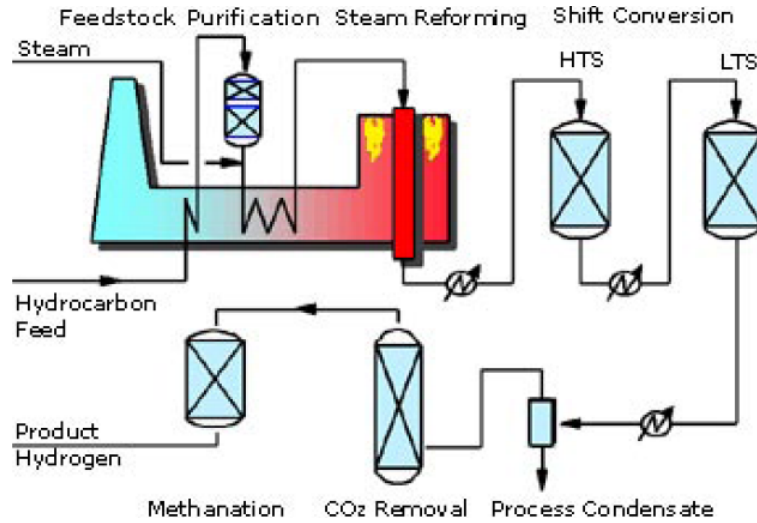


**Figure 2-7 Steam Methane Reforming Process**

Source: (Padro et al., 2003)

### *Partial Oxidation*

Hydrogen can also be produced by partial oxidation. With this method, natural gas is reacted with a limited amount of oxygen that is not enough to completely oxidize the hydrocarbons to carbon dioxide and water. Since there is less than the stoichiometric amount of oxygen available, the reaction products contain primarily hydrogen and carbon monoxide. The reaction is shown in Equation (2.14).



If air is used instead of pure oxygen, nitrogen is found in the products as well. These products are then turned into carbon dioxide and more hydrogen by a water-gas shift reaction as shown in Equation (2.15).



Unlike SMR, partial oxidation is an exothermic process. It is, typically, a much faster process than SMR and requires a smaller reactor vessel (Department of Energy, 2006). Often, downstream equipment is necessary to remove the large amount of heat generated by the

reactions, remove CO<sub>2</sub>, and purify the hydrogen (Epperly, 2004). It can be seen from the equations that this process produces less hydrogen in the first step than the SMR process.

### ***Autothermal Reforming***

As stated earlier, SMR is highly endothermic. To deal with this, an external source must supply the heat input required. Autothermal reforming (ATR) combines the exothermic partial oxidation process with the endothermic SMR process to form hydrogen. Truly autothermal reforming exactly balances the heat flow into and out of the reactor. If extra heat is needed, a burner or some other heat source can be added. These systems can be very productive, fast starting, and compact (Adamson, 2006). ATR reactors often consist of a ceramic-lined reactor that allows the heat from the partial oxidation reaction to be carried downstream into the SMR zone by the reaction gas mixture. This provides the heat necessary for the endothermic SMR reactions.

### ***Exhaust Gas Fuel Reforming***

Another way of producing hydrogen is through exhaust gas fuel reformation. This application is well suited for use on engines and involves the reaction of engine exhaust gas with hydrocarbon fuel to produce hydrogen rich gas. This gas can then be returned to the engine as fuel. Figure 2-8 shows one way an exhaust gas fuel reformer system may be set up. This is called reformed exhaust gas recirculation. It not only re-circulates the combustion products like normal exhaust gas recirculation, but it also contains hydrogen to further reduce emissions. This process works because the exhaust gas supplies oxygen and steam at high temperatures. This is similar to the ATR process described above because the hydrocarbon fuel is reacted with both steam and air (oxygen) to produce hydrogen. Exhaust gas fuel reforming uses the partial oxidation reactions as well as steam reforming reactions and water-gas shift reactions. The overall process is endothermic, and the required additional heat is supplied directly from the exhaust gases. At low temperatures (570°F), relatively low hydrogen content (less than 20% of the volume) is expected in the reformed gas (Yap et al., 2005).

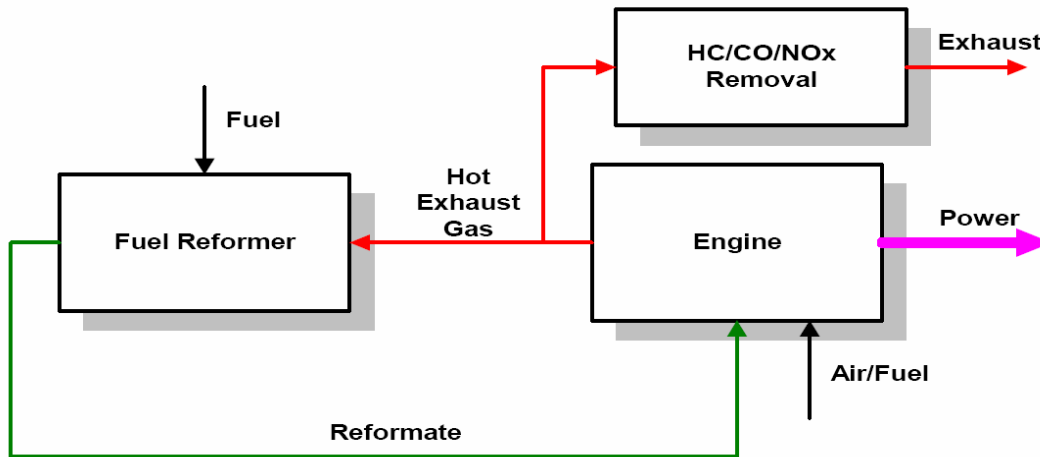
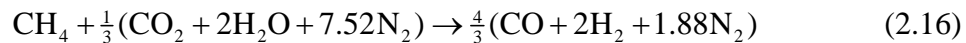


**Figure 2-8 Example of Engine-Reformer System**

Source: (Wyszynski et al., 2000)

Assuming stoichiometric combustion, the equation for exhaust gas reforming of methane is:



Combustion of the reformed fuel is then done through:



Theoretical and practical research into exhaust gas reforming of hydrocarbon fuels has been conducted at The University of Birmingham. This research has shown that the temperature of the exhaust gas at the inlet to the reactor has significant effects on the reforming process. Lower exhaust temperatures lead to the formation of carbon solids and to low reforming efficiencies. To achieve high amounts of hydrogen in the reformed gas, The University of Birmingham recommends supplying the reactor with exhaust gas at 1470°F (Jamal et al., 1996). This high temperature may be possible at high engine load. With exhaust temperatures between 1470-1560°F, it is possible to obtain high hydrogen yields (30% in reformed gas). At lower temperatures, usually 950-1300°F, up to 20% hydrogen in the reformed gas is predicted. These temperatures should be possible even at part load conditions. One way to elevate the temperature at part load conditions is to increase the air-to-fuel ratio. With more oxygen in the exhaust gas, a lower temperature can be used since more heat will be generated by the partial oxidation reactions (Wyszynski et al., 2000). The temperature of the exhaust gas at the inlet to

the reactor is not the only factor that affects the quality and quantity of the reformed fuel. Figure 2-9 shows some other factors that should be taken into account.

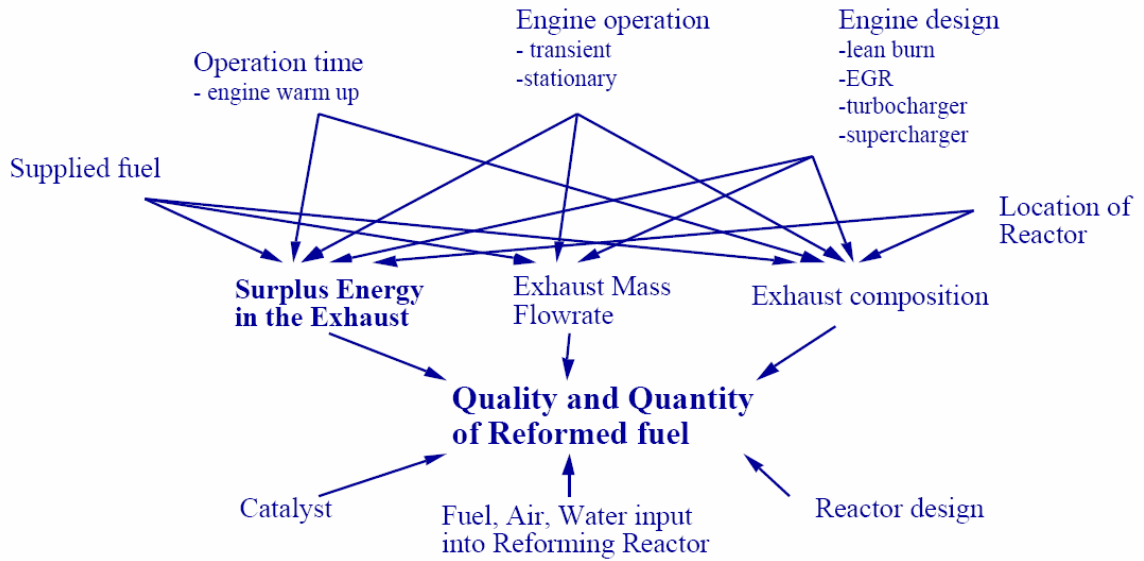


**Figure 2-9 Parameters Affecting the Quality and Quantity of Reformed Fuel**

Source: (Wyszynski et al., 2000)

The University of Birmingham has used a modified single cylinder, spark ignited engine to experiment with exhaust gas fuel reforming. The engine is a Medusa single cylinder with a bore of 3.15 in. and a stroke of 3.5 in. The compression ratio was raised from 10.5 to 15 to operate the engine with homogeneous charge compression ignition (HCCI). The engine throttle was kept wide open throughout the tests and the inlet airflow was constant. All the tests were performed at 1,500 rpm and the engine load was varied by fuel settings. Since HCCI requires high temperatures for ignition with methane fuel, a 3 kW electric air heater was installed in the intake duct. A mini reactor was used to reform the exhaust gas. The flows of exhaust gas, natural gas, and air into the reactor were controlled and a furnace was used to control the temperature of the reactor. The reactor itself was a 1 in. diameter stainless steel tube loaded with two monolith catalysts of 2.56 in. and 2.95 in. long by 0.98 in. diameter. Thermocouples monitored the temperature of the catalysts. After some initial trials with the reactor, pure methane was used instead of natural gas because sulfur in the natural gas was damaging the catalysts. The hydrogen and methane contents of the reformed gas were measured with a gas

chromatograph. Reformed gas flow back into the engine was kept at 5% of the intake air volume (Yap et al., 2005).

The tests performed with this engine showed, as expected, that the exhaust gas composition changed with engine load. As a result, the reactor formed varying concentrations of products in the reformed gas. A constant amount of hydrogen in the reformed gas was desired to maintain combustion stability (Yap et al., 2005). Varying the air, methane, and exhaust gas supplied to the reactor was proposed to maintain a constant amount of hydrogen formation. For these tests, 10% hydrogen was desired. To obtain this, air, methane, and exhaust gas were supplied to the reactor to keep the  $O_2/CH_4$  molar ratio between 0.59 and 0.68 and the  $H_2O/CH_4$  molar ratio between 0.26 and 0.33. The results showed that hydrogen addition to the intake air increased the start of combustion. HCCI operation requires high intake temperatures to initiate combustion, however now the temperature could be lowered.  $NO_x$  emissions were shown to decrease while CO and hydrocarbon emissions increased. Finally, no increase in fuel consumption was observed by using exhaust gas reformation (Yap et al., 2005).

### ***Partial Oxidation vs. Steam Methane Reforming***

While there are many different ways to produce hydrogen on-site, not all are ideal. For the engines operated in the gas industry, a simple, relatively low maintenance method would be best. After looking at the above methods, partial oxidation and steam methane reforming are the best candidates for gas industry applications. They are the simplest methods, and are not extremely sensitive to system changes. The other methods would most likely involve a complicated control system and significant operator attention.

Both methods are dangerous. Partial oxidation is more dangerous because the fuel and oxygen are mixed together at high temperatures. If the flammability range is reached, the mixture could ignite. With SMR, the danger is a leak in the reactor vessel. Since the leak would be a stream of primarily hydrogen in an oxygen rich environment at high temperatures, a flame could start. SMR requires more catalyst surface area because of a longer residence time. Partial oxidation has a short residence time, and thus requires less catalyst. However, the partial oxidation catalyst is more expensive than the one required for SMR. SMR would require water to be delivered in the field, while partial oxidation would only require air. The endothermic SMR process would also require an energy source, perhaps electricity. The exothermic partial

oxidation process requires some energy to start, but once started, requires no external energy source.

Picking the right method would require further research and testing. Experimental setups, as well as modeling, would most likely be involved. Perhaps one method would work better on certain engines while the other is better suited for others.

## **Major Findings**

After reviewing the literature, it was found that meeting emissions regulations is a challenge. The EPA is continually lowering emissions limits, and is now regulating engines that were previously exempt. Many factors in the combustion process were found to influence the formation of emissions. These factors include combustion stability, equivalence ratio, peak in-cylinder temperature, and the duration at this peak temperature.  $\text{NO}_x$  formation is especially sensitive to this peak in-cylinder temperature. Hydrogen's properties are suitable for blending with natural gas and lowering emissions. These are primarily its low ignition energy, high diffusivity, and fast flame speed. There are experimental results from various researchers that show hydrogen addition to natural gas does lower emissions both in four and two stroke cycle engines. These researchers also found that hydrogen has limitations. With stoichiometric mixtures, power can decrease with hydrogen addition. Also, due to its low ignition energy, hydrogen blended fuels can be susceptible to pre-ignition. With lean burn engines, pre-combustion chambers can create a large percentage of the overall engine  $\text{NO}_x$  due to their near stoichiometric mixture. Because of hydrogen's ability to lower  $\text{NO}_x$  and its fast flame speed, PCCs may benefit from a blended fuel. Since many of the engines used in the industry are located in remote locations, hydrogen may need to be generated on-site. Looking at various hydrogen production methods, it was found that the first stage in SMR and partial oxidation could be performed to produce hydrogen on site. From the research conducted in the literature review, it was concluded that further experimental testing was a viable next step.

## CHAPTER 3 - Governing Equations

In order to investigate the impact of hydrogen blended fuels, various parameters needed to be calculated. Since experimental research results in raw data, equations had to be defined to turn this raw data into a parameter of use, such as horsepower or mass flow rate. The following sections describe parameters of interest, and how they must be calculated if experimental data is present.

### Brake Horsepower

The brake power is calculated from the engine speed and torque. It is used in many other calculations such as brake specific emissions, and brake specific fuel consumption. Knowing the engine speed and load, Equation (3.1) calculates the brake horsepower (Ferguson and Kirkpatrick, 2001).

$$\dot{W}_b [\text{hp}] = \frac{\tau [\text{lb}_f] N [\text{rpm}]}{5252} \quad (3.1)$$

### Mass Flow Rate of Fuel

The mass flow rate of fuel is necessary when determining engine efficiency parameters such as brake specific fuel consumption. Since it is difficult to measure mass flow rate directly, measurements can be used in combination with equations to calculate the mass flow rate. In general, mass flow rate is given by (Moran and Shapiro, 2004) as:

$$\dot{m} = \rho AV \quad (3.2)$$

In the above equation, the velocity ( $V$ ) can be difficult to determine directly in experimental setups. It is convenient to utilize Bernoulli's equation with an orifice plate to solve this problem. An orifice plate is essentially a restriction in the flow that causes a pressure drop as shown in Figure 3-1.

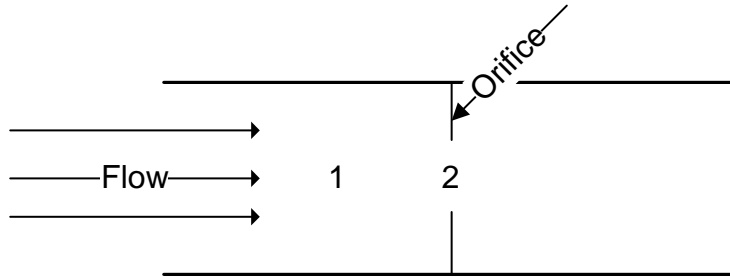


**Figure 3-1 Orifice Plate in a Pipe**

By using upstream and downstream pressure sensors, or a differential pressure sensor, this pressure drop can be measured. Assuming constant density and no significant change in potential energy, Bernoulli's equation from (Crowe et al., 2005) becomes:

$$\Delta p = \frac{1}{2} \rho (V_2^2 - V_1^2) \quad (3.3)$$

Solving Equation (3.2) for  $V$ , and substituting it into Equation (3.3), gives:

$$\dot{m} = \frac{A_2 \sqrt{2\rho\Delta p}}{\sqrt{1 - \left(\frac{A_2}{A_1}\right)^2}} \quad (3.4)$$

Defining  $\beta$  as the ratio of the diameters in area one and two, plugging in the area formula for a circle, and reducing, gives:

$$\dot{m} = \frac{\pi}{4} d_2^2 \frac{\sqrt{2\rho\Delta p}}{\sqrt{1 - \beta^4}} \quad (3.5)$$

This now gives the theoretical mass flow rate based on diameters, density, and a differential pressure. To improve the accuracy of this measurement, a coefficient of discharge ( $C_d$ ) and a combined thermal expansion factor ( $F_a$ ) are introduced. These coefficients are determined experimentally and provided by the manufacturer of the orifice plate. Another coefficient, the gas expansion coefficient, is calculated from:

$$Y = 1 - \left(0.41 + 0.35\beta^4\right) \frac{\Delta p}{p \frac{c_p}{c_v}} \quad (3.6)$$

Finally, the actual mass flow rate is calculated as given by (Crowe et al., 2005) as:

$$\dot{m} = C_d F_a Y \frac{\frac{\pi}{4} d_2^2 \sqrt{2\rho\Delta p}}{\sqrt{1-\beta^4}} \quad (3.7)$$

The density of the fuel is calculated from the ideal gas model as:

$$\rho = \frac{p}{\frac{R_u}{M} T} \quad (3.8)$$

Equation (3.7) contains coefficients supplied by the manufacture, measured density, and a measured differential pressure. The required measurements are made in an experimental setup. The experimentally determined coefficients ensure reliable calculations.

## Fuel Blending Calculations

Not only did a physical system need to be built to blend the fuel, but calculations needed to be performed to ensure the proper amounts of hydrogen and natural gas were blended. The gas models used needed to be accurate for the test conditions. When blending mixtures of gases, there are different methods that can be used. The simplest approach is to treat the mixture as an ideal gas. Ideal gas mixtures consist of two or more gases whose molecules are not affecting each other.

To check the validity of the ideal gas approximation in this research, mixture final pressures and partial pressures were calculated using the ideal gas equation of state, as well as the van der Waals equation of state. The results of the two models were then compared. All calculations were done assuming natural gas was added to the tank first, and then hydrogen was added to complete the mixture.

Treating the mixture as a real gas, the van der Waals equation of state, Equation (3.9) was used in place of the ideal gas equation of state. Van der Waals noted that gas molecules actually occupy more than the negligibly small volume presumed by the ideal gas model and also exert attractive forces on one another (Moran and Shapiro, 2004).

$$p = \frac{R_u T}{\bar{v} - b} - \frac{a}{\bar{v}^2} \quad (3.9)$$

The constant  $b$  is intended to account for the finite volume occupied by the molecules and the term  $\frac{a}{\bar{v}^2}$  accounts for the forces of attraction between molecules. It is interesting to note that if  $a$  and  $b$  are set to zero, the ideal gas equation results. Values for constants  $a$  and  $b$  are found from:

$$a = \frac{27}{64} \frac{R_u^2 T_c^2}{p_c} \quad (3.10)$$

$$b = \frac{R_u T_c}{8 p_c} \quad (3.11)$$

When performing the real gas model calculations for the mixture, the constants  $a$  and  $b$  were first calculated for both hydrogen and natural gas. Then, the moles of natural gas were calculated by specifying a pressure for the natural gas, calculating the molar specific volume, and then calculating the number of moles by multiplying by the known tank volume as shown in Equation (3.12). To stay consistent, the specified pressure ( $p_N$ ) corresponds to the partial pressure of natural gas used in the ideal gas model.

$$p_N = \frac{R_u T}{\bar{v}_N - b_N} - \frac{a_N}{\bar{v}_N^2} \rightarrow \bar{v}_N \quad (3.12)$$

$$N_N = \bar{v}_N V_{Tank}$$

With the number of natural gas moles known, hydrogen can be added. By specifying the molar percentage of hydrogen desired in the mixture, the number of hydrogen moles that need to be added to the tank is calculated by (Moran and Shapiro, 2004) as:

$$y_H = \frac{n_H}{n_H + n_N} \rightarrow n_H \quad (3.13)$$

Now, the mixture constants  $a$  and  $b$  are calculated with:

$$a_{Mix} = y_H a_H + y_N a_N \quad (3.14)$$

$$b_{Mix} = y_H b_H + y_N b_N \quad (3.15)$$

Finally, the mixture pressure is calculated using:

$$P_{Mix} = \frac{R_u T}{\frac{V_{Tank}}{n_H + n_N} - b_{Mix}} - \frac{a_{Mix}}{\left(\frac{V_{Tank}}{n_H + n_N}\right)^2} \quad (3.16)$$

As a further check, the compressibility factor of the mixture as given by (Moran and Shapiro, 2004), is found from values obtained with the real gas model through:

$$Z = \frac{P\bar{v}}{R_u T} \quad (3.17)$$

A compressibility factor near one indicates the mixture can be treated as an ideal gas.

Appendix A shows an example calculation for the real gas model described above. After the calculations were performed with the real gas model, the mixture was treated as ideal to compare the results. The ideal gas model is described next.

In an ideal gas, the actual pressure ( $p$ ) is small relative to the critical pressure ( $p_c$ ), and/or the actual temperature ( $T$ ) is large relative to the critical temperature ( $T_c$ ). These factors are used to calculate the reduced pressure ( $p_R$ ) and temperature ( $T_R$ ) (Moran and Shapiro, 2004).

$$p_R = \frac{P}{p_c} \quad (3.18)$$

$$T_R = \frac{T}{T_c} \quad (3.19)$$

With the reduced pressure and temperature, a compressibility factor ( $Z$ ) can be determined for a component using a compressibility chart. Again, if  $Z$  is near one, a gas can be treated as ideal.

The critical pressure is 673 psia for natural gas and 188.1 psia for hydrogen. The critical temperature is 344°R for natural gas and 59.8°R for hydrogen (Moran and Shapiro, 2004).

When working with an ideal gas mixture, Kay's rule can be used to determine a mole fraction ( $y_i$ ) averaged critical temperature and critical pressure. Equations (3.20) and (3.21) show Kay's rule to find a mixture critical pressure and temperature of  $j$  components (Moran and Shapiro, 2004).

$$T_c = \sum_{i=1}^j y_i T_{c,i} \quad (3.20)$$

$$p_c = \sum_{i=1}^j y_i p_{c,i} \quad (3.21)$$

The mixture critical pressure and temperature from Kay's rule can then be used in Equations (3.18) and (3.19) to find a mixture reduced pressure and temperature. The values obtained are then used in conjunction with a compressibility chart to determine the mixture compressibility factor. Assuming an actual temperature and pressure of 540°R and 200 psia, respectively, the compressibility factors of hydrogen and natural gas mixtures are near one, indicating an ideal gas. Appendix B shows the compressibility factors for hydrogen and natural gas mixtures with varying volumetric percentages of hydrogen.

To calculate mixture pressures assuming an ideal gas, the Dalton model was used. This model is consistent with the concept of an ideal gas being made up of molecules that exert negligible forces on each other and whose volume is negligible relative to the volume occupied by the gas. Due to the negligible intermolecular forces and small fraction of volume taken up by each molecule, the Dalton model assumes that each mixture component behaves as an ideal gas as if it were alone at the temperature and volume of the mixture. This means that the individual components do not exert the mixture pressure but rather a partial pressure. The sum of all these partial pressures would be the mixture pressure. The partial pressure ( $p_i$ ) of component  $i$  is the pressure that  $n_i$  moles of component  $i$  would exert if the component were all alone in the volume ( $\mathcal{V}$ ) at the mixture temperature and can be evaluated using the ideal gas equation of state from (Moran and Shapiro, 2004):

$$p_i = \frac{n_i R_u T}{\mathcal{V}} \quad (3.22)$$

Since the molar percentage ( $y_i$ ) of component  $i$  is the moles of that component divided by the total moles in the mixture, and using the ideal gas law, the following can be derived.

$$\frac{p_i}{p} = \frac{\frac{n_i R_u T}{\mathcal{V}}}{\frac{n R_u T}{\mathcal{V}}} = \frac{n_i}{n} = y_i \quad (3.23)$$

The mixture temperature ( $T$ ), volume ( $\mathcal{V}$ ), and universal gas constant ( $R_u$ ) are the same for each component as well as the mixture. The partial pressures in an ideal gas mixture are calculated by:

$$p_i = y_i P \quad (3.24)$$

It is important to realize that the pressures used in these calculations need to be absolute. This means that pressure readings from the tank gage need to have the atmospheric pressure added to them before they are used in the formulas. Failure to do this would result in improper fuel mixtures. For the testing done here, the final mixture pressure was fixed to ensure sufficient fuel was available in the blending chamber for at least 30 minutes of test time. This mixture pressure turned out to be approximately 180 psig. Again, this is a gage pressure, and is adjusted based on the atmospheric pressure during blending. For the comparison calculations, a fixed mixture pressure of 200 psia was used.

Comparing the mixture pressure calculated from Equation (3.16), derived using the real gas model, to the fixed final mixture pressure used in the ideal gas model will determine if the gas mixture can be treated as ideal with little uncertainty. Looking at Table 3-1, the final mixture pressure calculated with the real gas model is within 0.3% of the final mixture pressure used in the ideal gas model. This shows that treating the mixture as an ideal gas is a valid assumption. The compressibility factor calculated from van der Waals equation is also near one.

**Table 3-1 Real Gas and Ideal Gas Mixture Pressures**

		Percent Hydrogen by Volume		
		10%	20%	30%
<b>Pre-Charge Pressure of Natural Gas (psia)</b>	<b>Ideal Gas</b>	180	160	140
	<b>Real Gas</b>	180	160	140
<b>Final Mixture Pressure (psia)</b>	<b>Ideal Gas</b>	200	200	200
	<b>Real Gas</b>	200.208	200.412	200.611
<b>Real Gas Z based on van der Waals</b>		0.976	0.980	0.984
<b>Molar Specific Volume based on van der Waals (ft<sup>3</sup>/lbmol)</b>		28.24	28.32	28.40

After completing the above checks, the gas mixture for this research was treated as ideal. Because of this, the mixing process can be performed based on the Dalton model. With the final mixture pressure ( $p$ ) and molar percentages of each component ( $y_i$ ) known, the partial pressure of

each component ( $p_i$ ) was calculated. The blending chamber started with pure natural gas at atmospheric conditions. Next, the partial pressure of hydrogen was calculated based on the final mixture pressure and the desired molar percentage of hydrogen. Hydrogen was then admitted to the blending chamber until the appropriate gage pressure was reached. Next, compressed natural gas was admitted into the blending chamber until the final mixture gage pressure was reached. This produced the desired blend of fuel. Again, the pressures used in the calculations were absolute pressures based on the current atmospheric conditions. Appendix C shows sample calculations for blending fuel.

### **Accounting for Hydrogen Addition**

As just discussed, the mixture of hydrogen and natural gas can be treated as ideal for the conditions of this research. In many calculations, such as brake specific fuel consumption and fuel density, it is necessary to know properties of the fuel. These properties, such as heating values and molecular weights, will vary as hydrogen is added. For ideal, non-reacting gas mixtures, the following from (Moran and Shapiro, 2004) can be applied where the desired molar property is  $\bar{x}$  :

$$\bar{x} = \sum_{i=1}^j y_i \bar{x}_i \quad (3.25)$$

These values can be converted from a molar basis to a mass basis as follows:

$$\bar{x} = Mx \quad (3.26)$$

### **Measures of Efficiency**

The brake specific fuel consumption (*BSFC*) is a measure of the quantity of fuel required to produce a unit of power. This is a measure of engine efficiency, and is more meaningful than looking at fuel flow or brake horsepower alone. It can be calculated after brake horsepower and fuel flow rate are found (Heywood, 1988). In the natural gas industry, it is common practice to include the lower heating value of the fuel in the calculation to take the properties of the fuel into account. For this research, the lower heating value of the fuel, after being corrected for hydrogen addition, was included in the calculation as shown in Equation (3.27). The volumetric flow rate at standard conditions was also used instead of the mass flow rate. While this equation is

different than that normally seen, it is common in the gas industry and necessary when comparing with data from other engines. Equation (3.27) will have units of Btu/hp-hr.

$$BSFC = \frac{\dot{V}_{fuel,st} \times LHV}{\dot{W}_b} \quad (3.27)$$

### Equivalence Ratio

Calculating the equivalence ratio on a two stroke cycle engine is no easy task. The difficulty comes from scavenging where the fresh intake charge mixes to some degree with the exhaust. Because of the pressure gradient across the engine, the inflowing air continues to mix with the residual exhaust, and a mixture of exhaust and air flows out of the exhaust port. Consequently, the trapped charge is a mixture of air and residual exhaust products. With four stroke cycle engines, it is possible to calculate equivalence ratio based on exhaust emissions. With two stroke cycle engines, due to scavenging, a portion of the incoming air does not take part in combustion. Even if the mass flow rate of fuel and air is precisely measured, the trapped equivalence ratio would not be known. In two stroke cycle engines, the actual trapped equivalence ratio is not known. For this research, an industry accepted method of calculating trapped equivalence ratio was used. The trapped equivalence ratio was calculated by dividing the stoichiometric air-to-fuel ratio by the trapped air-to-fuel ratio. The stoichiometric air-to-fuel ratio was corrected for hydrogen addition by balancing the stoichiometric combustion equation from (Ferguson and Kirkpatrick, 2001).



The subscripts  $x$  and  $y$  are found from a mole balance on the natural gas composition provided by the local gas company's gas analysis. If  $a$  and  $b$  are mole fractions, the stoichiometric air-to-fuel ratio becomes:

$$AF_{stoich} = 4.76 \left( bx + \frac{a}{2} + \frac{by}{4} \right) \left( \frac{M_{air}}{M_{fuel}} \right) \quad (3.29)$$

The actual air-to-fuel ratio was calculated using the mass of air trapped in the cylinder divided by the amount of fuel trapped in the cylinder. The mass of trapped air was calculated by

using the in-cylinder pressure and cylinder volume when the exhaust ports closed along with the intake temperature as follows:

$$m_{tr} = \frac{pV_{tr}M_{air}}{R_u T_{amb}} \quad (3.30)$$

Equation (3.30) assumes that there is only air in the cylinder at the ambient temperature. Actually, a mixture of air and exhaust will be present and the temperature will be increased due to heat transfer from the cylinder surfaces. Again, this is just an industry accepted approximation. The mass of trapped fuel was calculated by dividing the mass flow rate by the cycles per second, which is the engine speed divided by 60.

$$m_{fuel} = \frac{\dot{m}_{fuel}}{N/60} \quad (3.31)$$

The actual air to fuel ratio is calculated by:

$$AF_{tr} = \frac{m_{tr}}{m_{fuel}} \quad (3.32)$$

Finally, the trapped equivalence ratio is calculated as discussed in the literature review by:

$$\phi_{tr} = \frac{AF_{stoich}}{AF} \quad (3.33)$$

## Delivery Ratio

When dealing with two stroke cycle engines, the delivery ratio ( $DR$ ) is a parameter that indicates the amount of fresh intake charge that is passed through the exhaust. The  $DR$ , as describe in (Heywood, 1988), is:

$$DR = \frac{\dot{m}_{total}}{m_{tr}N} = \frac{\dot{m}_{exhaust} - \dot{m}_{fuel}}{\dot{m}_{tr}} \quad (3.34)$$

In two stroke cycle engines, scavenging occurs where the fresh intake charge displaces the burned gases. During the process, some of the fresh intake charge is expelled into the exhaust stream. This results in fresh intake charge diluting the exhaust stream. Large  $DR$  values

indicate large amounts of intake charge in the exhaust stream, while small  $DR$  values indicate minimal intake charge escaping into the exhaust.  $DR$  values vary from engine to engine. Values of 1.4 to 2 are common, but can be higher depending on the engine. Just as with the trapped equivalence ratio, calculating the trapped air mass is only an estimate.

Measuring the true exhaust temperature is also complicated due to scavenging. Typically, exhaust temperature is measured by a thermocouple in the exhaust stream near the engine. Scavenging causes lower temperature intake charge to pass this thermocouple lowering the measured exhaust temperature. Because of this, ambient temperature can influence the exhaust temperature of two stroke cycle engines especially with high  $DR$  values. A method of calculating exhaust temperature by removing ambient temperature affects utilizes the  $DR$ . This method assumes that the measured exhaust temperature is a combination of the true exhaust temperature and the ambient temperature. The mass flow rates of trapped intake charge, intake air that slips into the exhaust during scavenging, and engine exhaust are used to weight the temperatures as follows:

$$T_{measured} = \frac{\dot{m}_r T_{exhaust} + \dot{m}_{air,slip} T_{amb}}{\dot{m}_{exhaust} - \dot{m}_{fuel}} \quad (3.35)$$

Using the  $DR$  definition of Equation (3.34), Equation (3.35) becomes:

$$T_{measured} = \frac{\dot{m}_r T_{exhaust} + \dot{m}_{air} T_{amb}}{DR \times \dot{m}_r} \quad (3.36)$$

The mass flow rate of intake air that slips into the exhaust is calculated by:

$$\dot{m}_{air,slip} = \dot{m}_{exhaust} - \dot{m}_{fuel} - \dot{m}_r \quad (3.37)$$

Substituting Equation (3.37) into Equation (3.36) and simplifying with Equation (3.34), a equation for the true exhaust temperature becomes:

$$T_{exhaust} = DR \times T_{measured} + (1 - DR) T_{amb} \quad (3.38)$$

The values of temperature in Equation (3.38) should be absolute.

## Emissions

Emissions measured with gas analyzers are given in parts per million by volume (ppm). Typically, emissions are reported on a mass basis. To make this conversion, the EPA recommends Method 19. Method 19 based on the O<sub>2</sub> F-Factor was used in this research. This method, as given by (Ely, 2004), uses the volumetric flow rate of fuel at standard conditions and the measured oxygen content in the exhaust to calculate the exhaust gas volumetric flow rate at standard conditions as in Equation (3.39).

$$\dot{V}_{exhaust,st} = HHV_{fuel} 10^{-6} F_{O_2} \dot{V}_{fuel,st} \left( \frac{20.9\%}{20.9\% - O_2\%_{measured}} \right) \quad (3.39)$$

where

- $\dot{V}_{exhaust,st}$  Exhaust flow rate (SCFH)
- $HHV_{fuel}$  Higher heating value of fuel (Btu/SCF)
- $\dot{V}_{fuel,st}$  Fuel flow rate (SCFH)

From Method 19, the parameter  $F_{O_2}$  is defined to be 8710 SCF<sub>exhaust</sub>/MMBtu. The calculated exhaust volumetric flow rate from Equation (3.39) is then used to calculate the mass emissions concentration ( $E_{mass}$ ) from the volumetric emissions concentration ( $E_{ppm}$ ).

$$E_{mass} = \dot{V}_{exhaust,st} d_E E_{ppm} \quad (3.40)$$

Values for the gas density factor ( $d_E$ ) are listed in Table 3-2.

**Table 3-2 Gas Density Factors for Emissions Calculations**

Source: (Ely, 2004)

Component	Density Factor
NO <sub>x</sub>	$1.194 \times 10^{-7} \text{ lb}_m/\text{SCF-ppm}$
CO	$7.26 \times 10^{-8} \text{ lb}_m/\text{SCF-ppm}$
O <sub>2</sub>	$4.155 \times 10^{-8} \text{ lb}_m/\text{SCF-ppm}$
NO	$7.792 \times 10^{-8} \text{ lb}_m/\text{SCF-ppm}$

Volumetric emissions values in Equation (3.40) must be dry. To be dry, moisture in the exhaust sample is removed before it is analyzed. The emissions sampling system will be discussed further in Chapter 4.

### Uncertainty Analysis

When looking at experimental data, it is important to take the uncertainty ( $\sigma$ ) in the measurements into account. For this research, each data point was taken multiple times to establish repeatability. If each of these tests produced the same results, it can be concluded the experiment is repeatable. The instruments used on the test cell were selected due to their high accuracy. However, even if the instrumentation is reading accurately, uncertainty is introduced when measured values are averaged. In preliminary testing, it was found that the uncertainty from the instruments was insignificant when compared to that from averaging the measured values together. This meant that the standard deviation from the data set was treated as the uncertainty in the measurement. This uncertainty was passed through the calculations to compute their uncertainty. This approach was presented by (Bevington and Robinson, 2003). Here, various formulas are presented for uncertainty calculation depending on the calculation being made. The uncertainty from addition or subtraction is:

$$\begin{aligned} x &= au \pm bv \\ \sigma_x^2 &= a^2\sigma_u^2 + b^2\sigma_v^2 \end{aligned} \quad (3.41)$$

The uncertainty from multiplication or division is:

$$\begin{aligned} x &= auv \quad \text{or} \quad x = \frac{au}{v} \\ \frac{\sigma_x^2}{x^2} &= \frac{\sigma_u^2}{u^2} + \frac{\sigma_v^2}{v^2} \end{aligned} \quad (3.42)$$

The uncertainty from raising a variable to a power is:

$$\begin{aligned} x &= a^{bu} \\ \frac{\sigma_x}{x} &= (b \ln a) \sigma_u \end{aligned} \quad (3.43)$$

An example of the uncertainty calculation performed when calculating horsepower is presented below.

Measured:

$$N = 363.15 \pm 3.71 \text{ rpm}$$

$$\tau = 1605.52 \pm 1.47 \text{ ft-lb}_f$$

$$\dot{W}_b = \frac{\tau N}{5252} = \frac{1605.52 \text{ ft-lb}_f \times 363.15 \text{ rpm}}{5252} = 111.014 \text{ hp (average value)}$$

$$\sigma_{\dot{W}_b} = \dot{W}_b \sqrt{\left(\frac{\sigma_N}{N}\right)^2 + \left(\frac{\sigma_T}{T}\right)^2} = 111.014 \text{ hp} \sqrt{\left(\frac{3.71 \text{ rpm}}{363.15 \text{ rpm}}\right)^2 + \left(\frac{1.47 \text{ ft-lb}_f}{1605.52 \text{ ft-lb}_f}\right)^2} = 1.139 \text{ hp}$$

The uncertainty of the power measurement is:

$$\dot{W}_b = 111.014 \pm 1.139 \text{ hp}$$

This method was followed for each calculation performed. The uncertainty of the experimental data will be included with the results. It is always helpful to know the uncertainty in a calculation, especially when it is being compared to other results. This allows for a conclusion to be made about experimental results based on their accuracy. Sometimes, data may seem to be trending a certain way, but when the uncertainty analysis is performed, it is found not to be the case due to high uncertainty.

When analyzing data, the coefficient of variation (*CV*) is sometimes referred to. The *CV* is useful because the standard deviation must be understood in the context of the mean. The *CV* is useful for comparing the degree of variation from one dataset to another, even if you have drastically different means. It is a relative measure of the standard deviation (relative about the mean). The *CV*, given by (Bevington and Robinson, 2003), is defined as:

$$CV = \frac{\sigma}{\mu} \quad (3.44)$$

The *CV* is often reported as a percentage. For this research, the *CV* will be applied to in-cylinder peak pressure data. Reporting in-cylinder peak pressure data using the *CV* is common in the industry, and allows engines with varying peak pressures to be compared to one another.

## CHAPTER 4 - Experimental Setup

To experimentally test the impact of hydrogen addition to natural gas, an Ajax DP-115 engine was used. This is a popular engine in the natural gas industry and gives a good representation of the two-stroke cycle engines found at gathering sites. The test cell that contains this engine is equipped with a dynamometer, an emissions sampling system, and a computer control system. A fuel blending system was designed and added to the test cell for the hydrogen testing. Detailed descriptions of each test cell component are described in the following sections.

### Test Engine

The test engine is an Ajax DP-115. This is a mature, lean burn, two stroke cycle, spark ignited, natural gas fueled engine. Since the DP-115 is a single cylinder engine, any changes made will not be masked by other cylinders as in a multi-cylinder engine. It is a good representation of how each cylinder will react in a multi-cylinder engine. Natural gas fuel is injected into the cylinder by a hydraulically actuated fuel valve in the cylinder head. Specifications for the engine are given in Table 4-1.

**Table 4-1 Test Engine Specifications**

<b>Number of Cylinders</b>	<b>One</b>
<b>Bore and Stroke</b>	<b>13.25 in. x 16 in.</b>
<b>Compression Ratio</b>	<b>8</b>
<b>Engine Full Speed</b>	<b>360 rpm</b>
<b>Engine Full Load</b>	<b>1600 ft-lb<sub>f</sub></b>
<b>Engine Maximum Horsepower @ 360 rpm</b>	<b>115 hp</b>

Prior to testing, the engine was retrofitted with the hydraulic governor shown in Figure 4-1, and air plenum shown in Figure 4-2. This engine originally had oil bath filters, but Ajax currently uses paper filters and an air plenum. The test engine also originally had a mechanical governor which used spinning weights to control the fuel valve, and thus engine speed. This type of governor requires constant adjustment under changing engine load. It also allows engine speed to vary significantly, which can create emissions swings. The hydraulic governor adjusts for changing loads and also maintains a constant engine speed. This constant engine speed ensures engine and emissions stability during testing. Currently, Ajax uses electronic governors on their new engines. Since matured engines, like the test engine, are difficult to retrofit with an electronic governor, Ajax uses the hydraulic governor instead. Both the hydraulic governor and air plenum make the test engine representative of engines currently used in the field.



**Figure 4-1 Hydraulic Governor Installed on Test Engine**



**Figure 4-2 Air Plenum Installed on Test Engine**

### **Dynamometer**

The test cell also includes a 2025A Midwest dynamometer for loading the engine. The dynamometer is controlled by a Dyn-Lok IV digital controller from Dyne Systems Co. This eddy current dynamometer was refurbished in 1989 and is capable of testing engines ranging from 100 to 1,800 bhp and 100 to 2,600 ft-lb<sub>f</sub> of torque. The dynamometer electromechanically absorbs the power delivered by the engine. Water pumped through the dynamometer removes the heat generated by the applied torque. This water then passes through a heat exchanger which is cooled by water circulation from a cooling tower near the test cell. Figure 4-3 shows the dynamometer coupled to the Ajax test engine. The engine has a clutch which is used to engage the dynamometer for loading.



**Figure 4-3 Dynamometer Coupled to Test Engine**

### **Pre-Combustion Chamber**

The test engine can also be fitted with the pre-combustion chamber shown in Figure 4-4. This pre-combustion chamber screws into one of the spark plug holes in the cylinder head as shown in Figure 4-5. The PCC was manufactured by Diesel Supply. It contains a 0.024 in. orifice in the fuel supply line and a 0.218 in. discharge nozzle. The discharge nozzle is the hole in the end of the PCC through which the flame is expelled into the main combustion chamber. Both the discharge hole and fuel orifice are small relative to other PCCs from Diesel Supply. The small discharge hole reduces the amount of air drawn into the PCC from the main combustion chamber, while the small orifice reduces the fuel admitted to the PCC. Together, this results in a slightly lean fuel-air mixture within the PCC when operated at the engine's fuel line pressure. Reducing the fuel pressure of the PCC will further lean out the mixture. The PCC receives cooling water from the dynamometer cooling loop, and fuel. The fuel can come from the city gas line or the blending system that will be discussed next.



**Figure 4-4 Pre-Combustion Chamber**

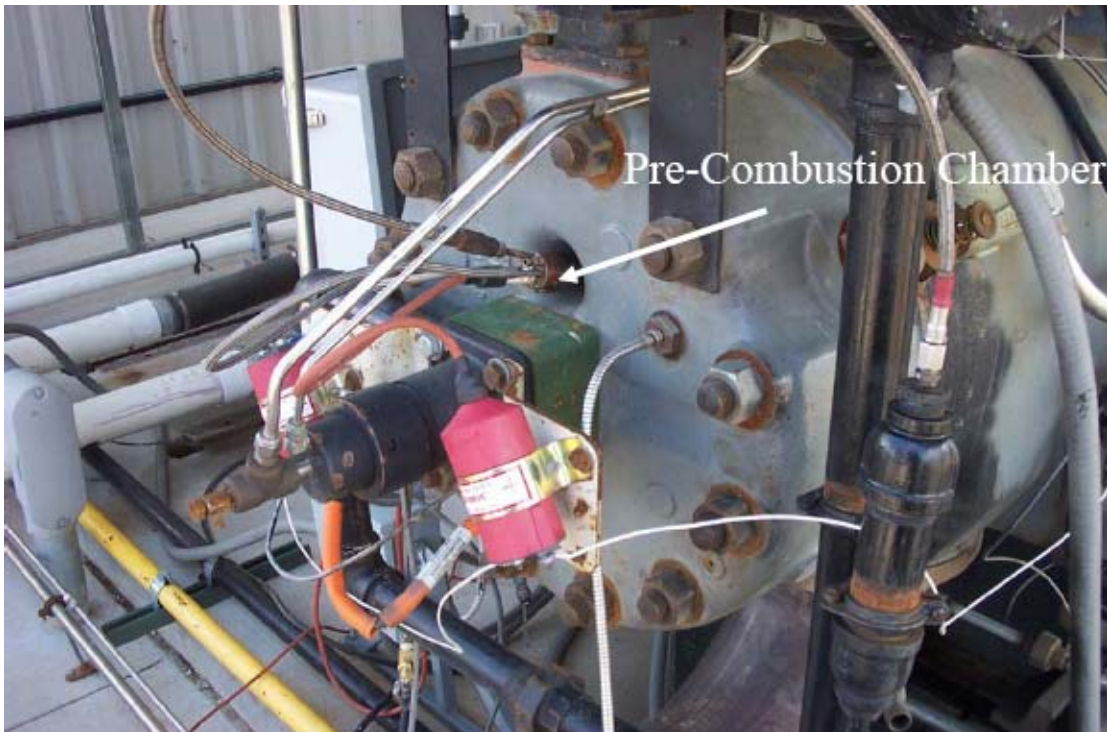


**Figure 4-5 Pre-Combustion Chamber Installed on Test Engine**

## Blending System

In order to test hydrogen blended fuels, the fuels had to be prepared and then delivered to the engine. The calculations in Chapter 3 showed that the fuel mixture can be treated as an ideal gas. However, an efficient and reliable blending system needed to be designed and built.

Two different blending system options were considered. First, a continuous mixing system was investigated. This system would have been very similar to the fuel blending system designed by Dresser-Rand which was described in the literature review. In this case, it would only blend hydrogen and natural gas. Compressed natural gas was available from an Ariel JG/2 gas compressor for the fuel blending. In the preliminary design, a large hydrogen tank would be purchased and kept on-site. The compressed natural gas and hydrogen would then be continually mixed by flow controllers to a specified volume percentage of hydrogen. A blending chamber downstream of the flow controllers would ensure enough residence time for proper mixing. After the blending chamber, the fuel would be delivered to the engine.

The second system that was considered was a simpler one. It consisted of essentially a large tank where batches of fuel could be prepared as opposed to the continuous mixing of the previous system. In this system, a manifold would be built that would allow compressed natural gas and hydrogen to be added to the tank. After the blended fuel spent some time in the tank to allow for mixing, it would be regulated down to the correct pressure and supplied to the engine.

After careful consideration, the second system was selected. This was done for two reasons. First, a substantial amount of uncertainty is introduced with the continuous mixing system. Since that system would involve a control device and valves, there are multiple variables that are constantly changing. With the second system, all of the mixing would be done with manual valves and a tank. This greatly reduces the uncertainty and complexity. It was also found that a large hydrogen tank could not be kept on-site for safety reasons. The most desirable feature of the continuous mixing system is that it would allow for continuous engine operation on blended fuel. However, since the hydrogen tank was going to be much smaller than originally thought, it would limit the operation time. The second system allowed for the hydrogen tank to be switched while the engine operated on pure natural gas. The simplicity of the second system allowed for much less uncertainty in the fuel blend composition and safer operation.

The second system is shown as built in Figure 4-6. The tank is connected to the manifold in Figure 4-7. The manifold allows for compressed natural gas and industrial grade

hydrogen to be added to the tank. Half inch tubing was used for the manifold as well as the connections between the tank and the engine. This reduced head loss and provided the necessary flow. The hydrogen tank is not shown in the figure, but would normally be directly behind the manifold between the three posts. Chains and the posts hold the hydrogen tank in place for safety. A pressure gage on the manifold gives the pressure in the tank, which is used during the blending process. A valve on the tank allows for purging between blends of fuel. This way the tank always starts the blending process with pure natural gas. A long pipe is attached to the purge valve to carry the purged gas up and away from the test cell for safety.



**Figure 4-6 Blending Chamber**



**Figure 4-7 Blending Manifold**

Once the desired amount of hydrogen and natural gas are blended in the tank, the manifold routes the blended fuel to the engine. At the engine, the blended fuel is regulated down to the required pressure for the engine fuel system (14 psig) and injected into the main gas line to the engine. Figure 4-8 shows this setup.



**Figure 4-8 Adjustable Pressure Regulator at Engine**

The engine can use pure natural gas from the city line as usual, or it can use fuel from the blending system. The same can be said for the PCC. Since the city line and the blended line both regulate the pressure and feed into a common line to the engine, the fuel source can be switched while the engine is running. The engine is switched back to the city natural gas source while the blending chamber is purged and prepared for the next test point. The hydrogen bottle can also be switched when empty without shutting down the engine. Figure 4-9 shows a schematic of the entire fuel delivery system as a graphical representation of Figure 4-6, Figure 4-7, and Figure 4-8. Compared to the continuous mixing system, the design is less complex and requires no automated control system.

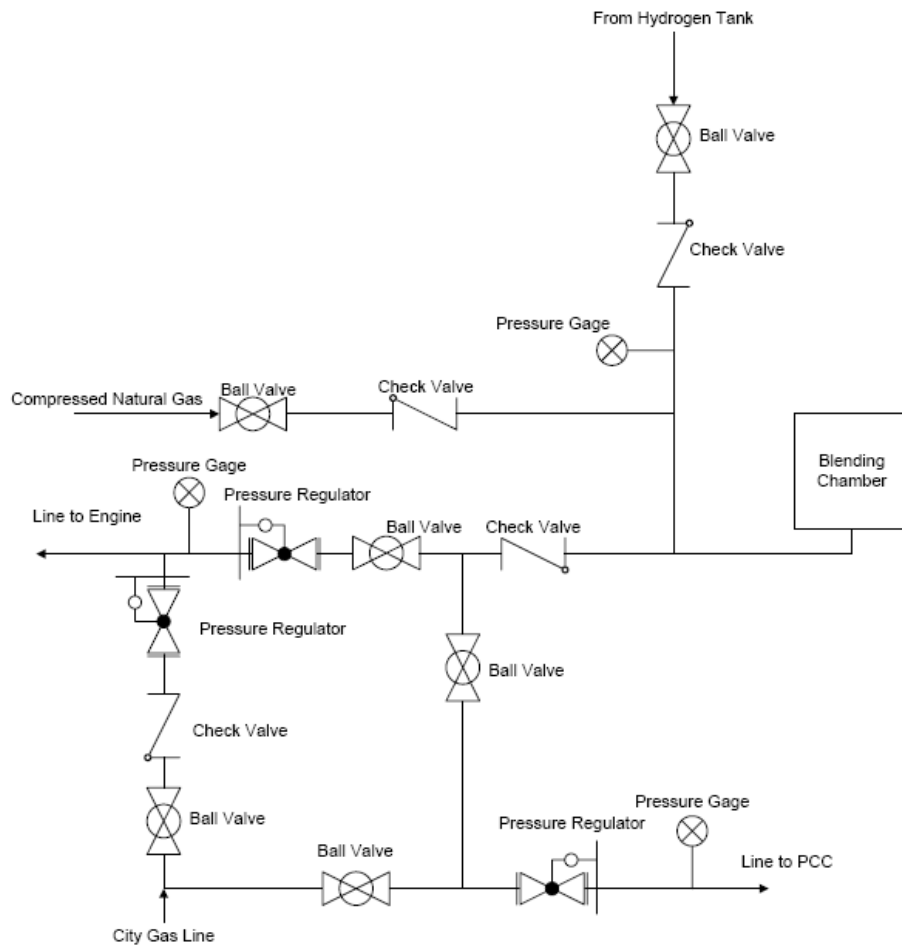


**Figure 4-9 Schematic of Fuel Delivery System**

Since the blending system is just an add-on to the original city fuel line, the engine can still operate on a continuous supply of natural gas as usual. This is helpful when warming up the engine and blending various fuels. This system also allows for the PCC to operate on the blended fuel while the engine’s main combustion chamber operates on pure natural gas. Any combination of fuel supplied to the PCC and main combustion chamber is possible. It is also important to note that check valves keep the blended fuel from contaminating lines that carry pure natural gas or pure hydrogen.

### **Data Collection and Instrumentation**

To determine the affect of hydrogen addition on the test engine, multiple parameters need to be calculated. The detailed equations and steps to calculate the parameters were described in Chapter 3. To calculate these parameters, measurements must be made on the engine. These measurements require not only instruments to capture raw data, but a data collection and analysis system. Table 4-2 contains a list of instrumentation installed on the engine, the range over which the instrument is calibrated, and the accuracy of each sensor. Instrumentation was added to both the engine and dynamometer. Other than engine load, measurements from the dynamometer were for safety purposes only.

**Table 4-2 Instrumentation Used to Analyze the Impact of Hydrogen**

<b>Measurement</b>	<b>Instrument</b>	<b>Range</b>	<b>Accuracy</b>
Ambient Temperature	Kele HO30K-TT-2	-20-140°F	1%
Ambient Pressure	Omega PX215	0-15 psia	0.25%
Ambient Humidity	Kele HO30K-TT-2	0-100%	3%
Engine Fuel Differential Pressure	American Sensor Technologies AST5100	0-1.5 psig	0.5%
PCC Fuel Differential Pressure	American Sensor Technologies AST5100	0-1.5 psig	0.5%
Engine Fuel Pressure	American Sensor Technologies AST4300	0-50 psig	0.25%
PCC Fuel Pressure	American Sensor Technologies AST4300	0-50 psig	0.25%

Engine Fuel Temperature	Type K Thermocouple	0-150°F	3.96°F
PCC Fuel Temperature	Type K Thermocouple	0-150°F	3.96°F
Engine Speed	Altronic Magnetic Pickup	0-25,000 Hz	0.5%
Exhaust Temperature	Type K Thermocouple	0-1200°F	3.96°F
Exhaust Pressure	American Sensor Technologies AST4710	0-30 psia	0.25%
Intake Pressure	American Sensor Technologies AST4710	0-30 psia	0.25%
Intake Temperature	Type K Thermocouple	-20-120°F	3.96°F
Dyno Coolant Inlet Temperature	Type K Thermocouple	-20-200°F	3.96°F
Dyno Coolant Outlet Temperature	Type K Thermocouple	-20-200°F	3.96°F
Engine Coolant Inlet Temperature	Type K Thermocouple	0-250°F	3.96°F
Engine Coolant Outlet Temperature	Type K Thermocouple	0-250°F	3.96°F
Combustion Cylinder Pressure	Optrand Fiber Optic	0-1,500 psig	1%
Dynamometer Load Cell	Sensotec Model 41	0-1,605 lb <sub>f</sub>	0.1%
O <sub>2</sub>	ECOM J2KN	0-21%	0.2%
CO	ECOM J2KN	0-65,000 ppm	0.2%
NO	ECOM J2KN	0-4,000 ppm	0.2%
NO <sub>2</sub>	ECOM J2KN	0-500 ppm	0.2%

The engine and dynamometer are monitored by a data acquisition system consisting of a computer with LabView software and National Instruments hardware, as well as Opto22 hardware and software. To be specific, there is a National Instruments PCI-6259 M-series multifunction DAQ card, Opto22 SNAP Ultimate Brain (SNAP UP1-ADS) controller, Opto22 SNAP Ethernet I/O Brain (SNAP B300-ENET) processor, and various Opto22 modules (analog current input and output, analog voltage input and output, digital input and output, and frequency input). This computer, shown in Figure 4-10, collects both low and high speed data, with the difference being the sampling rate.



**Figure 4-10 Data Acquisition Setup**

Engine parameters such as speed and water temperature are also monitored to ensure safe operation. The Opto22 user interface is shown in Figure 4-11. The data from the instruments is mapped and recorded by the engine mapping program provided by Advanced Engine Technologies (AETC) of Figure 4-12.

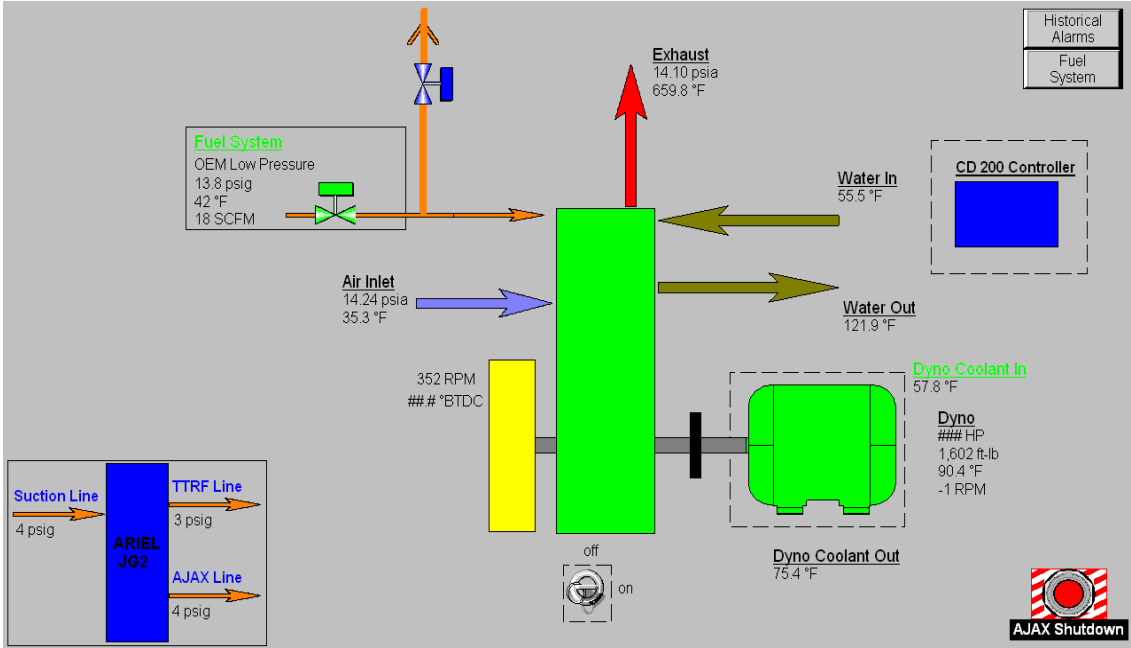


Figure 4-11 User Interface



Figure 4-12 AETC Mapping Program

The user interface displays data about the engine in real-time. Data such as engine coolant temperature, engine speed, and dynamometer coolant temperature should be constantly watched to eliminate dangerous and costly situations. This program also automatically monitors the instrumentation data and compares it to the list of safety shutdown values shown in Table 4-3. If the actual values reach these maximum values, the computer closes a pneumatic valve on the fuel line which shuts down the engine. The mapping program is capable of recording data every second for a user defined amount of time. Another useful function is the graph it displays. This graph can show if the engine is operating at steady state just by looking at the instrument readings. If the exhaust temperature stays within 1% of the average, the engine is stable. It can also identify inconsistent sensors, which may unexpectedly spike on the graph.

**Table 4-3 Safety Shutdowns**

Maximum Dyno Coolant Outlet Temperature	125°F
Maximum Dyno Torque	1615 ft-lb <sub>f</sub>
Maximum Engine Coolant Outlet Temperature	200°F
Maximum Engine RPM	400 rpm
Maximum Engine Fuel Pressure	20 psig

The raw data from the mapping program was imported into a spreadsheet where the average and standard deviation are calculated. These values were then used in the spreadsheet to carry out the calculations discussed in Chapter 3. Due to the measuring of multiple points for each test, the standard deviation is a good measure of the uncertainty. It was found that the uncertainty from the standard deviation was dominant over the instrument accuracy. Initially, it was believed that uncertainty from the thermocouples would be significant. After checking the test cell thermocouples against a calibrated thermocouple, the readings were found to be within 0.5°F of each other, showing that the thermocouple uncertainty was also less than that from repeated measurements.

Approximately 50 raw pressure traces were collected for each test point. These raw traces were imported into a spreadsheet with each column representing a complete cycle, and each row 0.1 degree of crank angle. A macro is used to automate data analysis of the raw traces

and calculates the average peak pressure, standard deviation of peak pressure, and average location of peak pressure for that test point.

Emissions data was collected by an ECOM J2KN analyzer. The analyzer was donated by ECOM. It is equipped with a software package that allows for wireless communication with the computer monitoring the test cell. It also contains a sample conditioning system that removes all moisture from the sample, resulting in dry values for emissions. Early in testing, a heated sample line was needed between the exhaust pipe and the analyzer. This line was donated by Ajax, and kept the sample above 320°F until it reached the analyzer. As shown in Figure 4-13, the heated line is connected to the exhaust pipe with a leak proof connection.

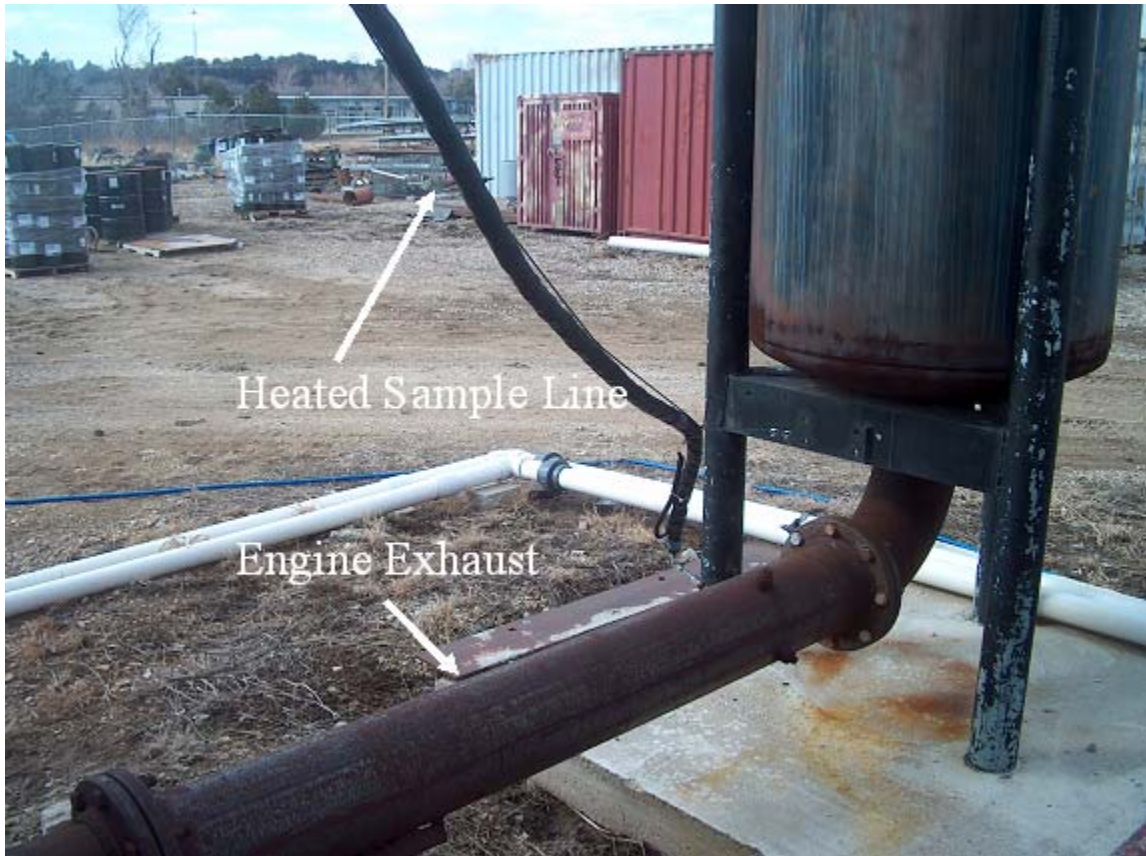


**Figure 4-13 Heat Emissions Sample Line**

A probe draws a sample from the center of the exhaust pipe. The purpose of keeping the exhaust sample at a high temperature is to keep condensation from forming. If condensation forms, components such as  $\text{NO}_x$  can be absorbed in the condensate and not read by the analyzer.

The sample probe is located before the silencer. Ideally, the sample would be taken from the end of the silencer to allow for complete mixing and equilibrium conditions. Through testing and the help of Ajax personnel, the length of pipe at the top of the test engine's silencer was determined to be insufficient. There was not enough pipe to keep ambient air from reaching the probe especially on windy days. A negative pressure wave is created in the exhaust during each cycle, resulting in some ambient air coming back in the top of the silencer. If the probe is too close to the pipe end, the sample becomes diluted. After considering the emissions taken from the location shown in Figure 4-13, emissions were deemed accurate with the help of Ajax personnel.

This method of data collection and analysis was designed with accuracy, safety, and simplicity in mind. Safety is always a concern when doing experimental testing, but when working with large rotating machinery, it is even more important. This method also requires relying on computer computations, which minimizes human error and data processing time.

## **CHAPTER 5 - Testing**

This chapter describes the experimental testing that was performed with the setup described in Chapter 4. The objective of this research was to investigate the impact of hydrogen addition to a two stroke cycle, lean burn, single cylinder engine. To accomplish this specific objective, two test matrices were constructed. The test matrix in Table 5-1 deals with the entire engine operating on the blended fuel without a PCC. The test matrix in Table 5-3 was constructed for PCC configuration. First, the test plan for the non-PCC configuration is described, including the parameters that were calculated and analyzed. Next, the actual data for the non-PCC configuration is presented with discussion on the results. The test matrix for PCC configuration is then described, followed by data and discussion for that configuration.

### **Test Plan for Non-PCC Configuration**

When completing Table 5-1, a spark timing of six degrees before top dead center (BTDC) was first used. Once the engine was warm, load was applied by the dynamometer, and the hydraulic governor was adjusted to reach full load and speed (1,600 ft-lb<sub>f</sub> and 360 rpm). The engine was tuned at this operating condition. Tuning the engine consisted of adjusting fuel pressure and fuel valve lift to achieve the lowest possible standard deviation in peak pressure. In the field, the engine would be tuned to the load and speed normally seen. After that, the engine would run continuously at that load and speed. Once the engine was loaded, it was allowed to stabilize for approximately 20 minutes. The engine was deemed stable by monitoring the exhaust temperature as described in Chapter 4. As shown in the test matrix, a baseline test was performed next while the engine was fueled by pure natural gas. After the baseline, a mixture of 10% hydrogen by volume was added to the engine and another test point was recorded. This consisted of operating the engine on fuel supplied by the blending chamber. Again, the engine was allowed to stabilize for 20 minutes before data was taken. Two more test points were taken with 20% and 30% hydrogen by volume. Both engine and emissions data were recorded, as well as physical observations for each test point. After completing the four test points at this spark timing, the engine was turned off so that the spark timing could be adjusted. Since hydrogen has a fast flame speed, it was desired to see how it will react to different spark timings. Besides 6

degrees BTDC, spark timings of 3 degrees BTDC and 11 degrees BTDC were used. The engine was then brought back up to full load and speed and the same procedure was followed for taking test points as with the previous spark timing. After the test matrix had been filled in once, the same test points were retaken at least one more time. The test points were retaken to show repeatability. They were retaken during various ambient conditions and were not taken consecutively. The test matrix for the non-PCC configuration is shown below in Table 5-1.

**Table 5-1 Non-PCC Test Matrix**

		Spark Timing (°BTDC)		
		3	6	11
Hydrogen Percentage	0%	Point 1	Point 5	Point 9
	10%	Point 2	Point 6	Point 10
	20%	Point 3	Point 7	Point 11
	30%	Point 4	Point 8	Point 12

The test matrix above was completed twice giving a total of 24 test points. Each point was analyzed to ensure reliable data. Points that were deemed unreliable were retaken. Unreliable points consisted of data with multiple outliers, often caused by the computer not being able to collect the data fast enough, or points in which engine speed varied by more than 10 rpm during the test. The test plan was constructed by investigating the typical field conditions and emulating those field conditions. Since this research is focused on allowing field engines to meet emissions regulations, it was important to simulate the field conditions as much as possible.

### **Test Results and Discussion for Non-PCC Configuration**

The following sections provide the experimental results for the non-PCC configuration. The results are discussed and trends in the data are pointed out. These results were obtained by supplying the blended fuel to the main combustion chamber of the engine.

### *Uncertainty in Experimental Results*

An uncertainty analysis was performed on the experimental data as described in Chapter 3. The uncertainty from experimental measurements was passed to the calculations. Table 5-2 provides the typical uncertainties of data presented in this chapter. The table is valid for both the non-PCC configuration and the PCC configuration and will be referred back to as the data is discussed.

**Table 5-2 Uncertainties**

<b>Parameter</b>	<b>Uncertainty</b>
Average Location of Peak Pressure	42.31%
Brake Specific Fuel Consumption (Btu/hp-hr)	6.84%
Exhaust Temperature (°F)	0.55%
NO <sub>x</sub> Emissions (g/hp-hr)	7.37%
NO Emissions (g/hp-hr)	7.51%
NO <sub>2</sub> Emissions (g/hp-hr)	7.41%
CO Emissions (g/hp-hr)	7.42%
Equivalence Ratio	10.31%

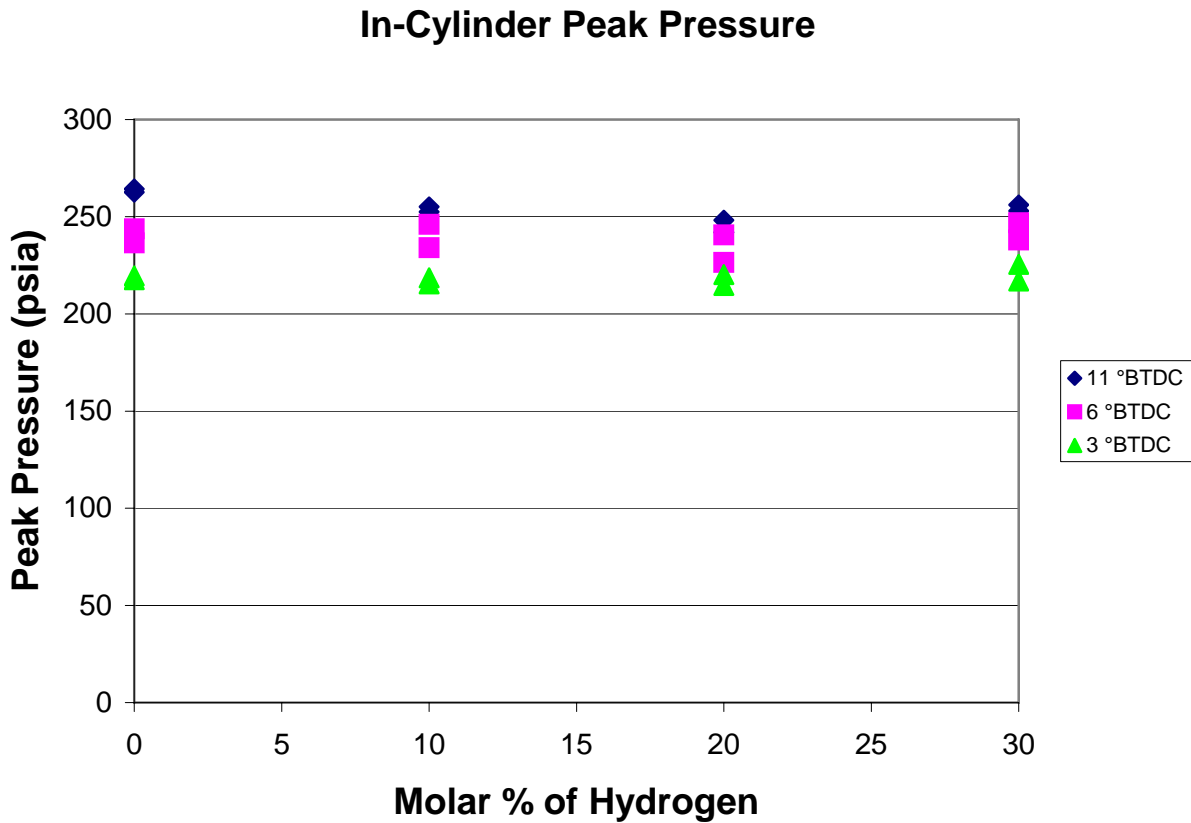
### *Physical Observations*

For each point, not only was data recorded, but special attention was taken to note physical observations such as how smoothly the engine ran and if there were any indications of misfires. No increases in misfires were physically observed as hydrogen was added and the engine seemed to run smoother with the blended fuel. This at least meant that the engine was firing more often. There appeared to be a decrease in the misfires, and there were no signs of backfires or knock.

### *In-Cylinder Peak Pressure*

Decreased in-cylinder peak pressure can be a drawback from hydrogen addition. Hydrogen displaces some of the air in the combustion chamber, creating a lower in-cylinder peak pressure. Hydrogen's lower volumetric heating value can contribute to lower peak pressures and decreased power output. These drawbacks are especially problematic near stoichiometric

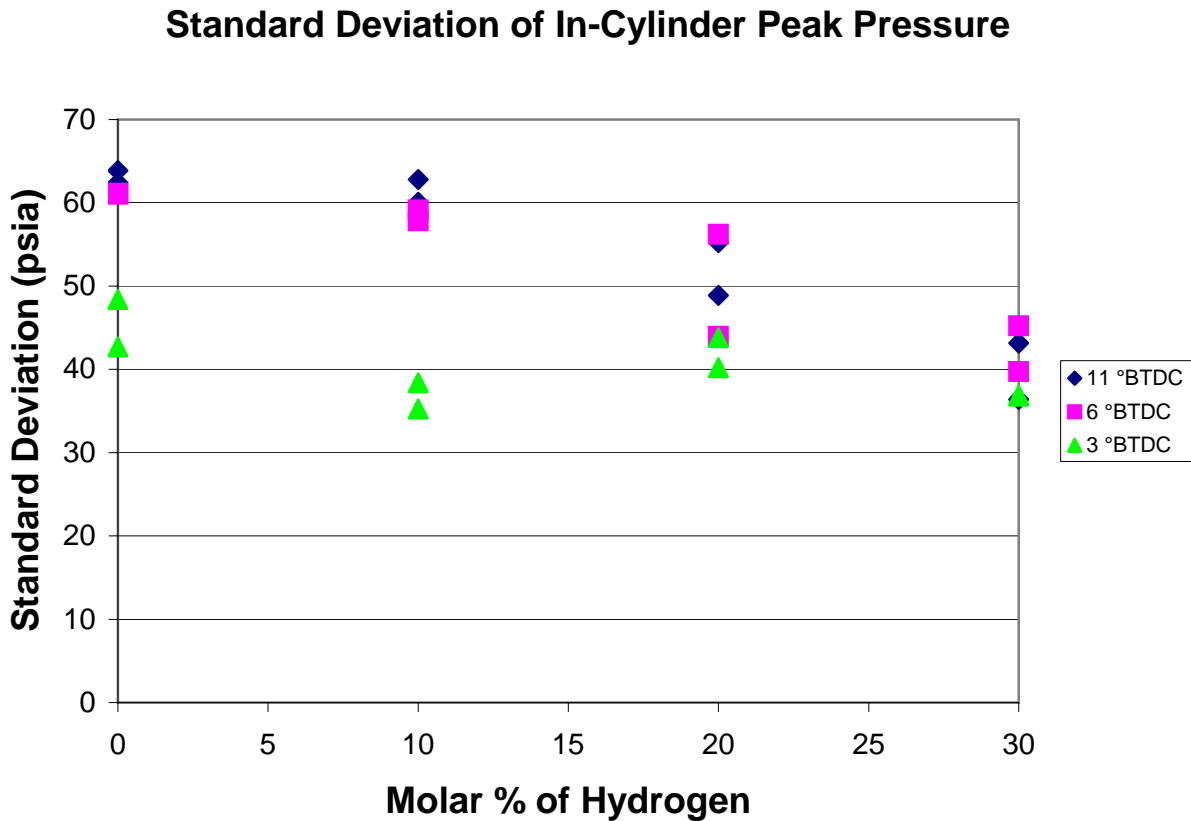
equivalence ratios. Figure 5-1 shows the in-cylinder peak pressures collected during testing. Four different test points are shown. Each point was repeated, giving a total of eight points displayed on the graph.



**Figure 5-1 In-Cylinder Peak Pressure**

As the spark timing was retarded, the in-cylinder peak pressure decreased. For the most advanced spark timing of 11 degrees BTDC, the in-cylinder peak pressure decreased approximately 6% from the baseline with 20% hydrogen addition. This was the minimum experienced for that spark timing. With 30% hydrogen addition, the spark timing started to increase. The increase could be due to a shortened combustion duration caused by hydrogen addition. Also, since the in-cylinder peak pressure values are averaged, a decrease in misfires, which resulted in lower in-cylinder peak pressures being factored into the average, could have increased the average. For the most retarded spark timing of 3 degrees BTDC, no significant change in in-cylinder peak pressure can be found.

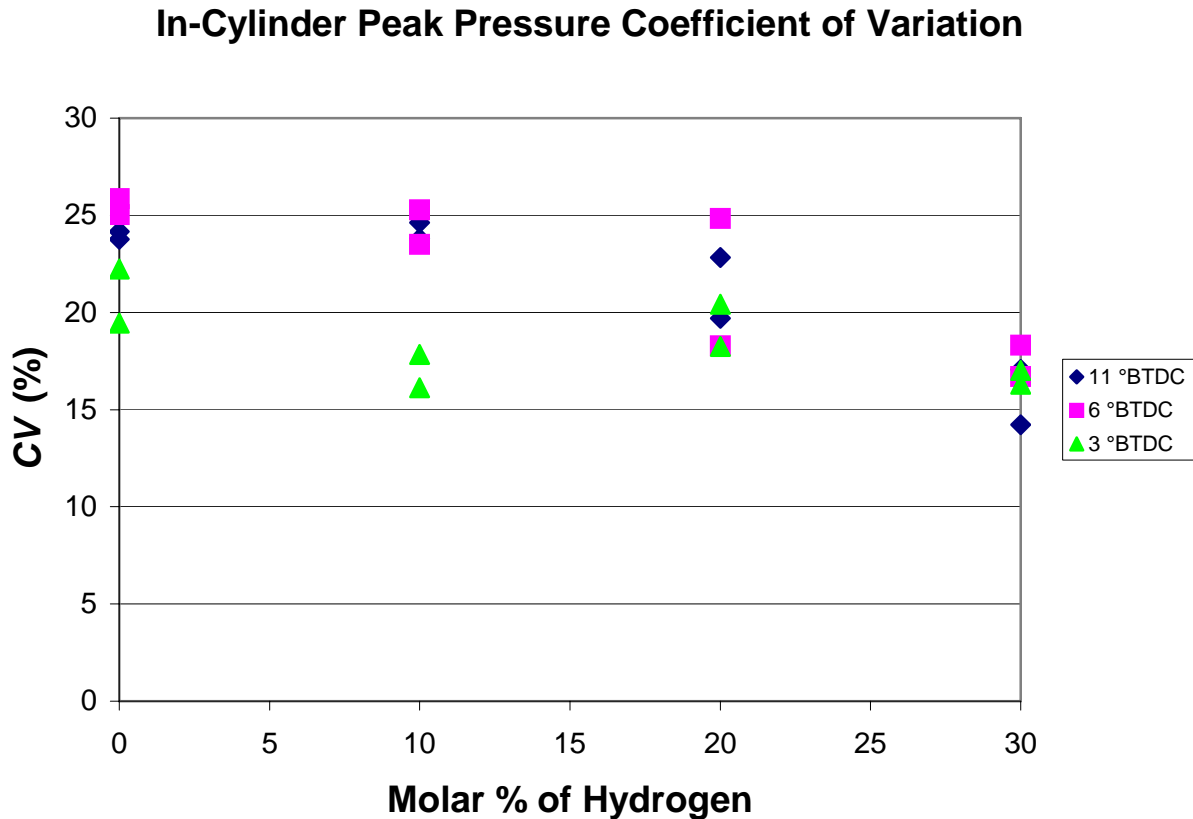
Physical observations during testing gave the appearance of decreased misfires. The standard deviation of in-cylinder peak pressure is representative of the amount of misfires. Lower standard deviation means fewer misfires. Figure 5-2 shows the standard deviation of in-cylinder peak pressure for all spark timings as hydrogen was added.



**Figure 5-2 Standard Deviation of In-Cylinder Peak Pressure**

The graph shows a general decrease in standard deviation as the hydrogen percentage was increased. The decrease was more prevalent for the most advanced ignition timing of 11 degrees BTDC. As the spark timing was retarded, the standard deviation decreased less. The spark timing of 3 degrees BTDC showed a decrease in standard deviation of approximately 20% for 10% hydrogen, but then increased nearly the same for 20% hydrogen. The standard deviation for 11 degrees BTDC was unaffected by 10% hydrogen addition, and began to decrease with 20% ending with a total decrease of 37% with 30% hydrogen addition.

Another way of analyzing the pressure data is looking at the coefficient of variation. The *CV* removes the in-cylinder peak pressure magnitude, and allows the data to be compared to each other even though the in-cylinder peak pressures have different magnitudes. Figure 5-3 shows the in-cylinder peak pressure coefficient of variation.



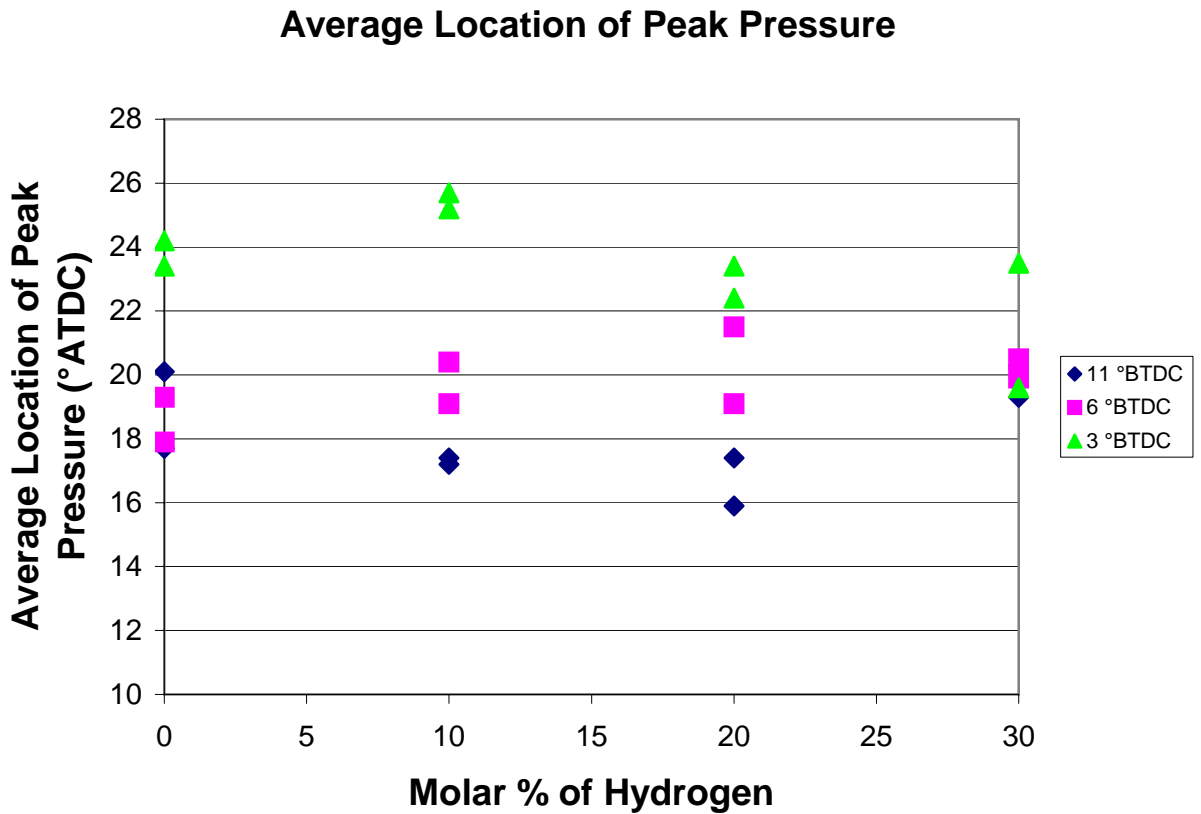
**Figure 5-3 In-Cylinder Peak Pressure Coefficient of Variation**

Figure 5-3 shows that hydrogen addition had a larger impact on the 11 degrees BTDC spark timing. The *CV* decreased almost 42% from baseline with 30% hydrogen addition. The 3 degrees BTDC spark timing had a minimum *CV* with 10% hydrogen addition. A spark timing of 6 degrees BTDC shows the highest *CV* over the test points, suggesting more misfires at that spark timing. With 30% hydrogen, the *CV*s for all three spark timings are nearly the same.

The behavior of Figure 5-3 is most likely because of hydrogen's high diffusivity and low ignition energy. As the spark timing was retarded, more mixing of fuel and air occurred within

the combustion chamber. When the spark occurred, the mixture was more compressed and mixed than with a more advanced spark timing, increasing the probability of combustion. With the most advanced spark timing and pure natural gas, combustion was more difficult to start since the probability is lower of an ignitable mixture being near the spark plug at the time of spark. As hydrogen was added to the fuel, it dispersed rapidly creating a more thoroughly mixed charge. Also, since hydrogen has a lower flammability limit and lower ignition energy than natural gas, combustion could occur at the spark plug when it could not with pure natural gas. The data shows that hydrogen addition does decrease misfires.

A faster flame speed could also change the location of peak pressure. Figure 5-4 shows the average location of peak pressure. The figure shows that as the spark timing was retarded, the location of peak pressure moved further away from TDC. This was expected. Hydrogen's fast flame speed should make the peak pressure occur sooner. This appears to happen for 20% hydrogen addition and spark timings of 11 and 3 degrees BTDC. However, 10% hydrogen addition caused the peak pressure to occur later with spark timings of 6 and 3 degrees BTDC. Referring back to Table 5-2, the uncertainty in this data is large. The large uncertainty is due to a high standard deviation in the location of peak pressure data brought about by misfires and the program not being able to calculate TDC for each cycle before recording the data. Conclusions about the variation in location of peak pressure are difficult to make with a large uncertainty.

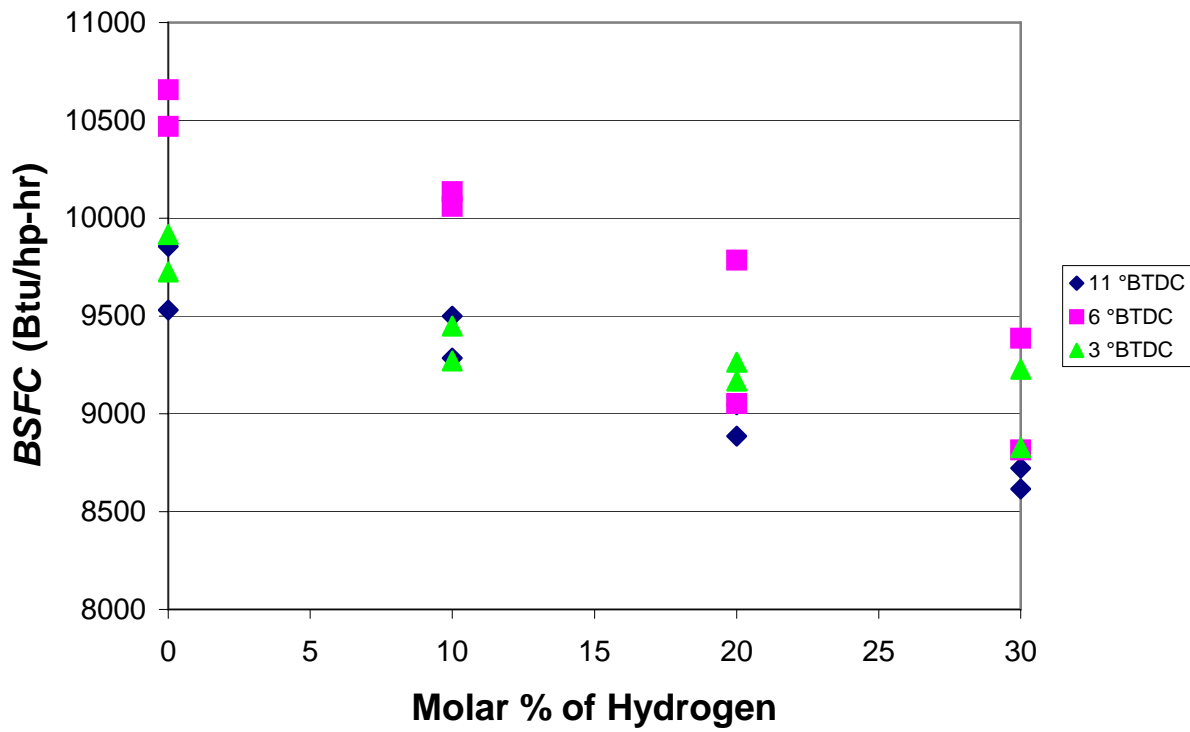


**Figure 5-4 Average Location of Peak Pressure**

### *Brake Specific Fuel Consumption*

As stated in Chapter 3 *BSFC* is a measure of engine efficiency. Figure 5-5 shows the variation in *BSFC* as hydrogen was added for all three spark timings. The *BSFC* was corrected for hydrogen addition.

## Brake Specific Fuel Consumption



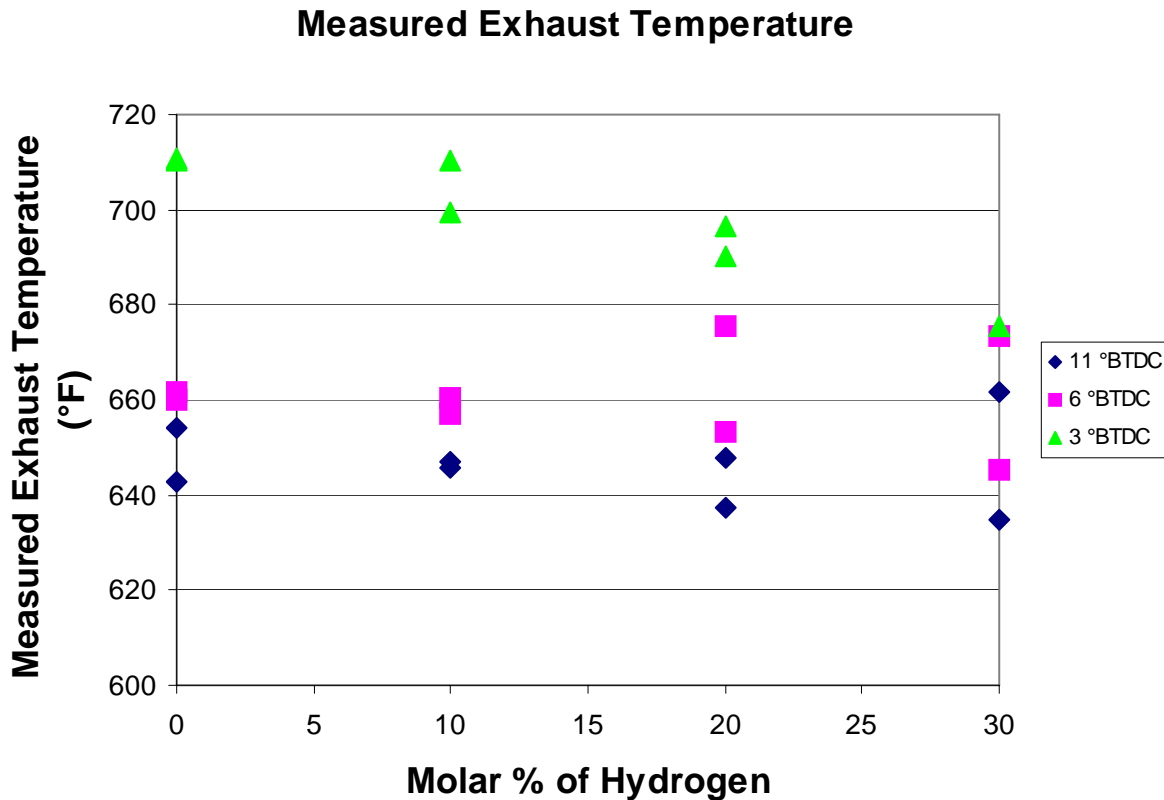
**Figure 5-5 Brake Specific Fuel Consumption**

Figure 5-5 shows that the engine was more efficient as hydrogen was added. Each spark timing had a decrease in *BSFC* of at least 10% with 30% hydrogen addition. As hydrogen was added, fuel consumption decreased. The volumetric heating value of the fuel also decreased. Typically, when the volumetric heating value of the fuel is decreased, the engine consumes more fuel to produce the same power. That was not the case in this experiment. The hydrogen decreased misfires, which meant more of the cycles were producing power. More power cycles meant the engine could maintain load and momentum on less fuel. The decrease in volumetric heating value also decreased the *BSFC*. Even though the fuel contained less energy per unit volume, combustion still initiated and the peak pressure decreased at most by 6%. Since the peak pressure did not significantly reduce, engine power was not compromised. The fuel-air mixture, while containing less energy, was more thoroughly mixed and required less energy to ignite. This too contributed to maintaining engine performance with hydrogen addition. While the results of Figure 5-5 suggest further increasing the hydrogen percentage would be beneficial,

that may not be the case. As hydrogen percentages increase further, the risk of backfires and pre-ignition increase as well. Combustion stability would decline, and possible engine damage could result.

### *Exhaust Temperature*

Since the test engine is a single cylinder, the exhaust temperature is not masked by other cylinders. With multi-cylinder engines, a poorly performing cylinder may not be recognized by analyzing exhaust temperature alone. Since hydrogen has a lower flammability limit, leaner fuel-air mixtures are possible. Leaner fuel-air mixtures lower the combustion temperature. If combustion occurs at a lower temperature, the exhaust temperature should also decrease. Figure 5-6 shows the measured exhaust temperature.



**Figure 5-6 Measured Exhaust Temperature**

Figure 5-6 shows a decrease in the measured exhaust temperature. This would indicate that the combustion temperature is decreasing as hydrogen is added. The measured exhaust

temperature is higher for the spark timing of 3 degrees BTDC than 11 and 6 degrees BTDC. Since the combustion duration remains the same with varying spark timings, retarding the spark timing moves the end of combustion closer to when the exhaust ports open. With less time for the combustion gases to expand and cool between the end of combustion and the exhaust ports opening, retarded ignition timings have higher exhaust temperatures.

With two stroke cycle engines, the measured exhaust temperature can be influenced by ambient conditions. Ambient conditions affect measured exhaust temperature by scavenging allowing ambient air into the exhaust stream. The measured exhaust temperature is lower than the temperature of the combustion products, which is the true exhaust temperature. The *DR* of the test engine is approximately 1.4, meaning the engine takes in 40% more air than needed for combustion. The excess air passes into the exhaust stream and lowers the measured exhaust temperature. The procedure discussed in Chapter 3 dealing with the *DR* was used to remove the affects of ambient conditions. Figure 5-7 shows the exhaust temperature after the correction for ambient conditions and the *DR*.

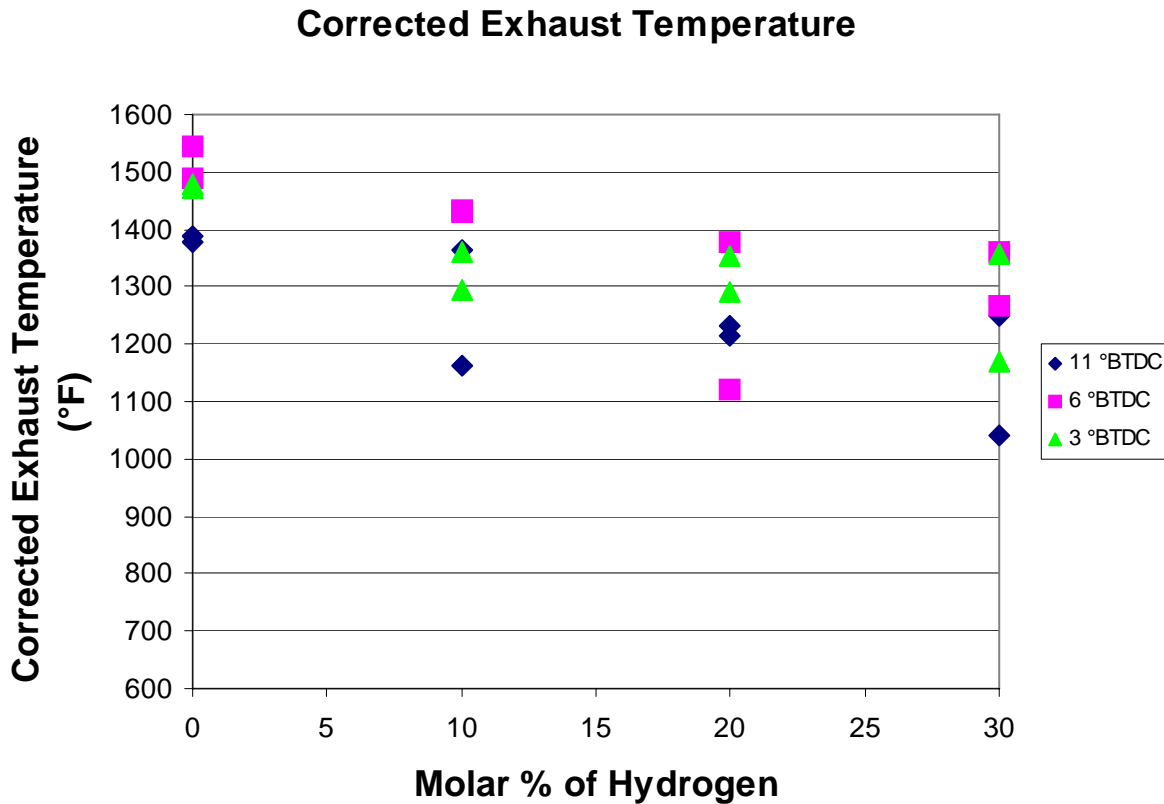
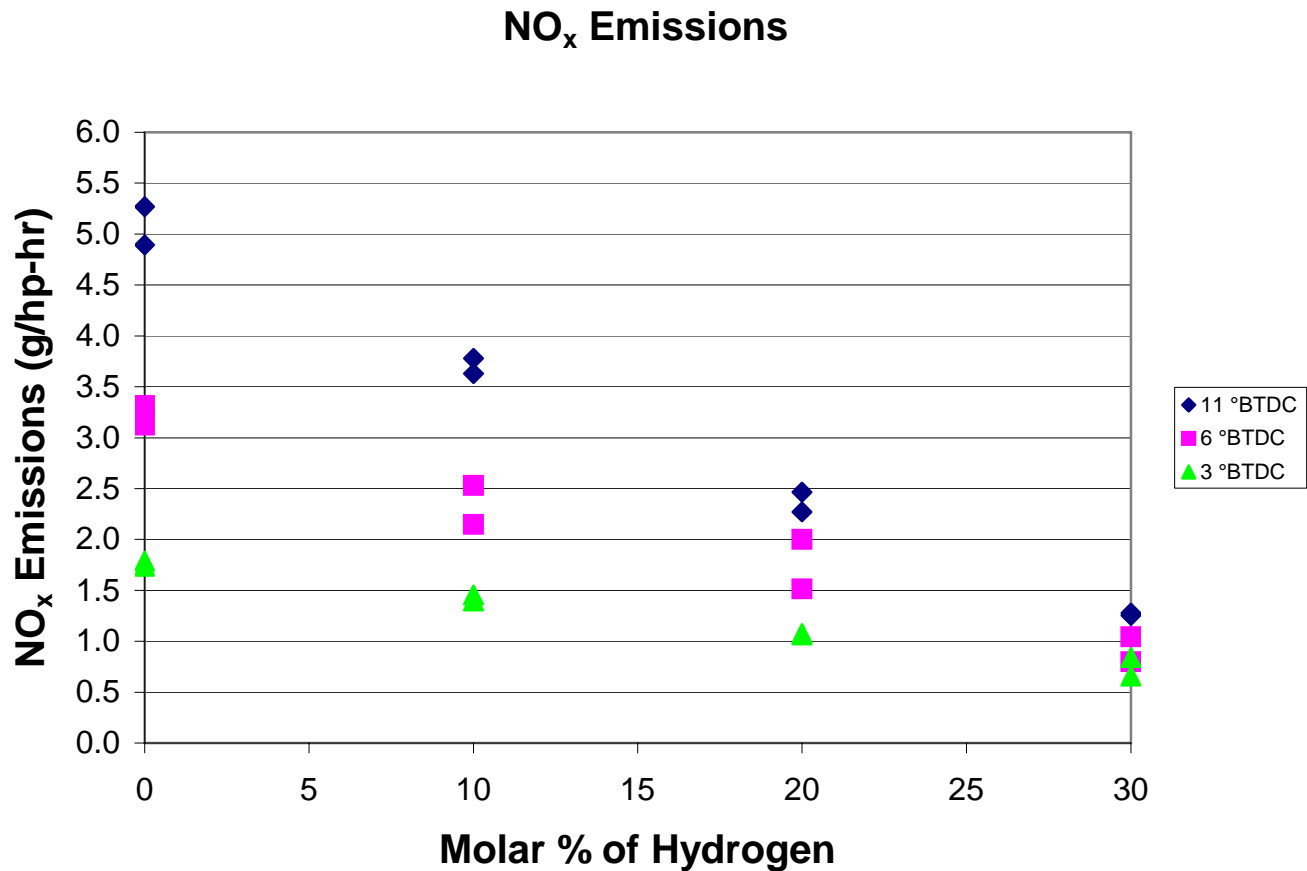


Figure 5-7 Corrected Exhaust Temperature

After the correction, a decrease in exhaust temperature is still seen. The values in Figure 5-7 should indicate the actual combustion temperature. The corrected exhaust temperatures do not show as strong of dependence on spark timing as in Figure 5-6. This is expected, since combustion should occur at nearly the same temperature within the cylinder regardless of when it was initiated.

### *NO<sub>x</sub> Emissions*

Decreased NO<sub>x</sub> levels were found when the emissions data was analyzed. Figure 5-8 shows the NO<sub>x</sub> emissions as the percentage of hydrogen in the blended fuel was increased.



**Figure 5-8 NO<sub>x</sub> Emissions**

While NO<sub>x</sub> decreased for all three spark timings, the amount of reduction was less as the spark timing was retarded. With a spark timing of 11 degrees BTDC, NO<sub>x</sub> was reduced by 75% with 30% hydrogen addition. With 30% hydrogen addition, the timing of 6 degrees BTDC had a

reduction of 68%, and the timing of 3 degrees BTDC has a reduction of 57%. Even 10% hydrogen reduced NO<sub>x</sub> emissions. For the spark timing of 3 degrees BTDC, which experienced the lowest overall NO<sub>x</sub> reduction, an 18% decrease occurred with only 10% hydrogen addition.

When NO emissions are considered alone, the NO<sub>x</sub> trend is again seen. Figure 5-9 shows the NO emissions as hydrogen was added. Just as with Figure 5-8, the emissions values decrease as the hydrogen percentage is increased. NO emissions contribute to the majority of the NO<sub>x</sub> emissions.

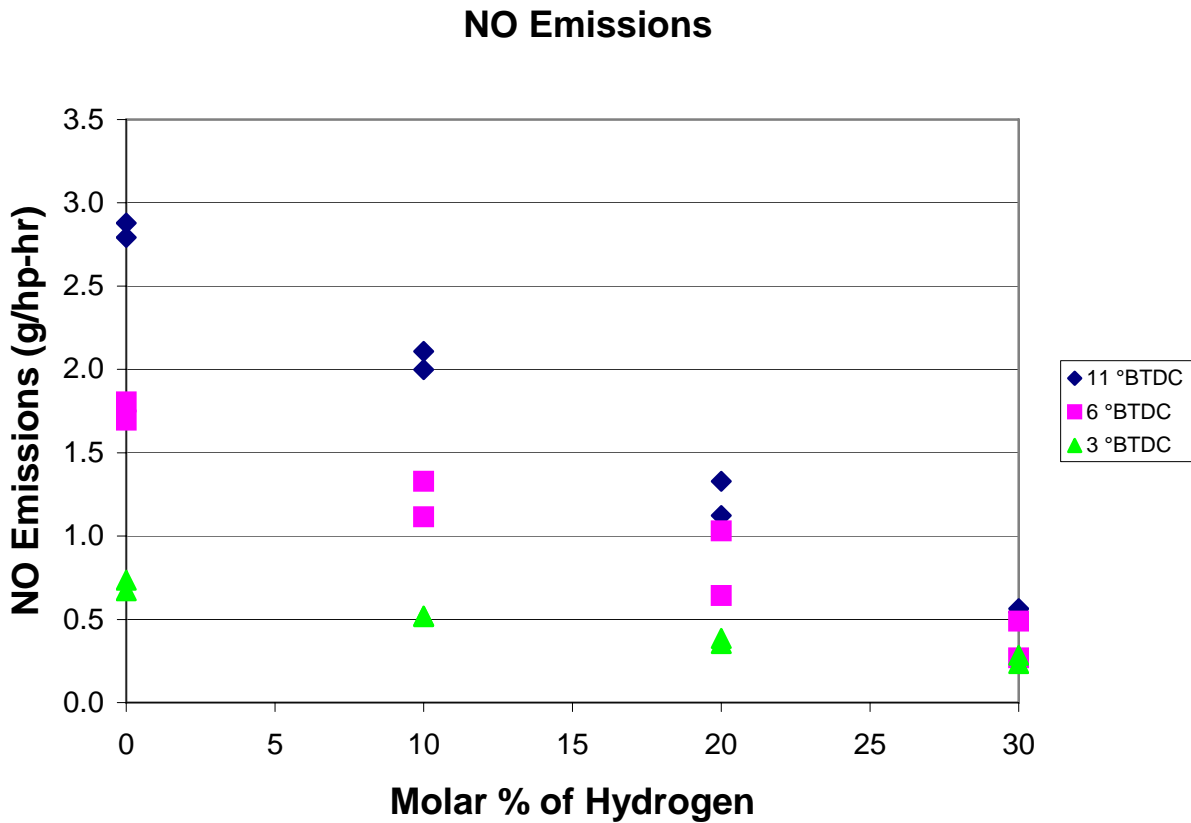


**Figure 5-9 NO Emissions**

Figure 5-10 shows the NO<sub>2</sub> emissions. The graph shows that NO<sub>2</sub> emissions did decrease, but were lower than NO emissions. This is typical for the test engine. Interestingly, retarding the spark timing did not have the same affect on NO<sub>2</sub> emissions as NO emissions. NO emissions reduced as spark timing was retarded. That is not the case with NO<sub>2</sub> emissions. A relationship between NO<sub>2</sub> emissions and spark timing does not appear to exist from this data.

Because of chemical equilibrium and dissociation, the final amounts of NO and NO<sub>2</sub> may vary as the test point is retaken. Since the concentration of NO<sub>2</sub> is less than that of NO, the dissociation is more apparent in the NO<sub>2</sub> data. The overall NO<sub>x</sub> should be nearly constant, as seen in Figure 5-8.

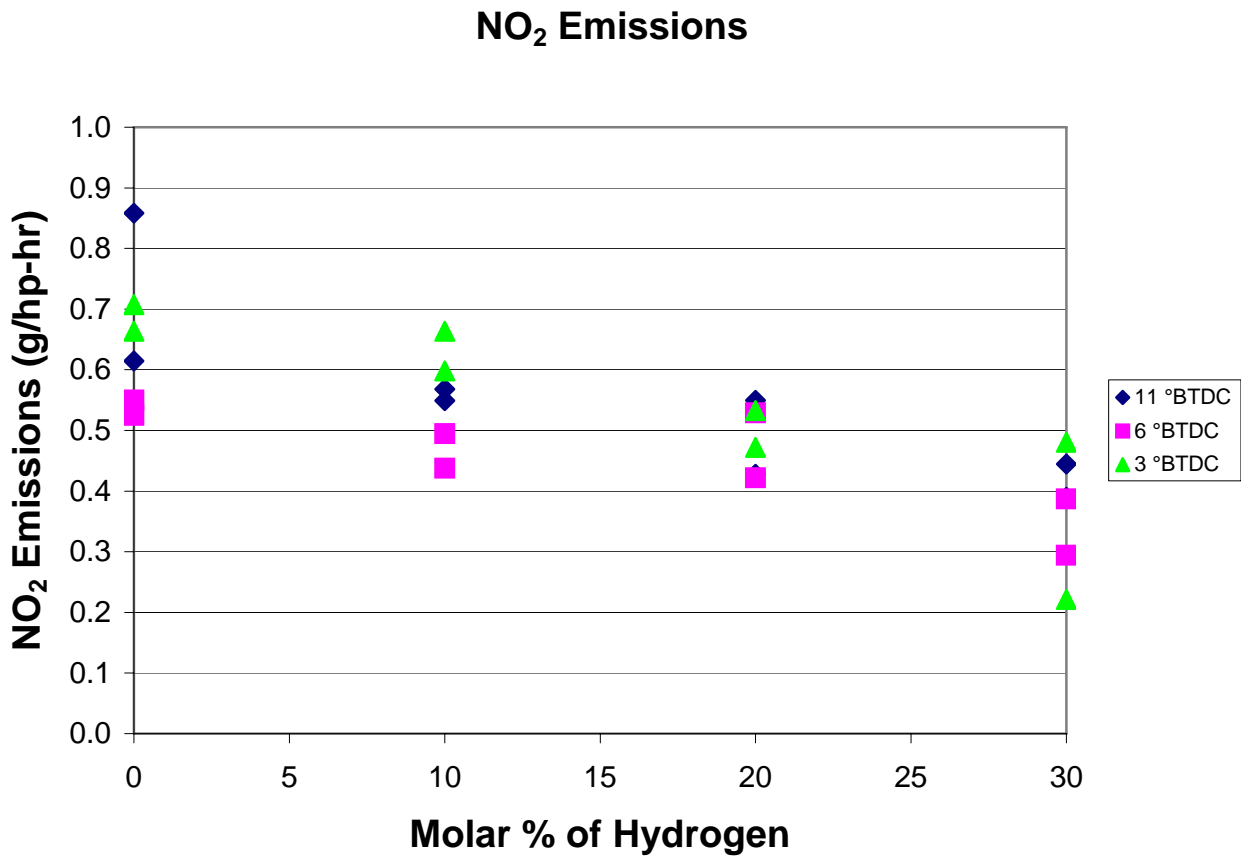


**Figure 5-10 NO<sub>2</sub> Emissions**

### *CO Emissions*

The changes in CO emissions were not as large as those in NO<sub>x</sub>. Figure 5-11 shows the variation in CO emissions as hydrogen was added to the blended fuel.

## CO Emissions

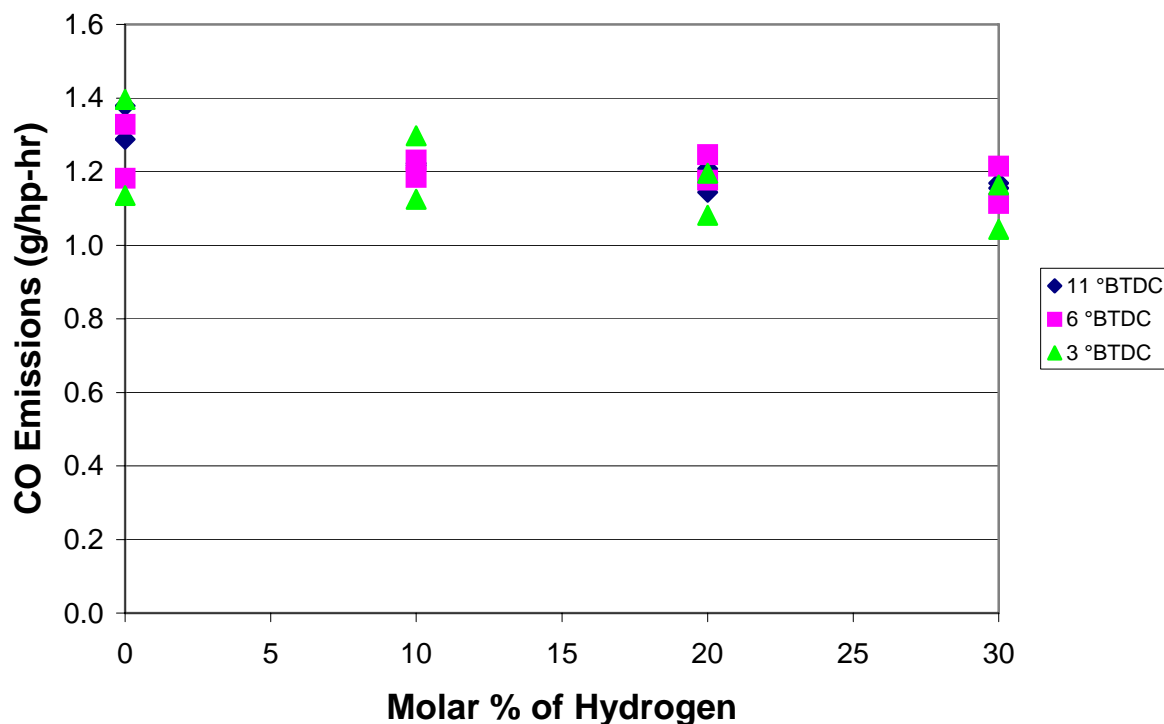


**Figure 5-11 CO Emissions**

Looking at only the mean values, the CO emissions decreased slightly. However, when taking the uncertainty into account, it can not be determined if CO emissions did in fact decrease. A more conservative conclusion is that CO emissions remained constant. The data does show there was no significant increase in CO. Usually, CO emissions will rise as  $\text{NO}_x$  emissions decrease, but that was not the case in this experiment. Hydrogen contains no carbon, so when blended with natural gas, the blended fuel contained less carbon as well. This means there was less carbon available to form CO. From these results, the potential exists of lowering  $\text{NO}_x$  emissions to meet regulations without pushing CO out of regulation

### *Trapped Equivalence Ratio*

As stated in Chapter 2, emissions are a function of equivalence ratio. Adding hydrogen decreases the stoichiometric air-to-fuel ratio. Because hydrogen requires less energy to ignite, leaner mixtures can be used. Figure 5-12 shows the variation in trapped equivalence ratio as hydrogen was added with each spark timing.

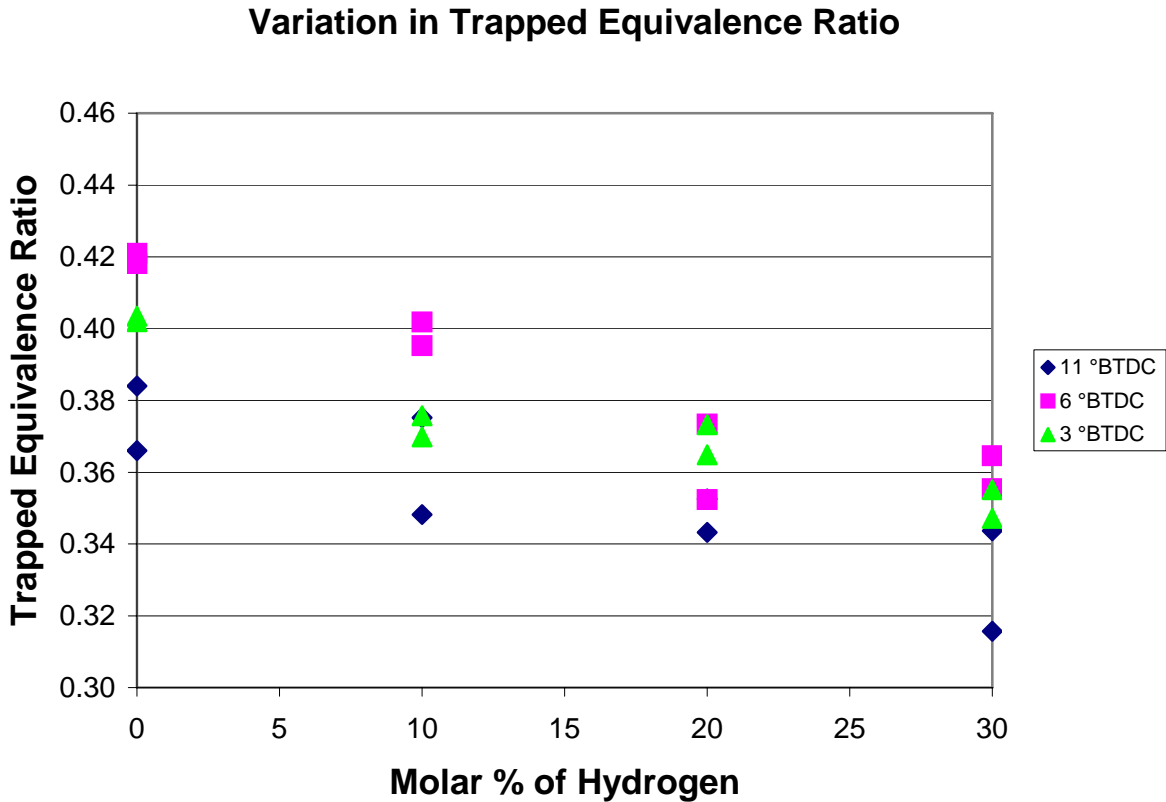


**Figure 5-12 Equivalence Ratio**

As hydrogen was added, the equivalence ratio averages decreased. Taking the uncertainty into account, a significant decrease cannot be concluded. Even with a constant equivalence ratio, the amount of fuel supplied to the engine decreased. Since the stoichiometric air-to-fuel ratio decreased with hydrogen addition, the actual air-to-fuel ratio had to decrease as well to keep a constant equivalence ratio.

## Summary of Non-PCC Tests

Results showed that hydrogen addition lowered the peak pressure coefficient of variation. Hydrogen addition had the largest impact on the 11 degrees BTDC spark timing. The *CV* decreased almost 42% from baseline with 30% hydrogen addition for that spark timing. The 3 degrees BTDC spark timing had a minimum *CV* with 10% hydrogen addition. A spark timing of 6 degrees BTDC shows the highest *CV* over the test points. This would suggest more misfires at that spark timing. With 30% hydrogen, the *CVs* for all three spark timings were within a few percent of each other. A large uncertainty in the location of peak pressure meant the results were inconclusive. The *BSFC* decreased approximately the same for each spark timing as hydrogen was added. Each spark timing showed an average 10% reduction from baseline with 30% hydrogen. As hydrogen was added, fuel consumption decreased. The volumetric heating value of the fuel also decreased. The decrease in volumetric heating value also decreased the *BSFC*. The measured exhaust temperature was found to be depended on ambient conditions. After correcting for the ambient impact, exhaust temperatures still seemed to vary for repeated test points, but did indicate an average decrease with 30% hydrogen addition of approximately 10% from baseline with each spark timing.  $\text{NO}_x$  levels decreased as hydrogen addition was added. While  $\text{NO}_x$  decreased for all three spark timings, the amount of reduction was less as the spark timing was retarded. The spark timing of 3 degrees BTDC showed a decrease of 57% from baseline with 30% hydrogen. The spark timing of 6 degrees BTDC showed a decrease of 68% from baseline with 30% hydrogen. The spark timing of 11 degrees BTDC showed a decrease of 75% from baseline with 30% hydrogen. The data also showed no increase in CO as hydrogen was added, giving the potential of lowering  $\text{NO}_x$  emissions without pushing CO emissions out of regulation. Finally, even though the average equivalence ratio values decreased as hydrogen was added for all three spark timings, no conclusion could be made after taking uncertainty into account. Overall, hydrogen addition lowered  $\text{NO}_x$  emissions while improving engine efficiency and maintaining combustion stability.

## Test Plan for PCC Configuration

After the test matrix of Table 5-1 was completed, the PCC was installed and the test matrix of Table 5-3 was completed. A spark timing of 3 degrees BTDC was used for the PCC testing. The spark timing was selected based on the results from the non-PCC testing. A spark

timing of 3 degrees BTDC not only provided the lowest in-cylinder peak pressure *CV*, but also had the lowest NO<sub>x</sub> emissions values of the three spark timings used. All test points were again conducted at full load and speed (1,600 ft-lb<sub>f</sub> and 360 rpm). First, the PCC was operated on pure natural gas. Typically, the PCC is operated at the engine fuel line pressure, which was the first point. The approximate fuel line pressure for the test engine is 14 psig. Next, a reduced PCC pressure of 10 psig was used to create a leaner mixture within the PCC. A reduced pressure of 10 psig was found to produce the lowest *CV* in preliminary testing. After those two points were completed, a blend of 30% hydrogen was supplied to the PCC while the main combustion chamber still operated on pure natural gas. Again, the PCC was operated at the engine fuel line pressure and 10 psig. Just as with the non-PCC configuration, the test points were retaken at least one more time to show repeatability. A blend of 30% hydrogen was used because it showed the lowest NO<sub>x</sub> levels for the non-PCC configuration. The test matrix for the PCC configuration is shown in Table 5-3.

**Table 5-3 PCC Test Matrix**

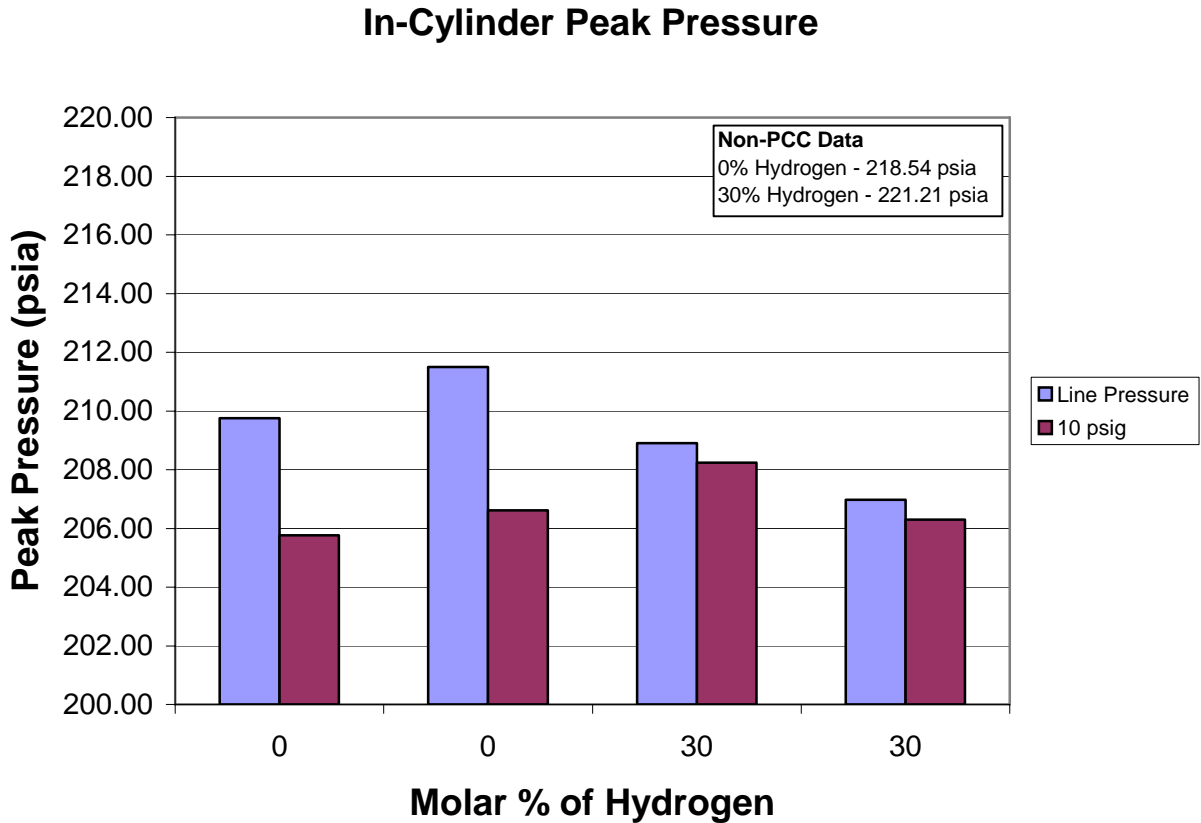
		PCC Pressure (psig)	
		Main Engine Fuel (14)	10
PCC Hydrogen Percentage	0%	Point 1	Point 2
	30%	Point 3	Point 4

### **Test Results and Discussion for PCC Configuration**

The following sections provide the experimental results for the PCC configuration. The results are discussed and trends in the data are pointed out. For comparison purposes, data from the non-PCC configuration is provided in the upper right hand corner of each graph. These results were obtained by supplying the blended fuel to the PCC only while the main combustion chamber of the engine was supplied pure natural gas. The uncertainties of Table 5-2 still apply to the following results.

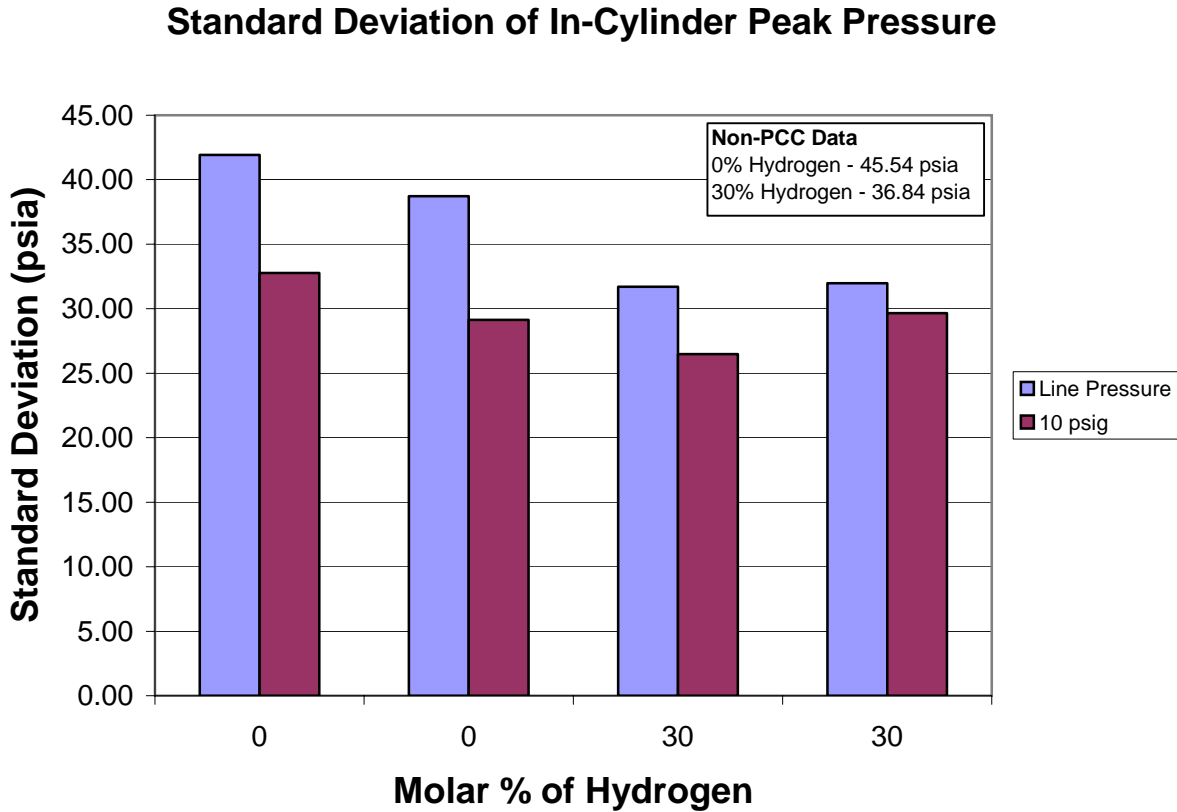
### *In-Cylinder Peak Pressure*

Figure 5-13 shows the in-cylinder peak pressure for the PCC configuration. Each bar represents a test point, and repeated test points are shown. Comparing the results with those of Figure 5-1, a decrease in peak pressure of approximately 4% occurred when the PCC was operated on the engine fuel line pressure without any hydrogen. When the PCC fuel pressure was reduced to 10 psig, the in-cylinder peak pressure decreased approximately 6% from the non-PCC configuration without hydrogen addition. As the hydrogen was added, the in-cylinder peak pressure appeared to decrease slightly with the line pressure and increase slightly with a pressure of 10 psig. When considering the uncertainty in these values from the standard deviation, no significant change in peak pressure can be found.



**Figure 5-13 In-Cylinder Peak Pressure with PCC**

Figure 5-14 shows the standard deviation of in-cylinder peak pressure with the PCC configuration. Comparing these results to those of Figure 5-2, a decrease in standard deviation is found with the PCC and a spark timing of 3 degrees BTDC.



**Figure 5-14 Standard Deviation in Peak Pressure with PCC**

With the PCC operating on the engine fuel line pressure and no hydrogen, a decrease in standard deviation of about 11% is found from operation without the PCC. When the PCC pressure was reduced to 10 psig, the standard deviation decreased 30% from non-PCC operation. As hydrogen was added to the PCC, the standard deviation values decreased about 20% from the values collected with pure natural gas and line pressure. With the reduced PCC pressure, the standard deviation showed almost no significant change with the hydrogen addition.

Figure 5-15 shows the in-cylinder peak pressure coefficient of variation. Comparing the results to those of Figure 5-3, without hydrogen addition and with the PCC at line pressure, an 11% decrease in CV was found with the PCC configuration. When the PCC pressure was reduced, the CV decreased approximately 27% without hydrogen addition from the non-PCC configuration. With 30% hydrogen addition and the reduced pressure, the CV decreased 10% from PCC operation with no hydrogen. With the PCC on line pressure, hydrogen addition decreased the CV approximately 21% from the PCC operation with no hydrogen addition. This shows that hydrogen addition had a more significant impact with the line pressure than the reduced pressure. Hydrogen addition with both pressures did decrease misfires, which is also confirmed by the standard deviation data of Figure 5-14.

### In-Cylinder Peak Pressure Coefficient of Variation

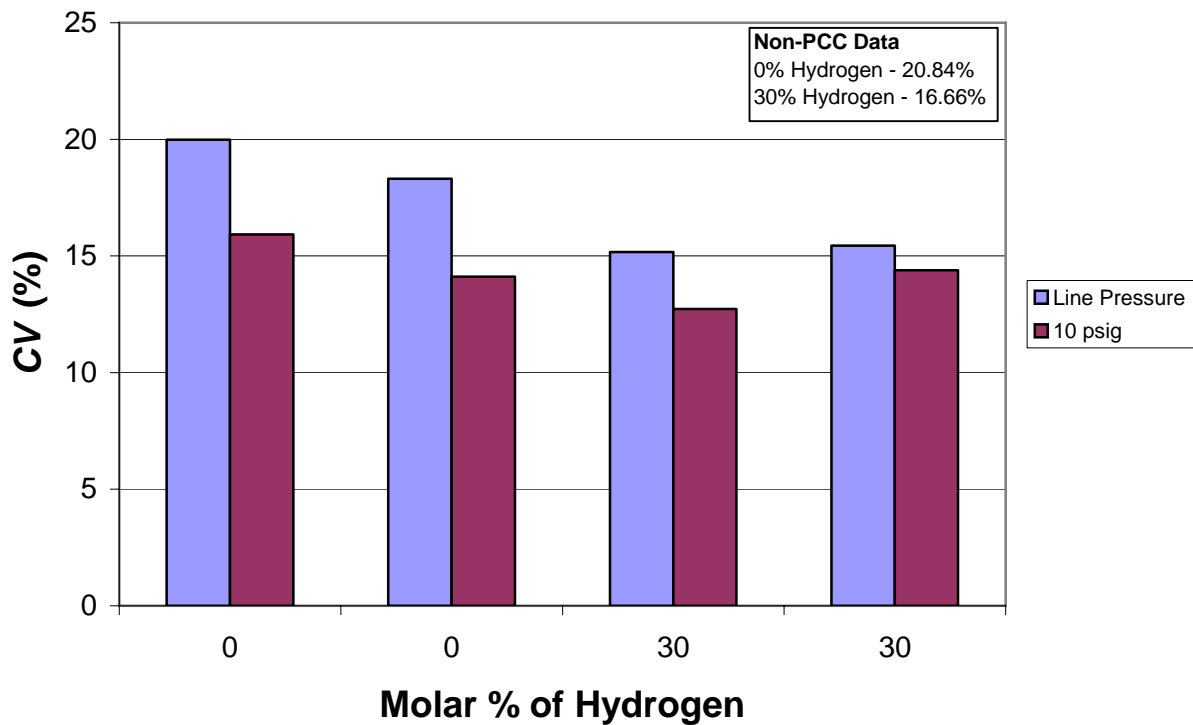
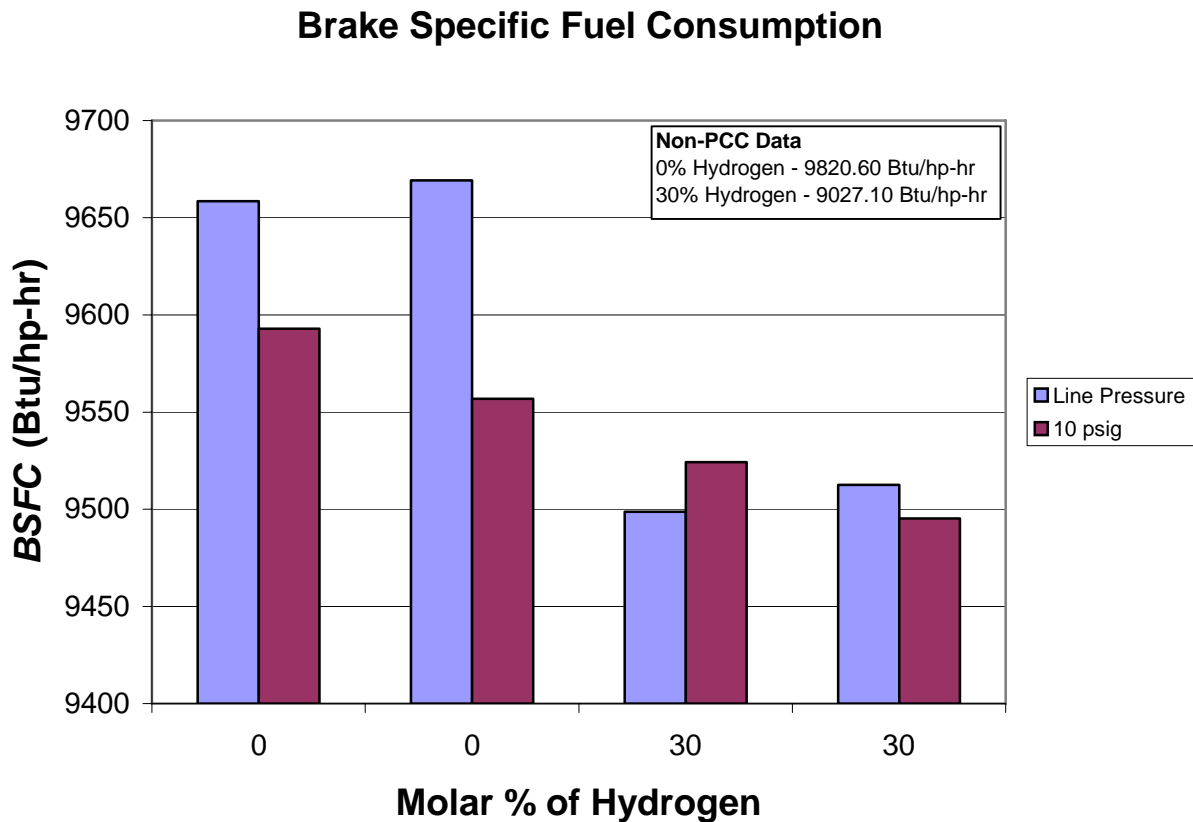


Figure 5-15 In-Cylinder Peak Pressure Coefficient of Variation with PCC

### ***Brake Specific Fuel Consumption***

Figure 5-16 shows the *BSFC* for the PCC configuration. Comparing the results to those of Figure 5-5 shows that when the PCC was operated at line pressure and no hydrogen, no change was found in the *BSFC* from the engine operating without the PCC. After the PCC fuel pressure was reduced, the *BSFC* shows a decrease of approximately 2% from the non-PCC configuration without hydrogen addition. Looking at only the PCC data, adding hydrogen decreased the *BSFC* approximately 2% with the line pressure and 0.5% for the reduced pressure. Since the PCC fuel flow was less than 2% of the total fuel flow into the engine, the amount of hydrogen in the PCC fuel was not included in the *BSFC* calculations. This means that the *BSFC* was not decreased with hydrogen addition because of a decreased fuel heating value. Although the average values show a decrease, after taking the uncertainty into account, no significant change can be found.



**Figure 5-16 Brake Specific Fuel Consumption with PCC**

### *NO<sub>x</sub> Emissions*

With the PCC configuration, adding hydrogen did not have as discernible impact on NO<sub>x</sub> emissions as it did with the non-PCC configuration. Figure 5-17 shows the NO<sub>x</sub> emissions for the PCC configuration. With the line pressure, the decrease in NO<sub>x</sub> emissions with hydrogen addition is about 15%. With the reduced fuel pressure of 10 psig, the NO<sub>x</sub> emissions appear to have increased slightly, however after considering the uncertainty in the data, no significant change is found. This is most likely due to the slightly lean mixture in the PCC with the line pressure. Since maximum NO<sub>x</sub> occurs for mixtures slightly lean of stoichiometric, the line pressure created the most NO<sub>x</sub> in the PCC. When the PCC fuel pressure was reduced, the mixture became leaner, which reduced the amount of NO<sub>x</sub> formed in the PCC.

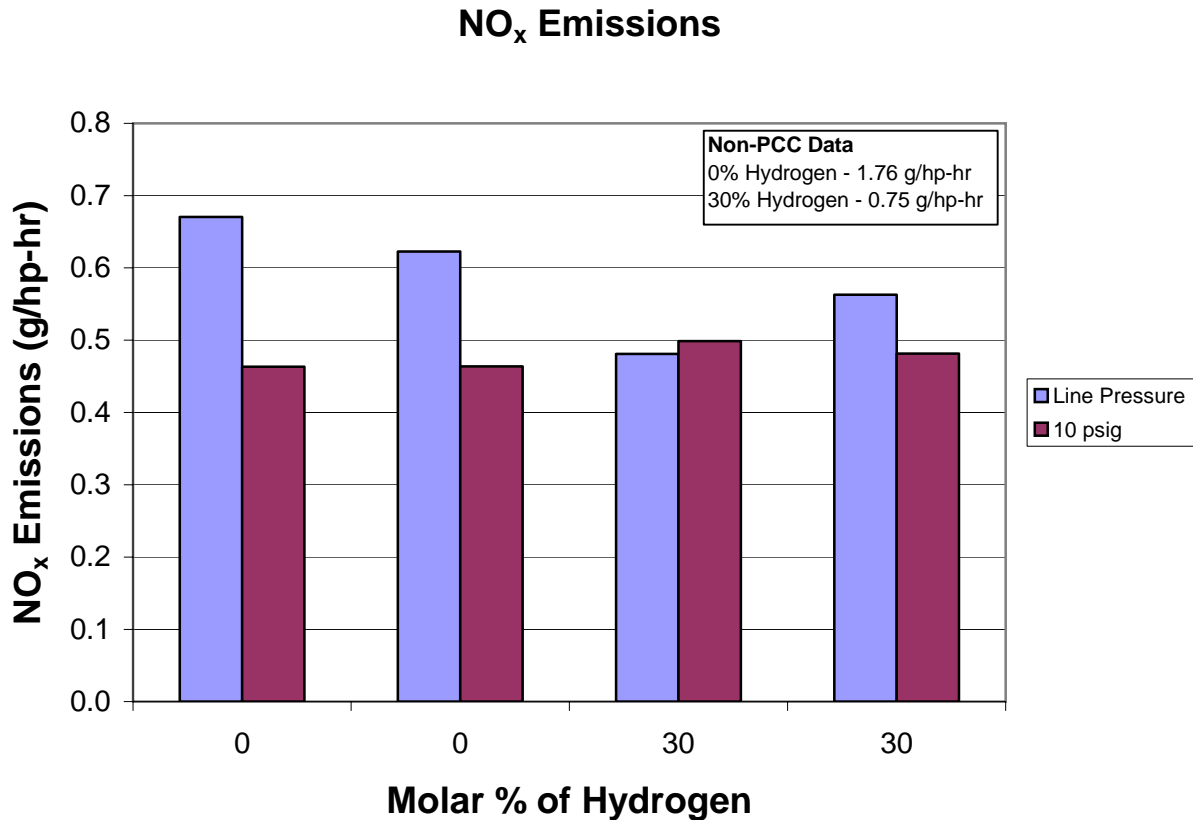


**Figure 5-17 NO<sub>x</sub> Emissions with PCC**

Comparing the data of Figure 5-17 to that of Figure 5-8, a decrease in NO<sub>x</sub> is found with the PCC configuration. Without hydrogen addition, NO<sub>x</sub> emissions decreased 62% with the

addition of the PCC at line pressure. When the PCC fuel pressure was reduced, NO<sub>x</sub> emissions reduced 73% from the non-PCC configuration. Both of these decreases occurred without any hydrogen addition. Only the PCC addition was necessary. With the non-PCC configuration, 30% hydrogen addition provided the lowest NO<sub>x</sub> emissions. This value is nearly the same as that produced by the addition of a PCC at line pressure and no hydrogen. The reduced PCC fuel pressure reduced the NO<sub>x</sub> emissions 20% from that value. Since the PCC operates with near stoichiometric fuel-air mixtures, more NO<sub>x</sub> is created per unit volume in the PCC than in the main combustion chamber. While the PCC can ignite leaner mixtures and lower total NO<sub>x</sub>, it does so while creating more NO<sub>x</sub> per unit volume than the main combustion chamber. The particular PCC used for this research contained less volume than typical PCCs. With less volume, the high levels of NO<sub>x</sub> formed in the PCC did not impact the overall engine NO<sub>x</sub> the way larger volume PCCs would. The data collected does not show a decrease in overall NO<sub>x</sub> with hydrogen addition. This does not mean the hydrogen did not decrease NO<sub>x</sub> production within the PCC, but that the amount of NO<sub>x</sub> from the PCC was insignificant relative to that of the main combustion chamber due to a large difference in volume. When looking at the NO and NO<sub>2</sub> emissions separately, no change was found in the NO<sub>2</sub> data as hydrogen was added to the PCC. The variation in NO<sub>x</sub> was due to variation in NO, just as with the non-PCC configuration. Even though the PCC addition decreased NO<sub>x</sub> emissions, the CO emissions did not remain the same as they did with hydrogen addition and no PCC.

### ***CO Emissions***

Figure 5-18 contains the CO emissions with the PCC configuration. Considering the uncertainties, both adjusting the PCC fuel pressure and adding hydrogen caused no change in CO emissions. After looking at Figure 5-11, an increase in CO emissions from the non-PCC configuration of about 15% occurred with the addition of the PCC on line pressure. Without a PCC, NO<sub>x</sub> levels were lowered without an increase in CO. Lowering NO<sub>x</sub> levels with a PCC comes with an increase in CO.

## CO Emissions

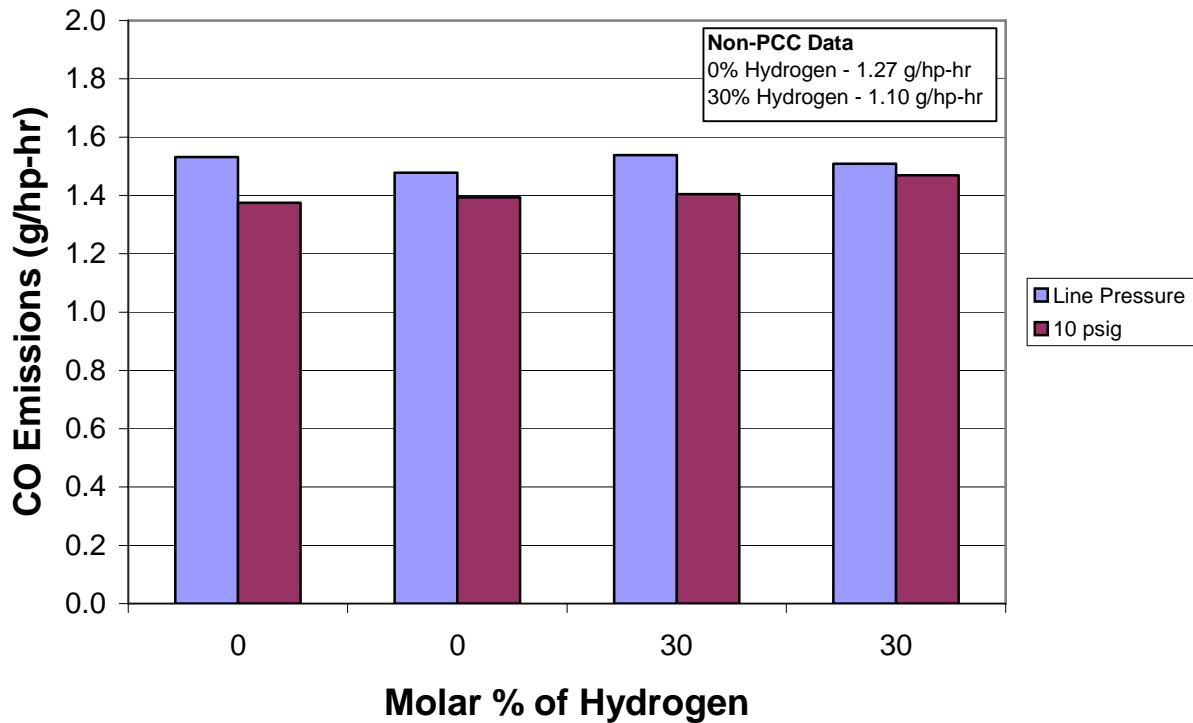


Figure 5-18 CO Emissions with PCC

### *Trapped Equivalence Ratio*

Figure 5-19 shows the trapped equivalence ratio for the PCC configuration. With the uncertainty, no variation can be found by either adjusting the PCC fuel pressure or adding hydrogen. Comparing the data of Figure 5-19 to that of Figure 5-12, again, there is no significant change in equivalence ratio. The conclusion can be made that, with uncertainty in the data, for a spark timing of 3 degrees BTDC, the trapped equivalence ratio stayed constant for all tests performed.

## Variation in Trapped Equivalence Ratio

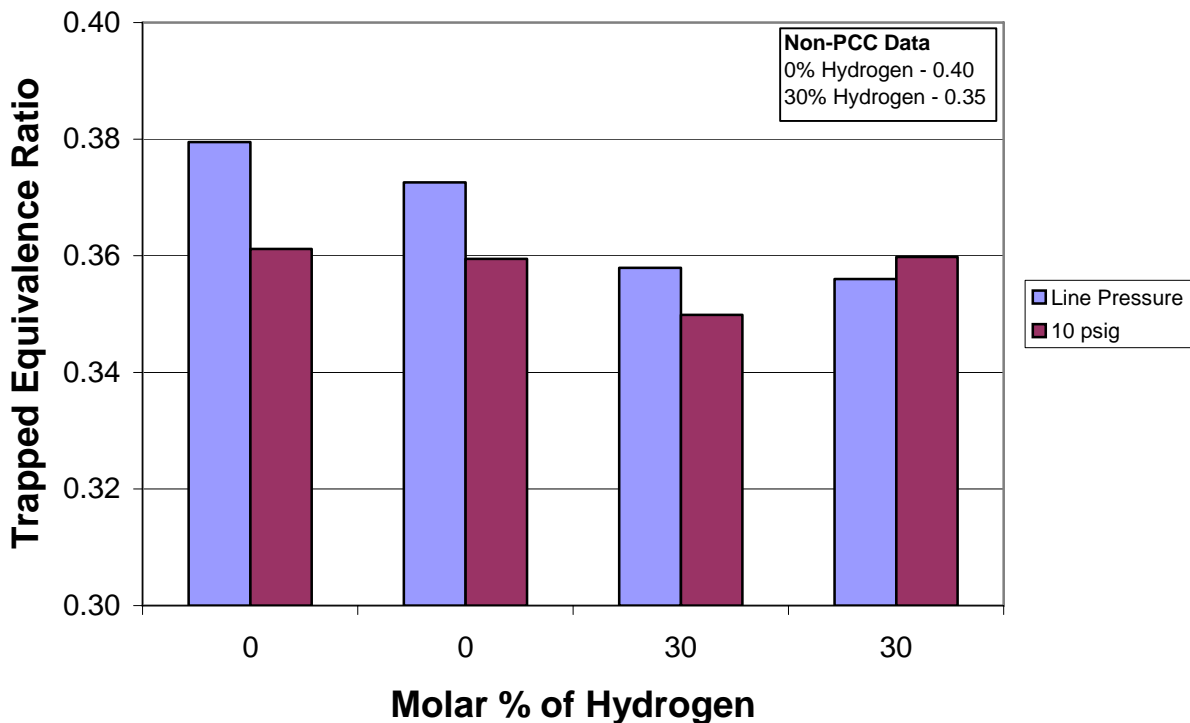


Figure 5-19 Trapped Equivalence Ratio with PCC

### Summary of PCC Tests

The data collected with the PCC configuration was not only compared to itself, but also to data collected with the non-PCC configuration. When the PCC was operated on the engine fuel line pressure, an 11% decrease in *CV* from the non-PCC configuration occurred with no hydrogen addition. When the PCC fuel pressure was decreased to 10 psig, the *CV* decreased 27% from the non-PCC configuration. With 30% hydrogen addition and the reduced pressure, the *CV* decreased 10% from PCC operation with no hydrogen. With the PCC on line pressure, hydrogen addition decreased the *CV* approximately 21% from the PCC operation with no hydrogen addition. This shows that hydrogen addition had a more significant impact for the line pressure than the reduced pressure. Hydrogen addition with both pressures did decrease misfires. No significant change in *BSFC* was found after considering the uncertainty in the calculations. Since the PCC fuel flow was less than 2% of the total fuel flow into the engine, the amount of hydrogen in the PCC fuel was not included in the *BSFC* calculations. With the PCC

configuration, adding hydrogen did not have as dramatic impact on NO<sub>x</sub> emissions as it did with the non-PCC configuration. With the line pressure, the decrease in NO<sub>x</sub> emissions with hydrogen addition is about 15%. With the reduced fuel pressure of 10 psig, the NO<sub>x</sub> emissions appear to have increased slightly, however after considering the uncertainty in the data, no significant change is found. Without hydrogen addition, NO<sub>x</sub> emissions decreased 62% with the addition of the PCC at line pressure. When the PCC fuel pressure was reduced, NO<sub>x</sub> emissions reduced 73% from the non-PCC configuration. Both of these decreases occurred without any hydrogen addition. Only the PCC addition was necessary. With the non-PCC configuration, 30% hydrogen addition provided the lowest NO<sub>x</sub> emissions. This value is nearly the same as that produced by the addition of a PCC at line pressure and no hydrogen. The reduced PCC fuel pressure reduced the NO<sub>x</sub> emissions 20% from that value. Considering the uncertainties, both adjusting the PCC fuel pressure and adding hydrogen caused no change in CO emissions. An increase in CO emissions from the non-PCC configuration of about 15% occurred with the addition of the PCC. No significant change in trapped equivalence ratio was found throughout the testing for both the PCC and non-PCC configurations with the spark timing of 3 degrees BTDC.

The impact of hydrogen addition on the PCC configuration was not as dramatic as for the non-PCC configuration. While hydrogen addition showed the ability to significantly lower NO<sub>x</sub> emissions without a PCC, the addition of a PCC without hydrogen addition showed similar NO<sub>x</sub> reduction capabilities. Compared to the non-PCC data, an increase in CO emissions occurred with the addition of the PCC. PCC addition maintained combustion stability without hydrogen addition and appears to be an effective way of lowering NO<sub>x</sub> emissions even without the use of hydrogen. This can only be said for the PCC used in this research. Other PCCs, especially those with larger volumes, may not produce the same results.

## CHAPTER 6 - Conclusions and Recommendations

The impact of hydrogen addition on performance and exhaust gas emissions of a large bore, lean burn, two stroke cycle engine was investigated. These results showed that hydrogen addition actually caused the engine to run more smoothly and increased combustion stability without the PCC. Without the PCC, there was a decrease in NO<sub>x</sub> emissions that did not come with an increase in CO emissions. The addition of the PCC showed similar NO<sub>x</sub> reduction capabilities without hydrogen addition. The following direct conclusions summarize the major findings of this thesis:

- For non-PCC configuration
  - Hydrogen addition had largest impact at the most advanced spark timing
  - Fewer misfires with hydrogen addition
  - No significant decrease in peak pressure with hydrogen addition
  - *BSFC* decreased with hydrogen addition showing more efficient engine operation
  - A nominal 10% hydrogen concentration by volume resulted in at least an 18% reduction in NO<sub>x</sub>
  - More NO<sub>x</sub> reduction with hydrogen addition as spark timing was advanced
  - Reduction in NO<sub>x</sub> did not cause increase in CO
  - *BSFC* decreased at least 10% with 30% hydrogen addition for all spark timings
  - Engine displayed a reduction in NO<sub>x</sub> and misfires with hydrogen addition and different spark timings
- For PCC configuration
  - Comparing to non-PCC data, a reduced PCC fuel pressure of 10 psig showed a decrease in the *CV* of 27% while PCC operation on the same fuel pressure as the engine showed a decrease in the *CV* of 11%
  - 30% hydrogen addition decreased misfires for both PCC fuel pressures (14 and 10 psig), but had the largest impact on the PCC with engine fuel line pressure decreasing the *CV* by 21%

- No significant change in *BSFC* occurred with PCC addition
- The addition of the PCC decreased  $\text{NO}_x$  by as much as 73% from the non-PCC configuration without any hydrogen addition
- The PCC reduced  $\text{NO}_x$  emissions to at least the concentration achieved with 30% hydrogen addition and no PCC
- A 15% increase in CO emissions were caused by the addition of the PCC
- Hydrogen addition has no impact on the CO emissions with the PCC

The results obtained in this research can be compared to those reported in the literature. Figure 6-1 shows the common results of various researchers. Most of the research available in the literature was conducted with rich burn, four stroke cycle engines. Therefore, the results may vary from those of this research. Research into hydrogen addition to PCCs is almost non-existent. Pratapas (2007) performed PCC testing similar to that conducted in this research. With the engine in non-PCC configuration, data showed it was possible to reach  $\text{NO}_x$  levels as low as what is currently achievable with PCC technology by adding hydrogen. A decrease in misfires was found with volume percentages of hydrogen above 5%. Data from the PCC testing showed that combustion stability with hydrogen addition was equivalent to combustion stability when operating on pure natural gas.  $\text{NO}_x$  emissions also appeared to be the same with and without hydrogen addition, while CO emissions decreased slightly with hydrogen addition. This is similar to data collected during this research.

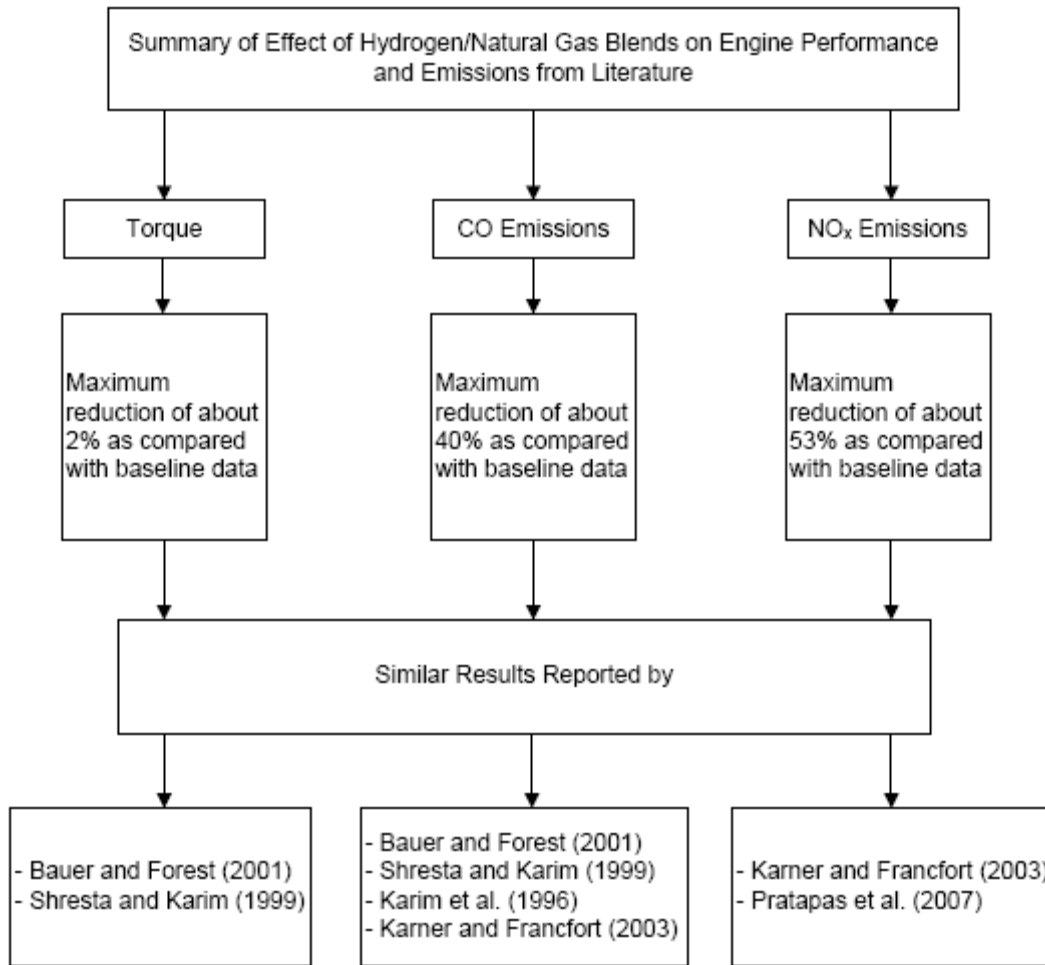


**Figure 6-1 Summary of Literature Results**

The results of this research show that hydrogen addition to a two stroke cycle, lean burn, single cylinder engine, without a PCC decreases NO<sub>x</sub> emissions and misfires while maintaining combustion stability and engine power. The addition of a PCC alone appears to lower NO<sub>x</sub> concentrations to those achievable with hydrogen addition and no PCC. However, the addition of the PCC increases CO emissions. These results make further PCC research a viable next step. This further research would include varying the PCC fuel line pressure and testing PCCs of varying volume. Larger PCC volumes may increase PCC NO<sub>x</sub> emissions that could be lowered by hydrogen addition. The use of the PCC from this research on different engines may not produce the same results. Different engines react differently to PCCs. Further work on calculating a true exhaust temperature not influenced by ambient conditions is necessary. The

model presented in Chapter 3 is simple, and a more precise model would allow more insight into in-cylinder temperatures. Further work into determining the location of peak pressure would make it possible to conclude the affects of hydrogen addition on combustion duration.

Hydrogen addition to natural gas seems to be a viable solution to reduce emissions while maintaining combustion stability and engine performance. However issues associated with hydrogen like on-site production and cost must be overcome.

## References

- Adamson, K. "Fuel Reforming." Fuel Cell Today (2006): 7 May 2007.
- Agrawal, A. K., et al. "Effect of EGR on the Exhaust Gas Temperature and Exhaust Opacity in Compression Ignition Engines." Sadhana 29.3 (2004): 275-84.
- Bauer, C. G., and T. W. Forest. "Effect of Hydrogen Addition on the Performance of Methane-Fueled Vehicles. Part I: Effect on S.I. Engine Performance." International Journal of Hydrogen Energy 26.1 (2001): 55-70.
- Beshouri, G., B. Willson, and K. S. Chapman. Pipeline Engine Emissions Control Roadmap: Technology Pathways to Cost-Effective Year 2010 Reciprocating Engine Emissions Compliance. Pipeline Research Council International, 2005.
- Bevington, P. R., and D. K. Robinson. "Error Analysis." Data Reduction and Error Analysis for the Physical Sciences. 3rd ed. New York, NY: McGraw-Hill, 2003. 36-49.
- Bowman, C. T. "Kinetics of Pollutant Formation and Destruction in Combustion." Progress in Energy and Combustion Science 1 (1975): 33-45.
- Chapman, K. S. Cost-Effective Reciprocating Engine Emissions Control and Monitoring for E&P Field and Gathering Engines Technical Progress Report, DOE Award DE-FC26-02NT15464. Vol. 3. Manhattan, KS: National Gas Machinery Laboratory, December 2003.
- Crowe, C. T., D. F. Elger, and J. A. Roberson. Engineering Fluid Mechanics. 8th ed. New York, NY: John Wiley & Sons, 2005.
- Department of Energy. Hydrogen Properties. Hydrogen Fuel Cell Engines and Related Technologies. United States Department of Energy, 2001a. 22 April 2007  
<[http://www1.eere.energy.gov/hydrogenandfuelcells/tech\\_validation/pdfs/fcm01r0.pdf](http://www1.eere.energy.gov/hydrogenandfuelcells/tech_validation/pdfs/fcm01r0.pdf)>.

- . Hydrogen use in Internal Combustion Engines. Hydrogen Fuel Cell Engines and Related Technologies. United States Department of Energy, 2001b. 33 April 2007  
<[http://www1.eere.energy.gov/hydrogenandfuelcells/tech\\_validation/pdfs/fcm03r0.pdf](http://www1.eere.energy.gov/hydrogenandfuelcells/tech_validation/pdfs/fcm03r0.pdf)>.
- . Natural Gas Reforming. United States Department of Energy, 2006. 25 Jan. 2007  
<[http://www1.eere.energy.gov/hydrogenandfuelcells/production/printable\\_versions/natural\\_gas.html](http://www1.eere.energy.gov/hydrogenandfuelcells/production/printable_versions/natural_gas.html)>.
- . Retooling Today's Engines for the Hydrogen Economy. FreedomCAR and Vehicle Technologies Program. United States Department of Energy-Energy Efficiency and Renewable Energy, 2005.
- Ely, C. "Emissions Data Collection, Calculations, and Interpretation." Engine Emissions Stack Testing and Analyzer Workshop. Oklahoma City, OK, 12-14 October 2004.
- Epperly, R. Hydrogen Production Technologies. The National Academy of Sciences, 2004.
- Ferguson, C. R., and A. R. Kirkpatrick. Internal Combustion Engines. New York, NY: John Wiley & Sons, 2001.
- Frey, C. H., and S. Li. "Quantification of Variability and Uncertainty in Stationary Natural Gas Fueled Internal Combustion Engine NO<sub>x</sub> and Total Organic Compounds Emission Factors." Annual Meeting of the Air and Waste Management Association. Orlando, FL, 24-28 June, 2001.
- Haimov, H., R. Faulkner, J. Chini, and V. Ammirato. CRB Reduces Compressor Emissions. Odessa, TX: Diesel Supply Company, 1998.
- Heywood, J. B. Internal Combustion Engine Fundamentals. New York, NY: McGraw-Hill, 1988.
- Jamal, Y., T. Wagner, and M. L. Wyszynski. "Exhaust Gas Reforming at Moderate Temperatures." International Journal of Hydrogen Energy 21.6 (1996): 507-19.

- Karim, G. A., I. Wierzba, and Y. Al-Alousi. "Methane-Hydrogen Mixtures as Fuels." International Journal of Hydrogen Energy 21.7 (1996): 625-31.
- Karim, G. A. "Hydrogen as a Spark Ignition Fuel." International Journal of Hydrogen Energy 28 (2003): 569-77.
- Karner, D., and J. Francfort. Hydrogen/CNG Blended Fuels Performance Testing in a Ford F-150. Energy Efficiency and Renewable Energy. United States Department of Energy, 2003.
- Kidder, J. K., and R. Potter. Recent Improvements in Two-Cycle Combustion Utilizing Screw-in Pre-Combustion Chambers and "High Pressure" Fuel Valves. Enginuity International, Inc., 2002.
- Moran, M. J., and H. J. Shapiro. Fundamentals of Engineering Thermodynamics. 5th ed. New York, NY: John Wiley & Sons, 2004.
- Padro, C. E. G., V. Putsche, and A. Harstein. Hydrogen Production-Steam Methane Reforming (SMR). New York State Energy Research and Development Authority, 2003.
- Pratapas, J. M., et al. "Thermo Chemical Recuperation (TCR) for Fuel Savings and Emissions Reduction at Compressor Engines." Gas Machinery Conference. Dallas, TX, 1-3 October 2007.
- Shrestha, S. O., and G. A. Karim. "Hydrogen as an Additive to Methane for Spark Ignition Engine Applications." International Journal of Hydrogen Energy 24.6 (1999): 577-86.
- Swain, M. Hydrogen: The Fuel of the Future. Plug Power Fuel Cell Systems, 2003.
- Turns, S. R. "Pollutant Emissions." An Introduction to Combustion. 2nd ed. New York, NY: McGraw-Hill, 2000. 550-88.
- Wyszynski, M. L., T. Megaritis, and R. S. Lehrle. Hydrogen from Exhaust Gas Fuel Reforming: Greener, Leaner, and Smoother Engines. Future Power Systems Group: The University of Birmingham, 2000.

Yap, D., et al. "Natural Gas HCCI Engine Operation with Exhaust Gas Fuel Reforming."  
International Journal of Hydrogen Energy 31.5 (2005): 587-95.

## Appendix A - Real Gas Fuel Blending Sample Calculation

$$\begin{array}{llll}
 V := 50.06 & R_{\text{bar}} := 10.732 & T_{\text{cN}} := 344 & P_{\text{cN}} := 673.07 \\
 T := 539.67 & & T_{\text{cH}} := 59.8 & P_{\text{cH}} := 188.11
 \end{array}$$

Calculate Constants for hydrogen and natural gas

$$a_{\text{N}} := \frac{27}{64} \frac{(R_{\text{bar}} T_{\text{cN}})^2}{P_{\text{cN}}} \quad a_{\text{N}} = 8.543 \times 10^3$$

$$a_{\text{H}} := \frac{27}{64} \frac{(R_{\text{bar}} T_{\text{cH}})^2}{P_{\text{cH}}} \quad a_{\text{H}} = 923.71$$

$$b_{\text{N}} := R_{\text{bar}} \frac{T_{\text{cN}}}{8 \cdot P_{\text{cN}}} \quad b_{\text{N}} = 0.686$$

$$b_{\text{H}} := R_{\text{bar}} \frac{T_{\text{cH}}}{8 \cdot P_{\text{cH}}} \quad b_{\text{H}} = 0.426$$

For a given precharge pressure of natural gas ( $P_{\text{N}}$ ), the moles of natural gas are calculated with the help of van der Waals equation.

$$v_{\text{N}} := 1 \quad P_{\text{N}} := 180$$

Given

$$P_{\text{N}} = R_{\text{bar}} \frac{T}{(v_{\text{N}} - b_{\text{N}})} - \frac{a_{\text{N}}}{v_{\text{N}}^2}$$

$$v_{\text{N}} := \text{Find}(v_{\text{N}})$$

$$N_{\text{N}} := \frac{V}{v_{\text{N}}}$$

$$N_{\text{N}} = 1.595$$

Hydrogen is now added.

Define what molar percentage of hydrogen is desired in the mixture and calculate how many moles of hydrogen are needed.

$$y_H := 0.1$$

$$y_N := 1 - y_H$$

$$N_H := 1$$

Given

$$y_H = \frac{N_H}{N_H + N_N}$$

$$N_H := \text{Find}(N_H)$$

$$N_H = 0.177$$

Now calculate total mixture pressure using van der Waals.

$$a_M := y_N \cdot a_N + y_H \cdot a_H$$

$$b_M := y_N \cdot b_N + y_H \cdot b_H$$

$$a_M = 7.781 \times 10^3$$

$$b_M = 0.66$$

$$v_M := \frac{V}{N_H + N_N}$$

$$P_M := R_{\text{bar}} \cdot \frac{T}{\frac{V}{N_H + N_N} - b_M} - \frac{a_M}{(v_M)^2}$$

$$P_M = 200.208 \quad \text{Total mixture pressure considering real gas}$$

$$Z := P_M \cdot \frac{v_M}{R_{\text{bar}} \cdot T}$$

$$Z = 0.976 \quad \text{Mixture compressibility factor considering real gas}$$

$$v_M = 28.244 \quad \text{Mixture molar specific volume considering real gas}$$

## Appendix B - Compressibility Factors

This table shows the compressibility factors of hydrogen and natural gas mixtures with an actual temperature and pressure of 540°R and 200 psia, respectively. The critical pressure is 673 psia for natural gas and 188.1 psia for hydrogen. The critical temperature is 344°R for natural gas and 59.8°R for hydrogen (Moran and Shapiro, 2004). Kay's rule was used to find the mixture critical pressure and temperature. Once the reduced pressure and temperature were calculated, the compressibility factor was read from a compressibility chart.

**Table B-1 Compressibility Factors for Fuel Mixtures**

<b>Hydrogen % by Volume</b>	<b>Mixture <math>T_c</math> (°R)</b>	<b>Mixture <math>p_c</math> (psia)</b>	<b>Reduced Temperature <math>T_R</math></b>	<b>Reduced Pressure <math>p_R</math></b>	<b>Compressibility Factor <math>Z</math></b>
<b>5</b>	329.79	648.76	1.6374	0.3083	0.980
<b>10</b>	315.58	624.51	1.7111	0.3203	0.985
<b>15</b>	301.37	600.27	1.7918	0.3332	0.988
<b>20</b>	287.16	576.02	1.8805	0.3472	0.990
<b>25</b>	272.95	551.78	1.9784	0.3625	0.993
<b>30</b>	258.74	527.53	2.0870	0.3791	0.995

## Appendix C - Ideal Gas Fuel Blending Sample Calculation

With a given final mixture pressure of 180 psig, a target 30% molar percentage of hydrogen, and atmospheric pressure of 14.3 psia, the following steps are performed to blend the fuel.

First, the blending chamber is purged so that only pure natural gas is present at atmospheric conditions. Next, hydrogen is added until the partial pressure is reached in the tank.

$$\begin{aligned} p_{H_2} &= 0.3(194.3 \text{ psia}) = 58.29 \text{ psia} \\ 58.29 \text{ psia} - 14.3 \text{ psia} &= 43.99 \text{ psig} \end{aligned} \tag{C.1}$$

After 43.99 psig is shown on the blending chamber gage, compressed natural gas is added until the blending chamber gage shows 165.7 psig, which is the final mixture pressure minus the atmospheric pressure. This gives a blended fuel with 30% hydrogen and 70% natural gas by volume.